creative commons
COMMONS DEED

저작자표시-비영리-변경금지 2.0 대한민국

이용자는 아래의 조건을 따르는 경우에 한하여 자유롭게

- 이 저작물을 복제, 배포, 전송, 전시, 공연 및 방송할 수 있습니다.

다음과 같은 조건을 따라야 합니다:

저작자표시. 귀하는 원저작자를 표시하여야 합니다.

비영리. 귀하는 이 저작물을 영리 목적으로 이용할 수 없습니다.

변경금지. 귀하는 이 저작물을 개작, 변형 또는 가공할 수 없습니다.

- 귀하는, 이 저작물의 재이용이나 배포의 경우, 이 저작물에 적용된 이용허락조건을 명확하게 나타내어야 합니다.
- 저작권자로부터 별도의 허가를 받으면 이러한 조건들은 적용되지 않습니다.

저작권법에 따른 이용자의 권리는 위의 내용에 의하여 영향을 받지 않습니다.

이것은 이용허락규약(Legal Code)을 이해하기 쉽게 요약한 것입니다.

Disclaimer

dCollection

이학박사학위논문

척추 동물 모계-접합체 전이 과정에서의 전령 RNA 꼬리 조절에 관한 연구

Study on the regulation of mRNA tailing during the maternal-to-zygotic transition in vertebrates

2017년 2월

서울대학교 대학원

생명과학부

여진아

이학박사학위논문

척추 동물 모계-접합체 전이 과정에서의 전령 RNA 꼬리 조절에 관한 연구

Study on the regulation of mRNA tailing during the maternal-to-zygotic transition in vertebrates

2017년 2월

서울대학교 대학원

생명과학부

여진아

Abstract

Study on the regulation of mRNA tailing during the maternal-to-zygotic transition in vertebrates

Jin-ah Yeo
School of Biological Sciences
The Graduate School
Seoul National University

During the maternal-to-zygotic transition (MZT), maternal transcriptome is degraded and replaced by *de novo*-synthesized zygotic transcripts in a highly coordinated manner. As zygotic genome is kept inactivated in fertilized eggs, maternal transcripts direct the early events of development and are regulated by post-transcriptional mechanisms such as cytoplasmic polyadenylation and differential RNA degradation. Timely decay of these maternal mRNAs is important because maternal transcripts must remain stable before the onset of zygotic genome activation (ZGA), but should be removed after ZGA so as not to interfere with the subsequent developmental events. However, it remains unknown how mRNA stability is temporally coordinated during early development in vertebrates.

To understand how mRNA tailing influences the transcriptome dynamics during the MZT, I applied a new high-throughput sequencing method called TAIL-seq to early zebrafish embryos. This method allows me to investigate poly(A) tail length and additional 3′ end modification at the genomic scale. I found that poly(A) tails of maternal mRNAs elongate globally after fertilization, whereas several groups of maternal transcripts remain

unchanged or are rapidly deadenylated shortly after fertilization, establishing the temporal regulation of maternal gene expression. After the onset of ZGA, maternal mRNAs are massively deadenylated and degraded. Interestingly, mRNA uridylation is dramatically induced during the MZT. Such induction of uridylation is consistently observed in mouse and *Xenopus* embryos but not in *Drosophila*, suggesting the conserved role of uridylation in vertebrate mRNA decay pathway.

Morpholino-mediated knockdown experiments and high-throughput mRNA sequencing revealed that mRNA uridylation plays a critical role in the progression ofthe MZT. When TUT4 (ZCCH11) and TUT7 (ZCCHC6), previously identified as mRNA uridylation enzymes in human cells, are knocked down in zebrafish, maternal mRNA clearance is significantly delayed, leading to impaired zygotic transcription and developmental defects during gastrulation. Maternal mRNAs with short poly(A) are preferentially targeted by TUT4 and TUT7, whereas maternal transcripts with long poly(A) are less affected by uridylation activity. I further found the essential role of uridylation in early embryonic development in *Xenopus laevis* by knockdown of TUT7. Wild-type TUT7 but not catalytically inactive TUT7 mRNA rescues the gastrulation defects and the uridylation reduction in the TUT7 morphants, indicating the specificity of the developmental phenotype caused by TUT7 morpholinos.

Based on my results, I propose that uridylation has a conserved role in maternal mRNA clearance during early embryonic development in vertebrates. During the MZT, mRNA uridylation is essential for precise clearance of maternal transcripts with short poly(A) tails, thereby directing the progression of early development.

Keywords: Uridylation; TAIL-seq; mRNA tailing; Maternal to zygotic transition; Poly(A) tail; maternal mRNA clearance

Student ID: 2010-20323

Contents

List of Figures

List of Tables

List of Abbreviations

cDNA	complementary DNA
dpf	day after fertilization
hpf	hour after fertilization
KD	Knockdown
MBT	Mid-Blastula Transition
MGA	Mid-preimplantation Gene Activation
miRNA	microRNA
MO	Morpholino
mRNA	messenger RNA
MZT	Maternal-to-Zygotic Transition
NTD	Nucelotidyl Transferase Domain
PABP	Poly(A) Binding Protein
PAP	Poly(A) Polymerase
PCA	Principle component analysis
PUP	Poly(U) polymerase
qPCR	quantitative Polymerase Chain Reaction
rRNA	ribosomal RNA

RT	Reverse Transcription
SB MO	Splicing Blocking Morpholino
TB MO	Translational Blocking Morpholino
TUT	Terminal uridylyl transferase
UTR	Untranslated Region
WT	Wild-type
ZGA	Zygotic Genome Activation

1. Introduction

1.1 The maternal to zygotic transition

The maternal to zygotic transition (MZT) is the first developmental transition event that occurs following fertilization in all animals. It has been extensively studied in various animal models including echinoderms (*Strongylocentrotus purpurarus*), nematodes (*Caenorhabditis elegans*), insects (*Drosophila melanogaster*), fish (*Danio rerio*), amphibians (*Xenopus*) and mammals (*Mus musculus*) (Figure 1) [1] (Tadros & Lipshitz, 2009). In all species, developmental control is first dependent on maternally deposited products and then switched into the mode that relies on newly synthesized zygotic products during the MZT. After fertilization, maternally supplied mRNAs and proteins drive the early development processes because the zygotic transcription is quiescent. During this period, the polyadenylation and deadenylation are regulated in a highly coordinated manner to allow the sequential translational control of maternal transcripts. Regulation of mRNA stability also has a critical role in differential expression of maternal transcripts during these early stages. Subsequently, transcriptome is dramatically remodeled via zygotic genome activation (ZGA), coinciding with widespread clearance of maternal transcripts. Timely elimination of maternally loaded mRNAs is required for the proper developmental progression.

Although the MZT is a universal process in all metazoan development, its timing and scale vary depending on species (Figure 1). In zebrafish and *Xenopus*, for instance, major zygotic transcription commences after ten and twelve cell cycles, respectively, coinciding

[1] Tadros, W. and Lipshitz, H. D., "The maternal-to-zygotic transition: a play in two acts", Development 136, 18 (2009), pp. 3033-42.

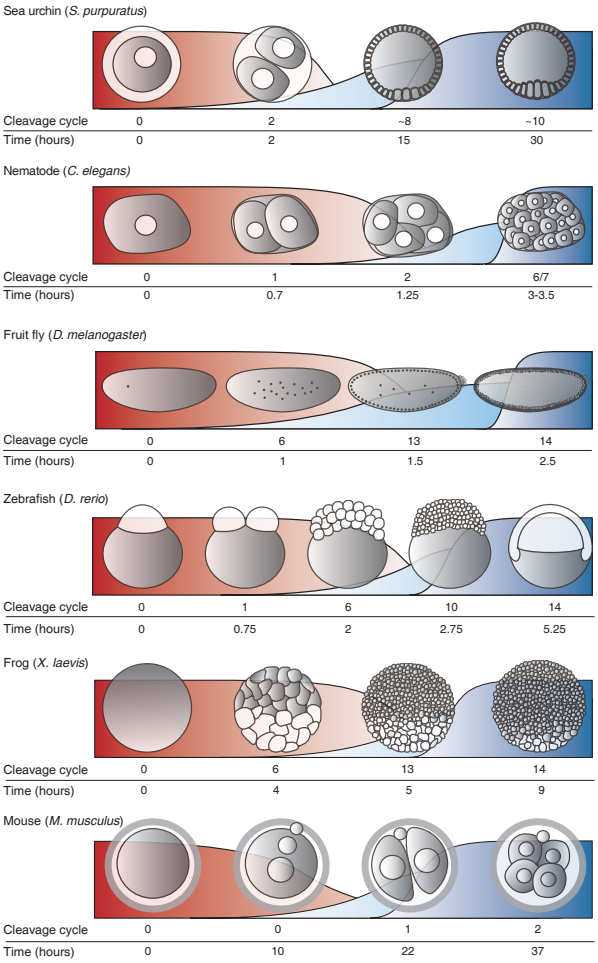

Figure 1. Illustration of embryonic developmental stages that span the maternal-to-zygotic transition (MZT) in several model organisms. Key embryonic stages for each model organism are depicted schematically above the corresponding cell cycle and time after fertilization. The red curves depict the degradation profiles of destabilized maternal mRNAs in each species. The light and dark blue curves represent the minor and major waves of zygotic genome activation, respectively.

with dramatic changes in the cell cycle (Newport & Kirschner, 1982; Kane & Kimmel, 1993). Upon fertilization, initial cell cycles are rapid and synchronous without gap phases, followed by asynchronous division with gap that coincides with initiation of major zygotic transcription. A developmental period when these changes in cell cycle are initiated is referred to as the midblastula transition (MBT). In mouse, however, the early cell cycles are slow and asynchronous, and major zygotic transcription initiates at the 2-cell stage (Hamatani et al., 2004). In general, major zygotic transcription is paralleled by the global degradation of maternal mRNAs although the timing and scale of maternal mRNA decay also vary across species (Tadros & Lipshitz, 2009). Diverse mechanisms regulating maternal mRNA clearance have been identified in different species, but it remains to undiscovered what mechanism is conserved across species (Yartseva & Giraldez, 2015).

1.2 Translational control by change in poly(A) tail length of maternal mRNAs

Translational control by poly(A) tail length is critical in early development of many animal species (Mendez & Richter, 2001; Weill et al., 2012). In the nucleus, mRNAs are co-transcriptionally capped by the addition of a 7-methylguanosine at the 5′ end, and cleaved and polyadenylated by canonical poly(A) polymerase (PAP) at the 3′ end. Once mRNAs are exported to the cytoplasm, the poly(A) tail and the 5′ cap form a closed loop through their interacting protein complex to facilitate translation initiation (Kahvejian et al., 2005; Wells et al., 1998). Thus, the regulation of poly(A) tails in the cytoplasm is one of the important mechanisms of translational control.

During oogenesis, maternal mRNAs are deposited in deadenylated forms and are

translationally silenced. In contrast to somatic cells in which deadenylation induces decapping and degradation of mRNAs, deadenylation is not linked to mRNA decay in oocytes and early embryos. Upon oocyte maturation or after fertilization, these dormant mRNAs are polyadenlyated and translationally reactivated to drive re-entry of oocyte into meiosis or early embryonic mitosis, respectively (Mendez & Richter, 2001; Weill et al., 2012). A subset of maternal mRNAs is sequentially activated by cytoplasmic polyadenylation during oocyte maturation, while some groups of maternal mRNAs are polyadenlyated and activated only after fertilization(Paillard & Osborne, 2003). Upon fertilization, a group of maternal mRNAs, which is polyadenylated during oocyte maturation, is rapidly deadenylated and inactivated (Paris & Philippe, 1990; Sheets et al., 1994). The sequential activation or inactivation of each mRNA depends on the polyadenylation/deadenylation governed by a combinatorial code of motifs in 3′ untranslated region (UTR) to recruit different sets of RNA binding proteins (Graindorge et al., 2008; Mendez & Richter, 2001; Pique et al., 2008). Recently, global poly(A) tail lengthening of maternal mRNAs is observed in zebrafish embryos. In mRNA-seq data of poly(A) enriched RNAs, a large number of maternal mRNAs increased in levels before the onset of ZGA (Aanes et al., 2011). Because validation by RT-qPCR using random primer differed from the pattern observed in poly(A) enriched mRNA-seq, increase of poly(A)+ transcripts might indicate increased cytoplasmic polyadenylation. Furthermore, comparison of poly(A) enriched and rRNA-depleted RNA-seq revealed that several hundred maternal transcripts undergo polyadenylation and deadenylation before the onset of ZGA in *Xenopus tropicalis* (Collart et al., 2014; Owens et al., 2016).

1.3 Mechanisms of maternal mRNA clearance during the MZT

In most animals, maternal mRNA clearance is accomplished by two major pathways (Figure 2): maternal decay pathway and zygotic decay pathway (Barckmann & Simonelig, 2013; Tadros & Lipshitz, 2009; Yartseva & Giraldez, 2015). The maternal decay pathway is programed by maternal factors and occurs independently of zygotic transcription, while the zygotic decay pathway is activated by newly synthesized zygotic factors after ZGA.

In *Xenopus*, fertilization triggers deadenylation of a subset of maternal transcripts for translational repression. The deadenylated mRNAs are degraded only after the MBT, suggesting temporal uncoupling between deadenylation and degradation (Audic et al., 1997; Duval et al., 1990; Voeltz & Steitz, 1998). In a previous study, translation inhibitor blocked mRNA degradation at the MBT, whereas transcriptional inhibitor did not affect the activation of mRNA decay (Duval et al., 1990). This indicates that the early decay of mRNAs is regulated by the translation of maternal factors but not by the new transcription of zygotic genes. More recently, two studies investigated how codon identity and translation affect mRNA stability during the MZT in zebrafish(Bazzini et al., 2016; Mishima & Tomari, 2016). They observed that mRNAs enriched in optimal codons (i.e., codons represented in highly expressed genes) are more stable than those enriched in non-optimal codon. They revealed that in maternal decay pathway, codon optimality affects mRNA stability in a translation-dependent manner and maternal mRNAs with non-optimal codon are highly deadenylated by the CCR4-NOT complex, suggesting that translation is determinant of mRNA stability during early development. In mouse, shortly after fertilization a subset of maternal mRNAs is selectively degraded through maternal decay pathway mediated by the 3′ UTR sequences (Alizadeh et al., 2005; Hamatani et al., 2004). Oocyte-specific mRNAs that are only required for oogenesis undergo rapid degradation after fertilization (Alizadeh et al., 2005).

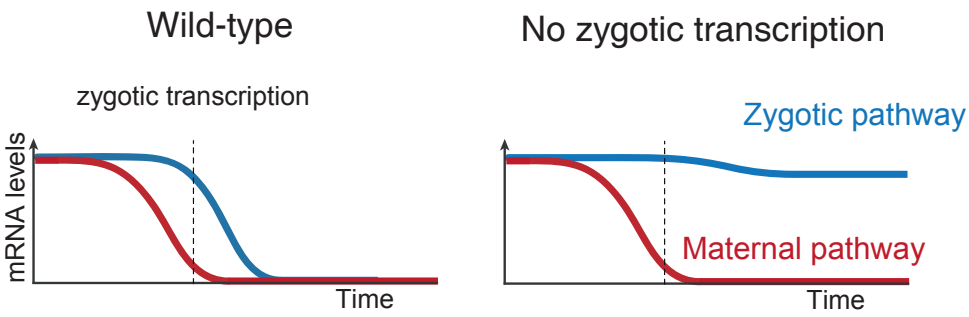

Figure 2. Maternal and zygotic pathways of maternal mRNA clearance. Maternal mRNAs under the regulation ofthe maternal factors (red) will be degraded independently of zygotic transcription, while mRNAs under the zygotic mechanisms (blue) will be stable in the absence of zygotic transcription.

Subsequently, zygotic pathway further eliminates maternal transcripts, coinciding with the major zygotic transcription(Hamatani et al., 2004) .

In both vertebrates and invertebrates, microRNAs (miRNAs) are implicated in zygotic decay pathway (Bushati et al., 2008; Giraldez et al., 2006; Lund et al., 2009). miRNA-dependent maternal mRNA decay was first identified in zebrafish, where miR-430 is expressed at the onset of zygotic transcription and triggers deadenylation and degradation of a subset maternal mRNAs that have miR-430 target sites (Bazzini et al., 2012; Giraldez et al., 2006). In *Xenopus*, the miR-430 ortholog miR-427, which has the same seed sequence with miR-430, mediates the rapid deadenylation of maternal mRNAs after the MBT (Lund et al., 2009). Similarly in Drosophila, the miR-309 cluster is highly expressed at the onset of ZGA and is involved in the degradation of hundred of maternal mRNAs (Bushati et al., 2008).

1.4 Transcriptome-wide measurement of poly(A) tail length

Recent advance in high-throughput sequencing methods enabled mRNA poly(A) length measurement at the genomic scale. First, TAIL-seq directly sequences the 3′ ends of mRNAs, allowing us to measure accurately poly(A) tail length and to determine additional 3′ end modification in a transcriptome-wide manner (Figure 3) [2](Chang et al., 2014). For mRNA enrichment without the bias by oligo dT, the TAIL-seq protocol initially removes rRNAs and short non-coding RNAs (<200nt) by affinity-based depletion and size fractionation, respectively. In order to keep the intact information of 3′ mRNA termini, the RNA sample is ligated to the 3′ adaptor that includes biotin residue prior to RNA

[2]Chang, H., Lim, J., Ha, M., & Kim, V. N. (2014). Tail-seq: Genome-wide determination of poly(a) tail length and 3′ end modifications. Mol Cell, 53(6), 1044–52.

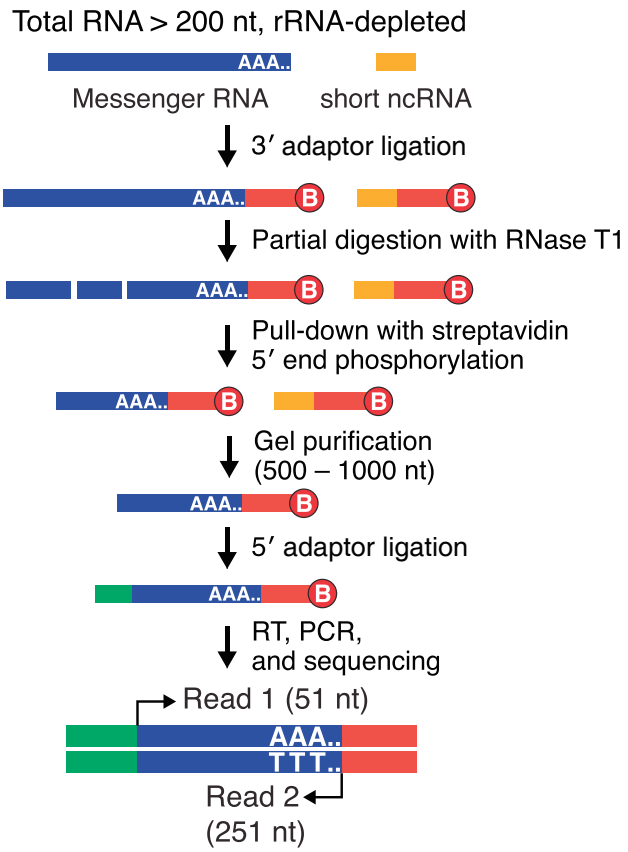

Figure 3. Experimental procedure for TAIL-seq.

fragmentation. Following partial digestion by RNase T1, the 3′ end fragments are purified by biotin-streptavidin interaction and ligated to the 5′ adaptor. Eventually, cDNA library is sequenced in paired-end illumina platform to generate sequences of 51 nt from the 5′ end, which is used for identification of transcripts and 231 nt from the 3′ end, which is used to determine 3′ end sequences. One of the unique advantages of TAIL-seq is that it provides the sequence information of the very end of RNA and thus allows us to investigate other modification apart from poly(A) tails. Interestingly, this method identified widespread uridylation and guanylation at the downstream of poly(A) tails in mammalian cells (Figure 4) [3]. More recently, a new version of TAIL-seq (mTAIL-seq) is developed to enhance sequencing depth for mRNAs by ~1,000-fold compared with the previous version (Lim et al., 2016). In mTAIL-seq, total RNA sample is ligated to the 3′ adaptor using splint ligation method, which allows enriching RNAs with a specific type of terminus and thereby increases the sequencing depth even with small amount of input RNA. This method revealed dynamic poly(A) tail regulation in *Drosophila* oocytes and embryos.

Second, poly(A) tail length profiling by sequencing (PAL-seq) measures fluorescence intensity that reflects the tail length of the cDNA (Subtelny et al., 2014). The PAL-seq utilizes largely similar strategies with TAIL-seq for preparation of cDNA library whereas the major difference is in the sequencing step, resulting that it does not provide a sequence information about the 3′ end modification. Using PAL-seq method, Subtelny *et al.* analyzed poly(A) tail profiling in various species, including yeast, fly, plant, mouse, human, zebrafish, and *Xenopus*. Interestingly, poly(A) tail length is strongly correlated with translational efficiency in early embryonic samples but not in non-embryonic samples. The correlation between poly(A) length and translational efficiency decreases at gastrulation, indicating a

[3] Chang, H., Lim, J., Ha, M., & Kim, V. N. (2014). Tail-seq: Genome-wide determination of poly(a) tail length and 3′ end modifications. Mol Cell, 53(6), 1044–52.

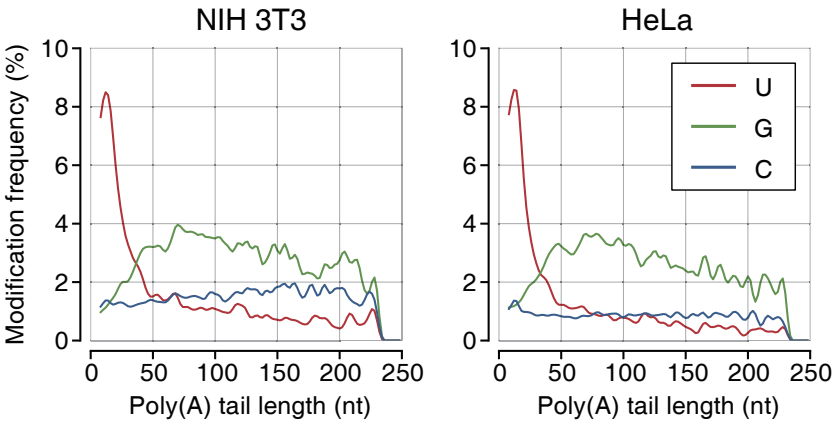

Figure 4. Relationship between modification and poly(A) tail length in NIH 3T3 and HeLa cells. TAIL-seq identified widespread uridylation and guanylation at the downstream of poly(A) tails in NIH 3T3 and HeLa cells. The density was calculated with 2 nt wide bins, then smoothened with Hanning window (width = 7).

developmental switch in the modes of translational control during the MZT.

1.5 Uridylation of RNAs

RNA tailing or 3′ non-templated nucleotide addition has a crucial role in determining the fate of RNAs and is one of the most abundant types of RNA modification, including adenylation, cytidylation, guadnylation, and uridylation (Lee et al., 2014; Munoz-Tello et al., 2015; Scheer et al., 2016) . The non-templated nucleotide addition is catalyzed by a group of template-independent ribonucleotidyl transferases that are also called terminal uridylyl transferases (TUTases) or poly(U) polymerases (PUPs), which belong to the Pol β-like nucleotidyltransferase superfamily (Aravind & Koonin, 1999; Kwak & Wickens, 2007; Martin & Keller, 2007; Norbury, 2013). Besides canonical poly(A) polymerase (PAPs), many noncanonical PAPs have been identified from fission yeast to mammals (Martin & Keller, 2007; Norbury, 2013; Scheer et al., 2016). Apart from the characteristic nucleotidyl transferase domain (NTD) and poly(A) polymerase-associated domain (PAP), noncanonical PAPs have diverse noncatalytic domains, indicating the variety of RNA substrates and cofactors of them. Humans have seven noncanonical PAPs with distinct subcellular localization and substrate specificity.

Recently, exciting progress has been made to understand the molecular function of terminal uridylation in RNA degradation. The role of uridylation in the RNA decay process was first identified in *Arabidopsis* and mammalian cells that the 3′ ends of miRNA-mediated cleavage products are modified by oligouridine addition (Shen & Goodman, 2004). In *Arabidopsis*, U-tails correlate with decapping and 5′ shortening of the cleaved products, implying that uridylation might promote the 5′ to 3′ decay pathway. In mammalian cells,

uridylation also stimulates the decay of replication-dependent histone mRNAs that lack a poly(A) tail (Martin & Keller, 2007). Upon inhibition of DNA replication or at the end of S-phase, uridylation of histone mRNAs triggers both 5′ to 3′ decay by LSM1, DCP2, and XRN1 and 3′ to 5′ decay by ERI1 and RNA exosome (Hoefig et al., 2013; Mullen & Marzluff, 2008; Slevin et al., 2014). Although several TUTase were reported to catalyze uridylation of histone mRNAs in earlier studies (Mullen & Marzluff, 2008; Schmidt et al., 2011; Su et al., 2013), recent study revealed that TUT7 acts dominantly in histone mRNA uridylation (Lackey et al., 2016). Furthermore, uridylation of polyadenylated mRNAs was first detected on mRNAs of fission yeast *S.pombe*, of which uridylation is catalyzed by Cid1 that is one of the TUTase in fission yeast (Rissland et al., 2007; Rissland & Norbury, 2009). The uridylation on the short poly(A) tails of mRNA promotes the 5′ to 3′ decay by facilitating the binding of LSM1-7 complex (Rissland & Norbury, 2009). Uridylation of mRNAs in *S. pombe* also induces 3′ to 5′ decay by the Dis3L2 that is member of the 3′-5′ exoribonuclease II/R family and acts independently of the exosome (Malecki et al., 2013).

More recently, a integral role of uridylation in mRNA decay pathway was identified in human cell lines by investigating the global effect of uridylation on mRNAs through the TAIL-seq analysis (Lim et al., 2014). In TAIL-seq result from mammal cell lines, uridylation is mainly found on deadenylated mRNAs (with poly(A) tails shorter than ~25 nt) and uridylation level has a negative correlation with global mRNA half-lives (Chang et al., 2014). Upon knockdown of both TUT4 and TUT7, which act redundantly, mRNA uridylation is globally depleted and mRNA half-lives are also globally increased. Moreover, depletion of 5′ to 3′ decay factors such as XRN1, LSM1, and DCP1/2 as well as 3′ to 5′ decay factors such as RRP41, and DIS3L2 results in the accumulation of uridylated mRNAs with short poly(A) tails. Based on these results, it was proposed that mRNAs are subject to uridylation following deadenylation, and then U-tails trigger decay of deadenylated

mRNAs by serving as a mark for recognition of downstream decay factors (Figure 5) [4](Lim et al., 2014). Therefore, uridylation leads deadenlylated mRNAs to both 5′ to 3′ and 3′ to 5′ decay pathways for rapid degradation, suggesting that uridylation is an integral step of fast-track mRNA decay pathway. In future studies, uridylation needs to be investigated in multiple biological contexts such as diverse organisms, developmental stages, or neuronal synapses to delineate the conserved roles of uridylation in mRNA metabolism.

As common model organisms for vertebrate development, zebrafish and *Xenopus* have superior advantages for the study of post-transcriptional regulation. Their early embryos are transcriptionally inactive. Transcription is naturally shut off at the beginning of oocyte maturation and only resumes at later stages of embryogenesis. Thus, it is needless to use transcription inhibitors to study post-transcriptional mechanism. In addition, their eggs, which are externally fertilized, are relatively large and produced in large quantities. This permits not only convenient manipulation but also easy microinjection of various molecules. For example, injection of chemically modified antisense oligonucleotide can efficiently inhibit the endogenous mRNA target and injecting a given mRNA leads to an overexpression of its protein. These facilitate loss- and gain-of-function approaches for important genes involved in early embryonic development. Notably, developmentally regulated changes in poly(A) tail length have been intensively characterized in these organisms. However, it still remains unknown about the role of non-templated modification besides poly(A) tailing during early embryonic development. More importantly, early embryo is one of physiological condition where global degradation of maternal mRNAs is necessary for the progression of early development. Therefore, applying TAIL-seq to the early embryos will provide crucial insights into the integral role of uridylation in RNA degradation.

[4]Lim, J. and Ha, M. and Chang, H. and Kwon, S. C. and Simanshu, D. K. and Patel, D. J. and Kim, V. N., "Uridylation by TUT4 and TUT7 marks mRNA for degradation", Cell 159, 6 (2014), pp. 1365-76.

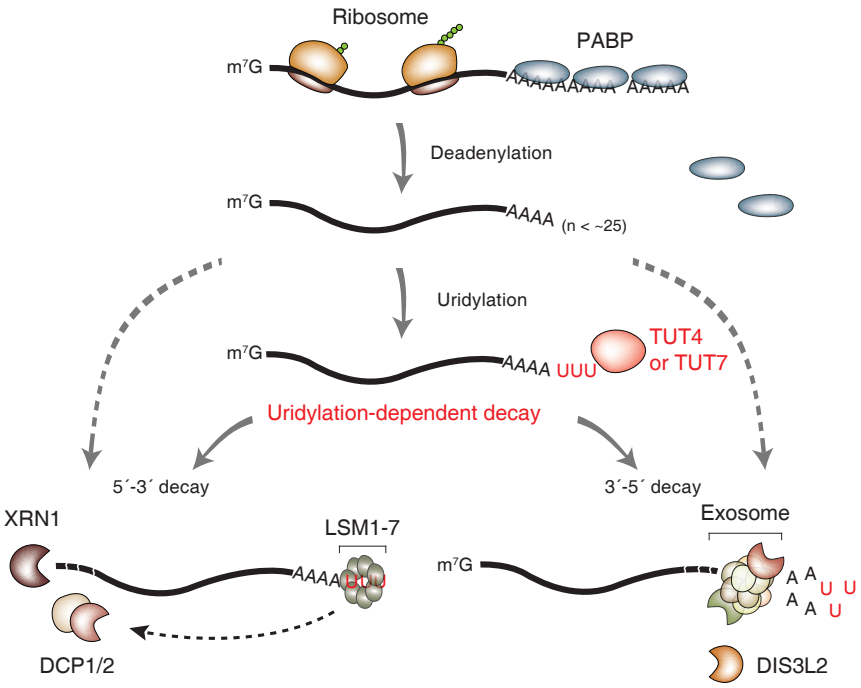

Figure 5. Uridylation-dependent mRNA decay in human. Upon deadenylation, mRNA lose PABP and instead gain a U tail by the redundant action of TUT4 and TUT7. The U tail is recognized by the downstream decay factors. The LSM1-7 complex binds to the U tail and facilitates decapping by the DCP1/2 complex. Decapped mRNAs are subject to degradation via the 5´-3´ exonuclease XRN1. Alternatively, the uridylated mRNA are degraded exonucleolytically by exosome or DIS3L2 from the 3´ end.

2. Results

2.1 Global distribution of mRNA poly(A) tail length during the MZT in vertebrates

To investigate how mRNA tailing is regulated at the genomic scale during the MZT, I applied TAIL-seq on zebrafish embryos[1]. I generated TAIL-seq libraries from six different developmental stages that span the MZT (Figure 6) [2](Kane & Kimmel, 1993). Fertilized 1-cell (0.2 hpf), 4-cell (1 hpf), and 64-cell (2 hpf) embryos cover the cleavage stages in which there is little transcription because de novo zygotic transcription initiates around 3 hpf (Harvey et al., 2013; Heyn et al., 2014; Kimmel et al., 1995). Sphere (4 hpf) embryo is at blastula stage, by which the first wave zygotic genes are transcribed (Lee et al., 2013). Shield (6 hpf) and 75%-epiboly (8 hpf) embryos are at gastrula stages, during which successive waves of transcriptional activation with increasing degree take place (Harvey et al., 2013).

Global distribution of poly(A) tail lengths showed that short poly(A) tails gradually increase during the cleavage stages presumably due to cytoplasmic polyadenylation since zygotic transcription is still inactive at these early stages (Figure 7). When the mRNA tags with poly(A) tails of 7-231 nt were plotted, the median lengths in global profile gradually increased from ~20 nt (0 hpf) to ~40 nt (4 hpf). I also found that conspicuous increase of longer portion [> 50 nucleotide (nt)] in poly(A) length occurs at sphere (4 hpf), possibly because newly transcribed mRNAs tend to have very long poly(A) tails (> 200 nt) after the onset of ZGA (Garneau et al., 2007). Even after ZGA, reads of short poly(A) tails

[1] All analyses in this section are carried out by Dr. Hyeshik Chang
[2] Zebrafish embryos are provided by Kyuwon Kim's lab

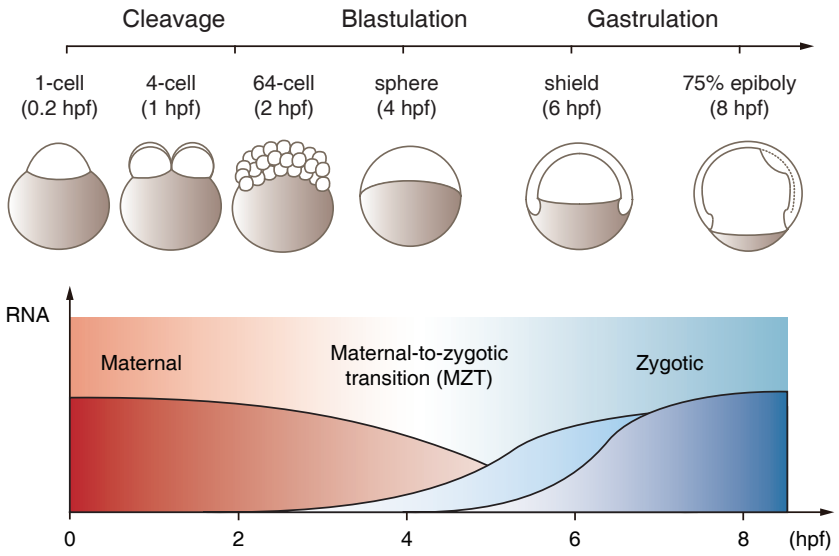

Figure 6. Illustration of zebrafish developmental stages examined in TAIL-seq analysis. Libraries were generated from 1-cell (0.2 hpf), 4-cell (1 hpf), 64-cell (2 hpf), sphere (4 hpf), shield (6 hpf), and 75%-epiboly (8 hpf) embryos. The graph depicts mRNA expression patterns during the MZT. The red curve represents the degradation profile of degraded maternal transcripts. The light and dark blue curves represent the minor and major waves, respectively, of ZGA.

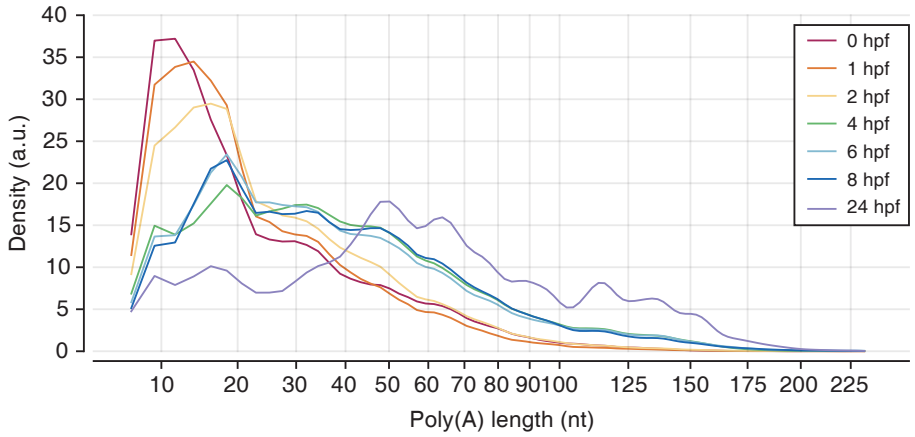

Figure 7. Global distribution of poly(A) tail lengths from six different developmental stages that span the MZT and at segmentation stage (24 hpf) in zebrafish. Poly(A) tail lengths from 7 nt to 231 nt are transformed by square root (x-axis) and the density was calculated by using kernel density estimation (band width = 0.07).

were still abundant, probably because a large fraction of maternally stored transcripts is still being degraded at this stage. This would result in much shorter median poly(A) length than that in mammalian somatic cell lines (~80 nt) (Chang et al., 2014). I confirmed that undifferentiated embryonic cells have different distribution of poly(A) tails from that of differentiated cells in zebrafish by carrying out TAIL-seq from zebrafish embryos at segmentation stage (24 hpf), when the somites develop and the primary organs begin to differentiate. TAIL-seq result showed that at segmentation stage, mRNAs with short poly(A) tails were already disappeared (Figure 7) and the poly(A) length distribution was similar with that of mammalian somatic cells (Chang et al., 2014). These results reveal that during the MZT, poly(A) tails are comprised of two different populations, with longer-tailed mRNAs under de novo synthesis and shorter-tailed mRNAs under maternal mRNA clearance; the distribution of poly(A) tail length is shifting from short tailed phase to long tailed phase along the course of differentiation after the MZT.

To confirm that global changes in poly(A) tail length during the MZT is conserved in vertebrates, I analyzed the distribution of poly(A) tails in *Xenopus* and mouse embryos. I generated TAIL-seq libraries from *Xenopus leav*is embryos at five different embryonic time points (Figure 8) [3]. The developmental stages examined include the cleavage stages (1-cell and 16-cell stage), early and late blastula stages (stage 7 and 9), and gastrula stage (stage12) (Nieuwkoop & Faber, 1994). In *Xenopus*, major zygotic transcription begins after twelve synchronous cell cycles (stage 8), which coincides with rapid decay of several hundred maternal mRNAs (Collart et al., 2014; Newport & Kirschner, 1982). Consistent with zebrafish embryos, global poly(A) length distribution of *Xenopus* shows that short poly(A) tails globally increase after fertilization, and the clear lengthening of poly(A) tails occurs after ZGA (Figure 9).

[3] Frog embryos are provided by Hosung Jung's lab

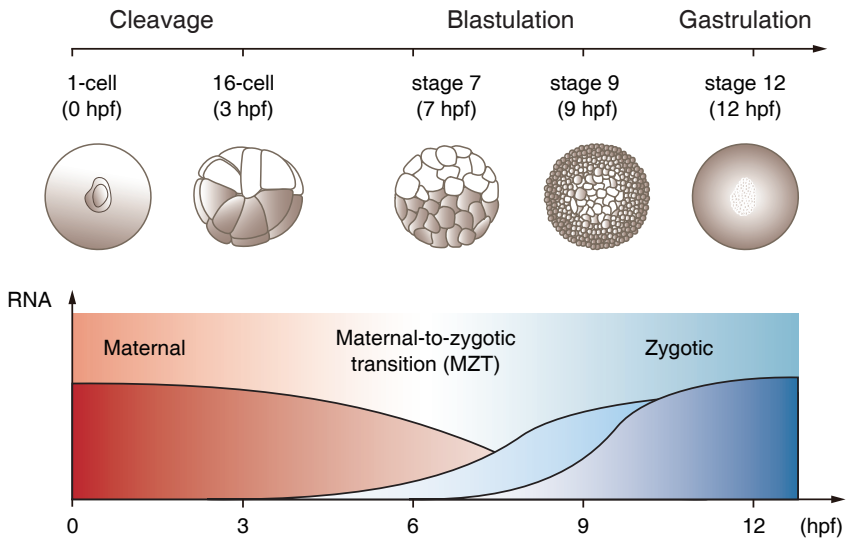

Figure 8. Illustration of *Xenopus* laevis developmental stages examined in TAIL-seq. Libraries were generated from 1-cell, 16-cell, stage 7, stage 9, and stage 12 embryos. In the graph, the red curve represents the degradation profile of maternal transcripts. The light and dark blue curves represent the minor and major waves, respectively, of ZGA.

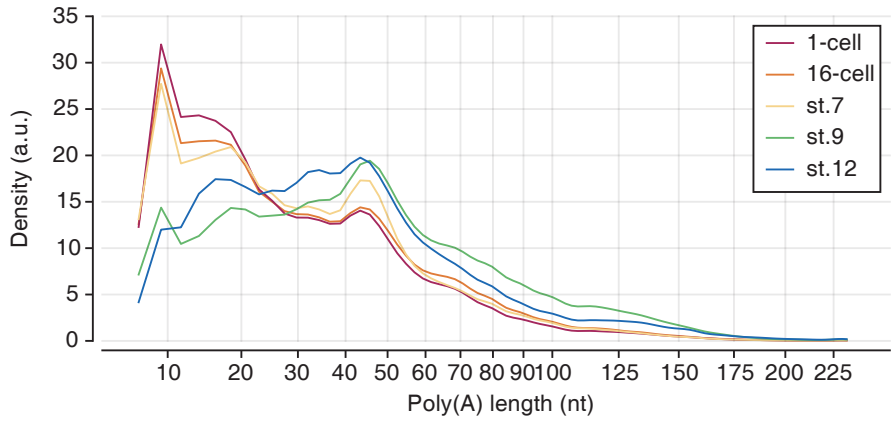

Figure 9. Global distribution of poly(A) tail lengths from five different developmental stages that span the MZT in *Xenopus laevis*. Poly(A) tail lengths from 7 nt to 231 nt are transformed by square root (x-axis) and the density was calculated by using kernel density estimation (band width = 0.07).

Unfortunately, it is difficult to prepare enough amount of total RNA from mouse embryo for TAIL-seq, which needs a large amount of RNA (~80 μg) for enough sequencing depth. Thus, I applied recently developed method, called mTAIL-seq, which uses splint ligation allowing enrichment of a specific type of terminus thereby increasing the sequencing depth even with small amount of input RNA (Lim et al., 2016). I carried out mTAIL-seq analysis using mouse embryos at four different time points, ranging from early 1-cell to the 8-cell stage (Figure 10) [4]. In mouse, the majority of maternal transcripts are degraded by the 2-cell stage and then the embryo exhibits two major waves of gene expression, including zygotic genome activation (ZGA) at the 2-cell stage and mid-preimplantation gene activation (MGA) at the 4-cell stage, although minor transcription wave begins at the late 1-cell stage (Hamatani et al., 2004; Park et al., 2013). I observed that relatively short poly(A) species of maternal transcripts globally increased between the early and late 1-cell stage, but after ZGA and MGA (the 2- and 8-cell stages), long poly(A) species remarkably increased probably due to the transcription-associated canonical polyadenylation (Figure 11).

Taken together, TAIL-seq analysis from vertebrate early embryos demonstrates that maternal transcripts, which are supplied in deadenylated state, are polyadenylated before the onset of ZGA, during which gene expression may be regulated by differential poly(A) tail length rather than mRNA stability. Subsequently, maternal mRNAs are rapidly degraded and zygotic transcription occurs in successive waves.

[4] Mouse embryos are provided by Macrogen inc. and mTAIL-seq libraries were generated by Dr. Jaechul Lim.

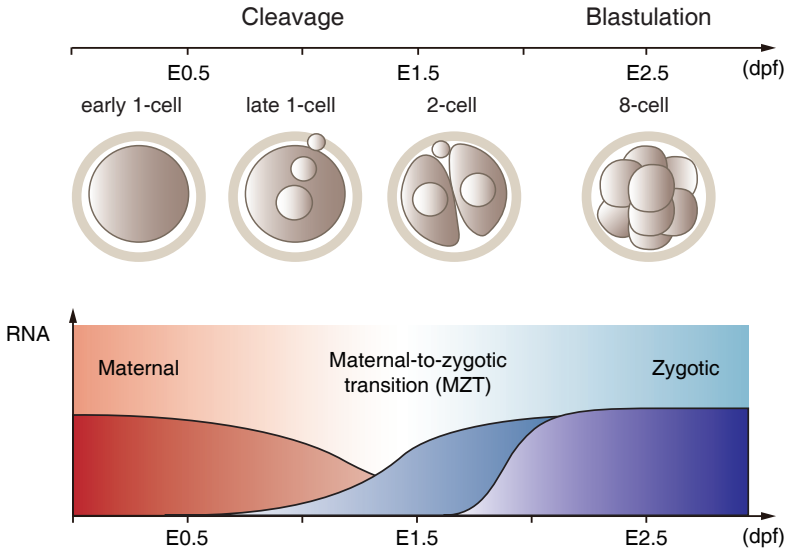

Figure 10. Illustration of mouse developmental stages examined in TAIL-seq. Libraries were generated from mouse embryos at early 1-cell, late 1-cell, 2-cell, and 8-cell stages. In the graph, the red curve depicts the maternal mRNA clearance. The blue and violet curves represent zygotic genome activation (ZGA) at the 2-cell stage and mid-preimplantation gene activation (MGA) at the 4-cell stage, respectively. X-axis represents the defined embryonic day of "day post fertilization" where E1 would indicate 1 day after fertilization.

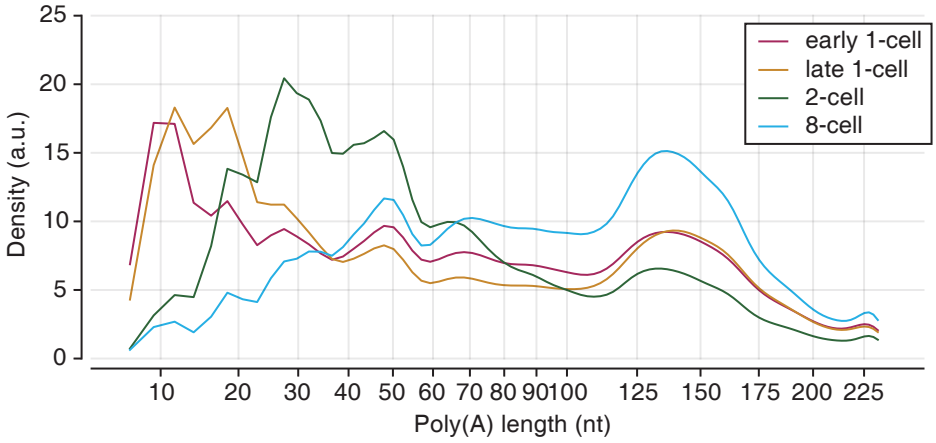

Figure 11. Global distribution of poly(A) tail lengths from four different developmental stages that span the MZT in mouse. Poly(A) tail lengths from 7 nt to 231 nt are transformed by square root (x-axis) and the density was calculated by using kernel density estimation (band width = 0.07).

2.2 Differential regulation of poly(A) tails during the MZT in zebrafish

During the MZT, the polyadenylation and deadenylation are regulated to allow the sequential translational control of maternal transcripts (Aanes et al., 2011). To analyze differential regulation of poly(A) tails at transcript level, I monitored poly(A) length changes of individual mRNAs from zebrafish TAIL-seq result (Figure 12A, The full list of poly(A) tail length changes are shown in Table 2). Expectedly, I found that poly(A) tail lengths are coordinated differently across mRNA species following fertilization. Generally, most of maternal mRNAs are initially in deadenylated forms, and their short poly(A) tails become gradually elongated until 4 hpf and then subsequently shortened at 6 hpf. However, individual genes show substantial variations in poly(A) tail lengthening, suggesting that maternal mRNAs are not polyadenylated at the same rate during early period of development. TAIL-seq enabled me to directly measure poly(A) length of individual genes and to reveal differential temporal dynamics of poly(A) tail length in a transcriptome-wide manner during early embryogenesis. Though previous studies revealed that cytoplasmic polyadenylation is a crucial mechanism that regulate translation of maternal mRNAs in early embryonic development, they could not directly identify the differential dynamics of poly(A) tails since they employed poly(A) enriched RNAs for genome-wide analysis (Aanes et al., 2011; Collart et al., 2014).

To examine transcriptome dynamics during the MZT, I profiled mRNA abundance changes at transcript level by using poly(A) tag count from TAIL-seq analysis in zebrafish. Following fertilization, mRNA abundance was largely unchanged until 4 hpf, indicating that most of maternally deposited mRNAs remain stable at these early stages (Figure 12B). A large fraction of maternal mRNAs was degraded rapidly between 4 and 6 hpf, whereas a

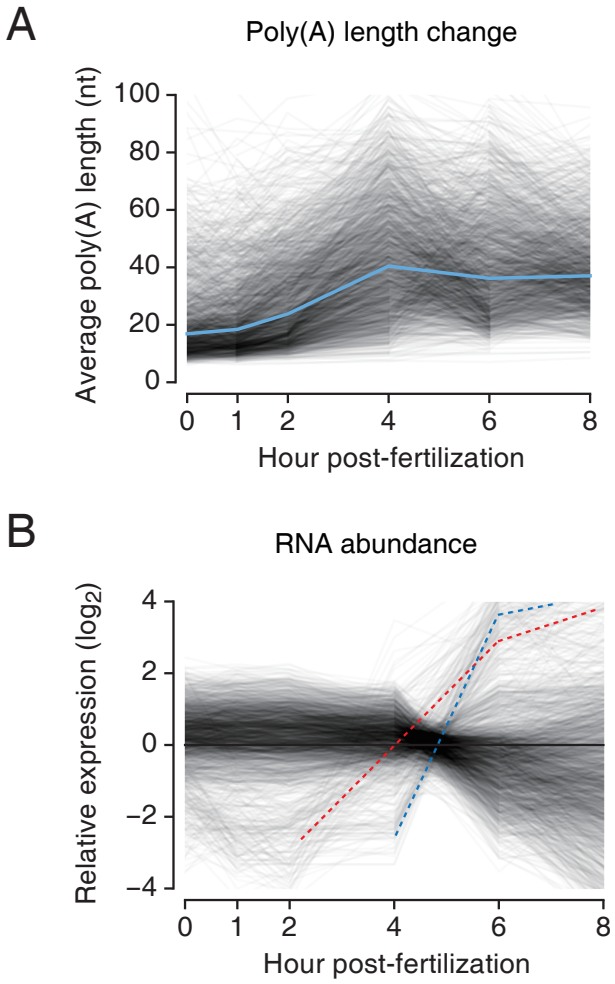

Figure 12. Poly(A) tail length changes (A) and RNA abundance changes (B) ofindividual transcripts in zebrafish. Each line represents a transcripts with ≥30 reads in at least four samples. In Fig. 12A, the light blue line represents the median poly(A) length. In Fig. 12B, the red and blue lines represent the first wave zygotic genes and subsequent wave genes, respectively.

small fraction of them was destabilized at earlier stage. Consistent with previous studies, newly expressed genes are also temporally regulated during the MZT (Harvey et al., 2013; Lee et al., 2013). TAIL-seq showed that the first-wave genes commence the transcription between 2 and 4 hpf (Figure 12B, red line), whereas the majority of zygotic genes initiate their expression after 4 hpf (Figure 12B, blue line).

To analyze the relationship between poly(A) length change with mRNA abundance change of individual transcripts, I classified mRNAs into three groups based on the expression pattern: maternal-only genes, maternal-zygotic genes, and zygotic-only genes (Figure 13). Maternal-only genes are largely stable in early time points and are degraded mostly between 4 and 6 hpf. Poly(A) tails of these transcripts are globally increased until 4 hpf and subsequently shortened, corresponding to the global degradation of maternal transcripts between 4 and 6 hpf. This points out that maternal mRNAs are cleared by deadenylation-mediated decay pathway during the MZT. The majority of genes expressed in the early embryos are both maternally and zygotically expressed (maternal-zygotic genes) and relatively unchanged during the MZT. These mRNAs are also polyadenylated gradually with higher levels than that of maternal-only genes, indicating that newly transcribed mRNAs have longer poly(A) tails. A few genes that are only zygotically expressed (zygotic-only genes) also have relatively long poly(A) tails after the onset of ZGA.

Typically, most maternal mRNAs are subject to cytoplasmic polyadenylation following fertilization with different temporal dynamics. For example, maternal mRNAs encoding transcription factors such as nanog, pou5f3, sox19b and sox11b were rapidly polyadenylated after fertilization indicating their early embryonic function (Figure 14A). Notably, maternal nanog transcripts exhibited relatively long poly(A) tails immediately after fertilization. Indeed, previous study revealed that nanog, pou5f1 and sox19b transcripts are highly translated before ZGA and are important for the initiation of ZGA in zebrafish (Lee et al.,

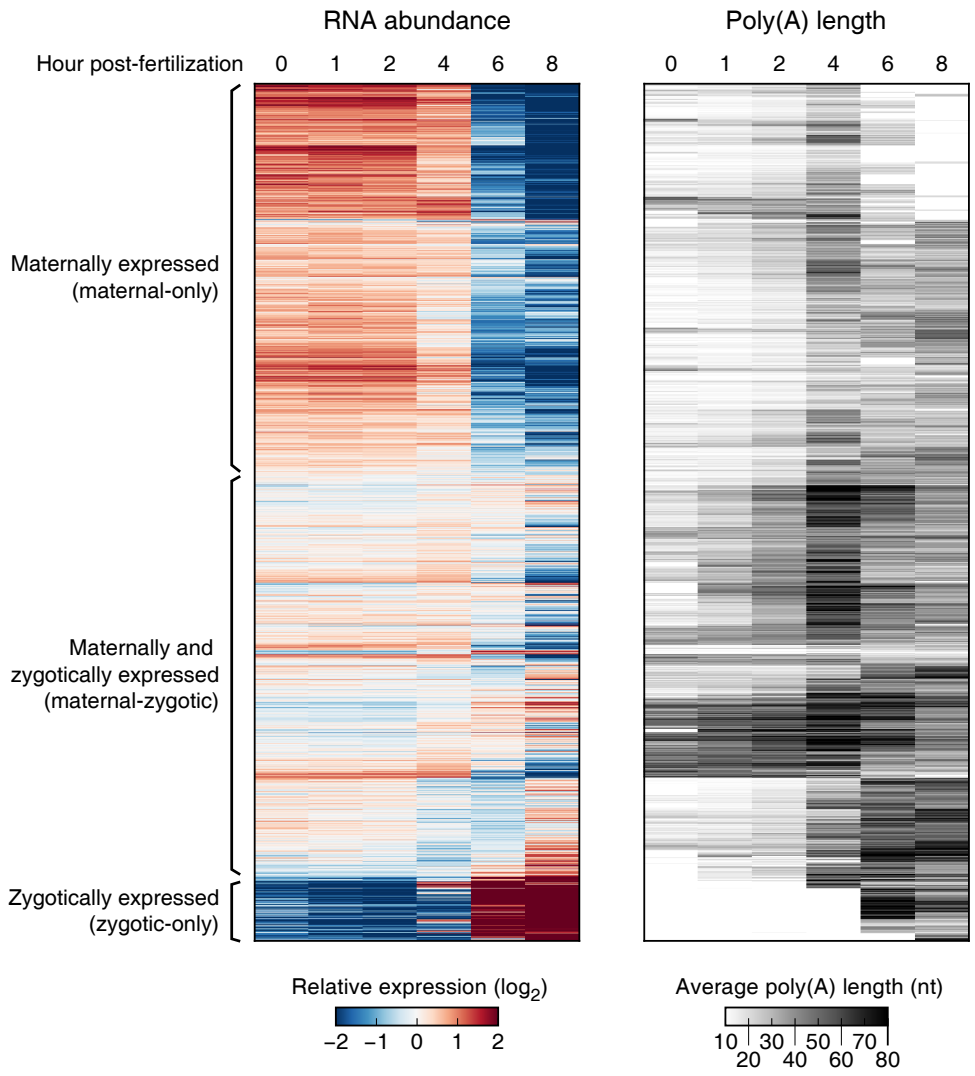

Figure 13. Relationship between mRNA abundance change (left) and poly(A) length change (right) of individual transcripts. mRNAs are classified into 3 groups based on the expression pattern: only maternally expressed genes, maternally and zygotically expressed genes, and only zygotically expressed genes. Each line represents a transcript with ≥50 reads in at least two samples.

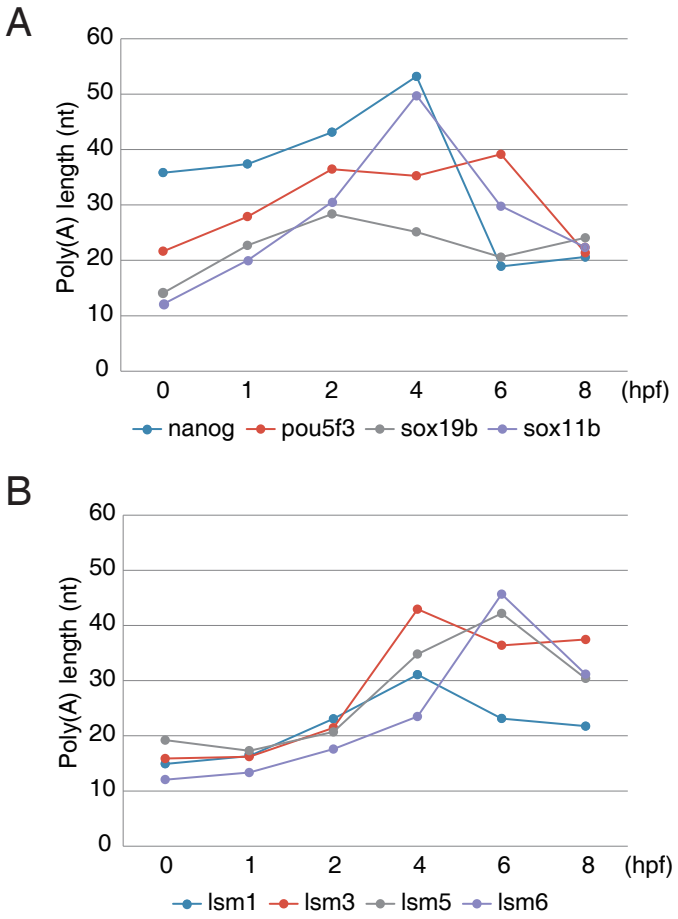

Figure 14. Examples of individual genes that show differential polyadenylation in zebrafish. (A) Maternal mRNAs encoding sequence-specific transcription factors such as nanog, pou5f3, sox19b and sox11b were rapidly polyadenylated after fertilization. (B) mRNAs encoding components of Lsm complex showed relatively delayed polyadenylation. The mean poly(A) length of each gene is presented in each graph.

2013). In addition, transcription factor sox11, which is one of the members of the SOXC family having an essential role in early vertebrate development (Klein & Moody, 2015), is highly polyadenylated soon after fertilization. On the contrary, some groups of genes were slowly polyadenylated after fertilization, indicating delayed translation activation. For example, mRNAs encoding components of Lsm complex, which functions in promoting the decapping of deadenylated mRNAs (Tharun et al., 2000), showed relatively delayed polyadenylation with a maximum level of poly(A) length after 4 hpf (Figure 14B).

There are, however, some mRNAs that are rapidly deadenylated or remained unchanged with their short poly(A) tails after fertilization (Figure 15), suggesting translational inactivation of these genes that perhaps have specific functions only in oocytes. Oocyte-specific genes may not only be unnecessary, but also detrimental to early embryonic development after fertilization. One example is maternal mRNA encoding siaz-interacting nuclear protein (sinup) that is markedly deadenylated following fertilization. Previously, overexpression of sinup resulted in abnormal expression of dorso-ventral patterning genes such as fgf8 and wnt8 during gastrulation and consequently caused developmental defects, suggesting that sinup expression should be tightly regulated during early embryonic development (Ro et al., 2005). In addition, overexpression of both uhrf1 and dnmt1, which are deadenylated after fertilization, resulted in significant defects during gastrulation in zebrafish embryos (Chu et al., 2012; Kent et al., 2016). Likewise, abundant oocyte-specific transcripts such as mos, aurka and kif11 are in deadenylated states and maintain their short poly(A) tails after fertilization (Figure 15B). In previous studies, these mRNAs are specifically regulated in oocytes, but not during early development (Legagneux et al., 1992; Suzuki et al., 2009; Paris & Philippe, 1990). These results suggested that oocyte-specific mRNAs should be translationally inactivated after fertilization, otherwise are detrimental to early embryogenesis.

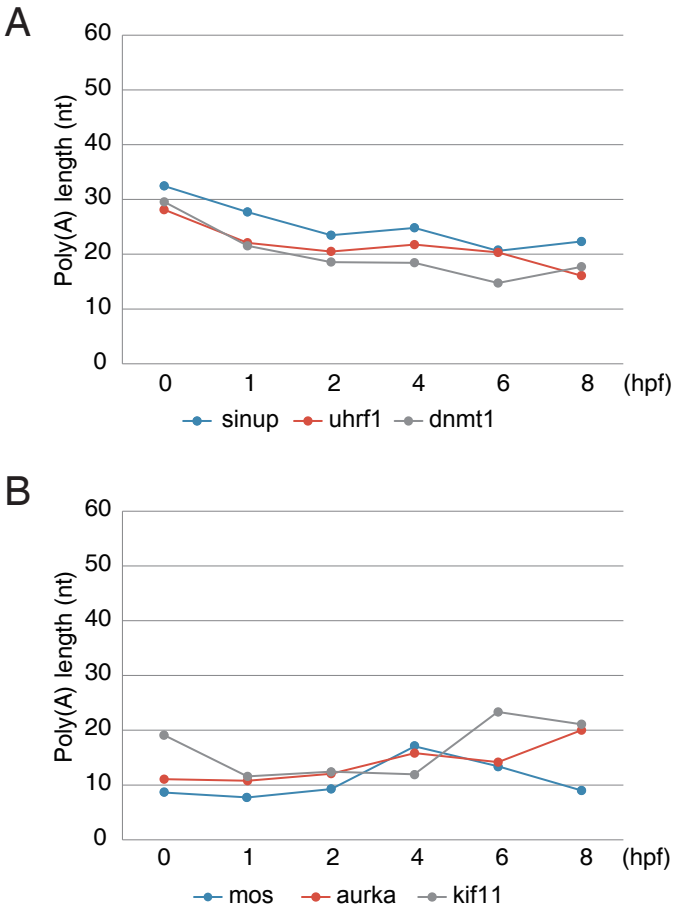

Figure 15. Examples of individual genes that show differential regulation of poly(A) tails in zebrafish. Oocyte-specific maternal transcripts are rapidly deadenylated (A) or remain unchanged with short poly(A) tails (B) after fertilization. The mean poly(A) length of each gene is presented in each graph.

Furthermore, by analyzing the ribosome profiling data that was previously published from other group (Subtelny et al., 2014), I confirmed the global correlation between poly(A) length from TAIL-seq analysis and translation efficiency before and during the MZT (2 hpf and 4 hpf). The correlation then disappeared at gastrulation stage (6 hpf) (Figure 16), in coherent with reported PAL-seq result (Subtelny et al., 2014). This result reveals that maternal transcripts undergo translational control through coordinated polyadenylation and deadenylation following fertilization whereas after gastrulation begins, translational efficiency is uncoupled from poly(A) tail length.

In conclusion, early embryos establish differential poly(A) length change depending on mRNA species in the absence of zygotic transcription, generating the temporal regulation of maternal gene expression. Subsequently, maternal mRNAs are rapidly deadenylated and degraded, which is accompanied with the major zygotic transcription and uncoupling of poly(A) length and translational efficiency.

2.3 Uridylation is induced simultaneously with maternal mRNA clearance during the MZT in vertebrates

Next, I asked whether zebrafish mRNAs have modifications at the 3′ end of poly(A) tails as described in mammalian somatic cells (Chang et al., 2014). Previously, TAIL-seq analysis discovered that the majority of mRNAs are subject to uridylation at the downstream of poly(A) tails and the oligo-U-tails are found mainly in short poly(A) mRNAs in both NIH3T3 and HeLa cells (Chang et al., 2014). Further study aiming at providing the action mechanism revealed that uridylation has a general role in mRNA degradation, accelerating the decay of deadenylated mRNAs (Lim et al., 2014). Considering that the MZT is one of

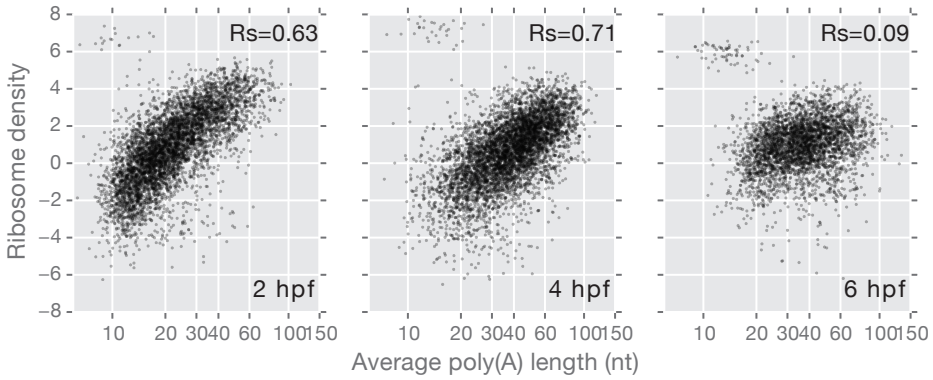

Figure 16. Comparison of poly(A) tail length with translational efficiency (TE) which was estimated by Subtelny *et al.* (Subtelny et al., 2014) during the MZT in zebrafish. Rs refers to Spearman correlation coefficient.

the biological contexts where global mRNA decay is required, uridylation may be involved in maternal mRNA clearance during the MZT.

Interestingly, I found that there is dramatic induction of 3′ uridylation of poly(A) tails during the MZT in zebrafish, whereas other modification is nearly unchanged (Figure 17). Average uridylation count (average U length per tail) is the sum of the number of all uridine residues on poly(A) tails divided by the total number of reads with poly(A) tails. Consistent with mammalian cells, U-tails are found mainly in mRNAs with short poly(A) tails (5-25 nt), indicating that uridylation occurs following deadenylation. Uridylation of short poly(A) tails is very low at pre-ZGA stages, but it increases remarkably after 2 hpf, coinciding with global degradation of maternal transcripts. This suggests that maternal mRNA clearance may be promoted by uridylation-mediated decay pathway.

Recent study applying TAIL-seq to early fly embryos showed that uridylation frequency in *Drosophila* is much lower than that in mammal cells, indicating that uridylation may play a limited role in invertebrates (Lim et al., 2016). To address whether the induced uridylation of mRNAs during the MZT is evolutionarily conserved in vertebrates, I additionally investigated genome-wide mRNA uridylation in *Xenopus* and mouse embryos. Surprisingly, I found that uridylation of short poly(A) tails dramatically increases, coinciding with the maternal mRNA clearance in both mouse and *Xenopus* (Figure 18), Because short poly(A) tails are preferentially uridylated, average uridylation is shown for short poly(A) tail range (5-25 nt)). Although mTAIL-seq method tends to underestimate the end modification of mRNAs (Lim et al., 2016), I could detect that mRNA uridyaltion significantly increases between the late 1-cell and 2-cell stage of mouse embryos. In *Xenopus*, there is a huge increase of uridylation between the stage 7 and 12, while the other type of modification remained unchanged. On the contrary, I could not detect up-regulation of uridylated mRNAs during the MZT in fly embryos (data not shown). These results

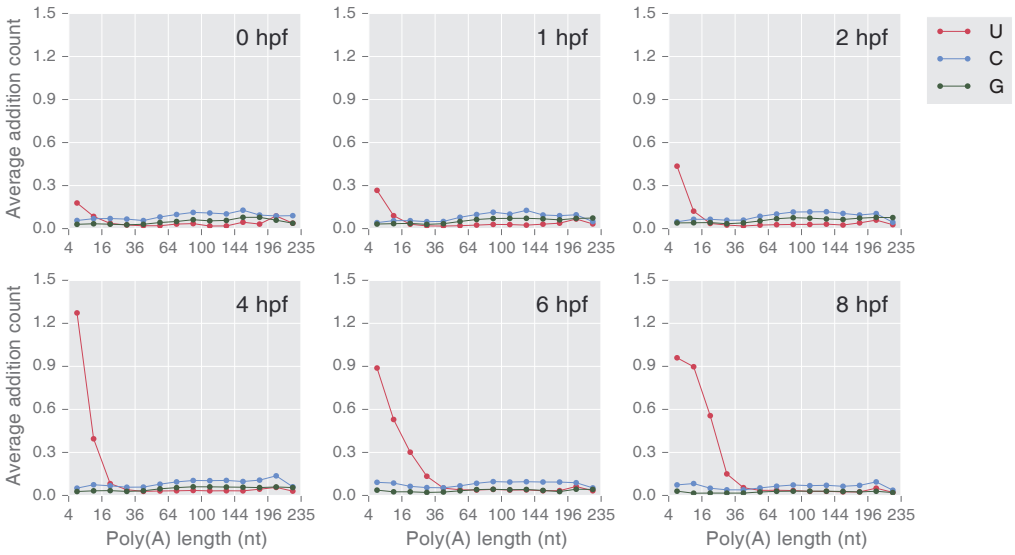

Figure 17. Dramatic increase in uridylation of short poly(A) tails during the MZT in zebrafish. Average addition count (y-axis) is mean length of consecutive non-A tails following poly(A) tails, which is the sum of the number of all modifications apart from adenylation on poly(A) tails divided by the total number of reads with poly(A) tails.

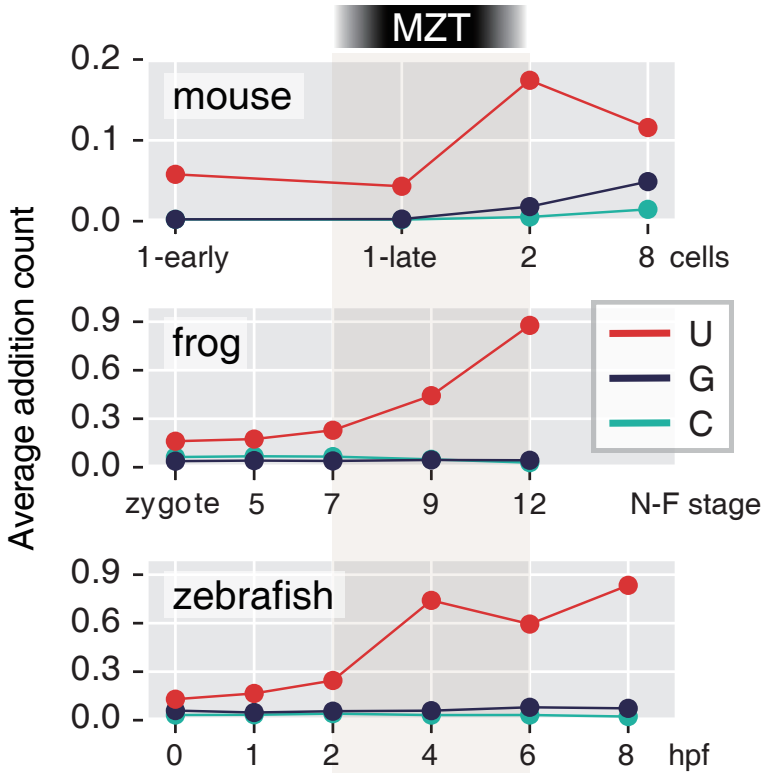

Figure 18. Uridylation on short poly(A) tails (5-25 nt) is induced simultaneously with maternal mRNA clearance in vertebrates. In zebrafish, uridylation reaches about 0.7 at 4 hpf, which means 7 out of 10 short poly(A) tails were uridylated.

demonstrate that induced mRNA uridyation during the MZT is evolutionarily conserved in vertebrates but not in invertebrates and that maternal mRNAs may be degraded via uridylation-dependent decay pathway in early vertebrate embryos.

2.4 TUT4 and/or TUT7 catalyze mRNA uridylation in zebrafish and *Xenopus* embryos

Recent studies revealed that TUT4 (also known as Zcchc11) and TUT7 (also known as Zcchc6) have highly similar domain organization and act redundantly in mRNA uridylation as well as miRNA uridylation in human cells (Heo et al., 2012; Lim et al., 2014). To identify enzymes responsible for mRNA uridylation in early embryos, I searched the candidates among the list of non-canonical nucleotidyl transferases including TUT4 and TUT7 (Figure 19). Fortunately, I found that zebrafish and *Xenopus* have close orthologs of human TUT4 and TUT7. In addition, a previous study discovered *Xenopus* TUT7 as mRNA uridylation enzyme in oocytes, in which TUT7 has a role in translation repression of polyadenylated RNAs (Lapointe & Wickens, 2013). Therefore, I examined whether TUT4 and TUT7 are responsible for mRNA uridylation in early embryos by performing knockdown (KD) experiments followed by TAIL-seq.

To transiently deplete a particular protein in embryo system, synthetic oligonucleotides, called morpholinos (MOs), are widely used (Eisen & Smith, 2008; Heasman et al., 2000; Nasevicius & Ekker, 2000). MOs are chemically modified oligos, about 25 nt length, with antisense complementarity to target RNAs. Two types of MOs are commonly used to inhibit the protein expression: translation blocking (TB) MOs and splicing blocking (SB) MOs. TB MOs are designed to bind to start codon (AUG) region and act by blocking the

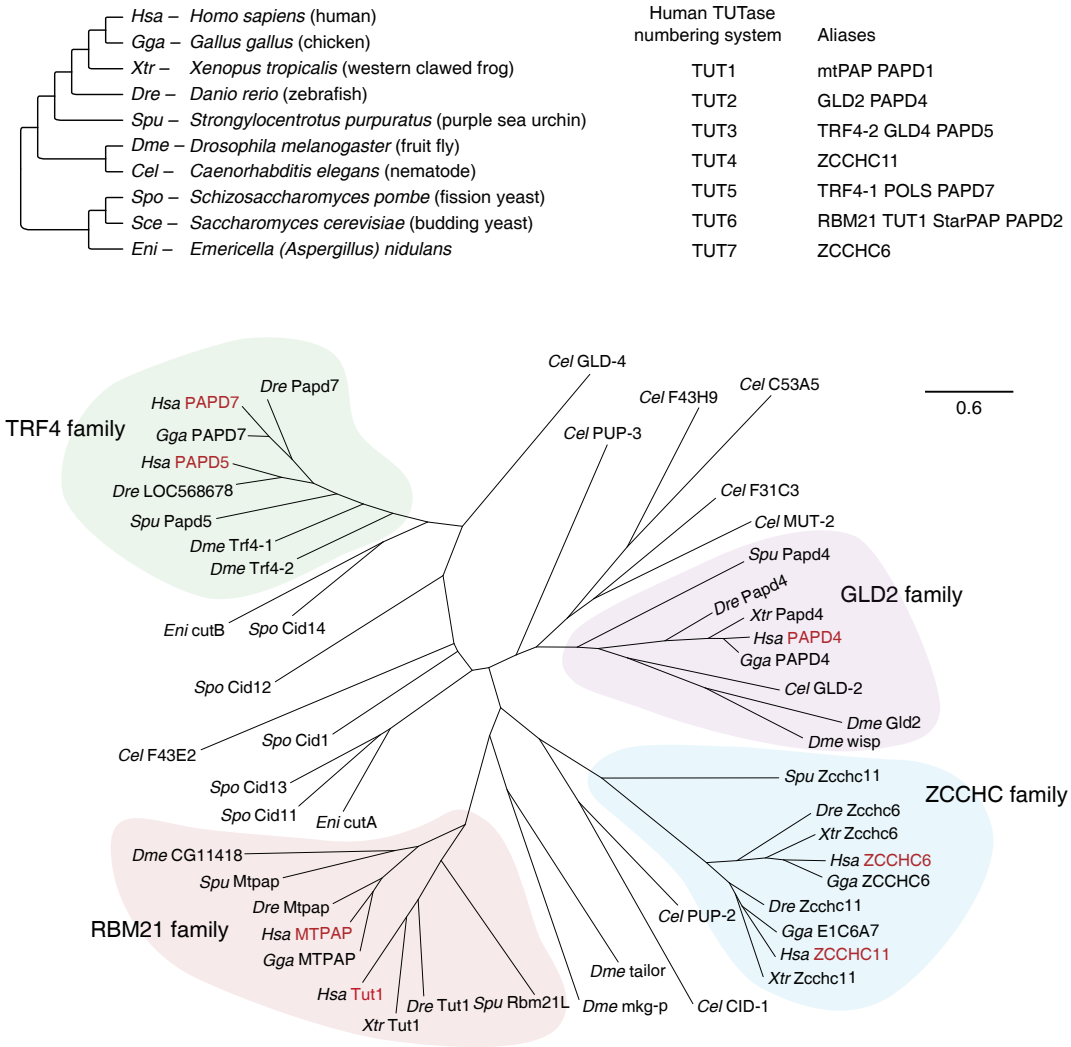

Figure 19. Phylogenetic tree of TUTase homologs in metazoan species. Human TUTases are shown in red labels. The families were grouped according to Minasaki and Eckmann (Minasaki & Eckmann, 2012).

translation initiation of mature mRNA. SB MOs are complement to splicing junction sites of pre-mRNAs and interfere with the RNA splicing procedure. MOs are injected into the yolk or cytoplasm of 1-cell stage embryo, and therefore could equally affect every cell in the developing embryo. Inside the embryo MOs bind to target RNAs, preventing translation or splicing of them.

I first injected splicing blocking (SB) MOs against TUT4 and TUT7 together into fertilized 1-cell zebrafish embryos and checked the knockdown efficiency using qPCR analysis from control MO or TUT4/7 SB MO-injected embryos (morphants) at 4, 6 and 24 hpf (Figure 20) [5]. At 24 hpf, expression levels of TUT4 and TUT7 decreased in TUT4/7 morphants, whereas until 6 hpf, it remained largely unchanged in TUT4/7 morphants compared to control morphants. Moreover, I found that uridylated short A tails greatly reduced at 24 hpf, while at 3 and 6 hpf, it remained nearly unaffected in TUT4/7 morphants compared to control morphants (Figure 21). Since SB MOs inhibit only the newly transcribed pre-mRNA but not maternally provided mature mRNAs, these results could be attributed to the function of maternally deposited TUT4/7 during the MZT. Consistently, previous study revealed that TUT4 or TUT7 SB MO resulted in developmental defects only after 24 hpf, and the majority of morphants died after 5 day post fertilization (dpf) (Thornton et al., 2014). Therefore, the lack of earlier phenotypes implies that in early embryos (before 6 hpf), the functions of TUT4/7 are derived from maternally deposited mRNAs.

To address this question, I injected AUG-targeting translation blocking (TB) MOs of TUT4 and TUT7 into fertilized 1-cell zebrafish embryos to knockdown maternally deposited TUT4 and TUT7 mRNAs, and then measured uridylation level of poly(A) tails in control and TUT4/7 morphants using TAIL-seq (Figure 22A). I checked the KD

[5] In collaboration with Jungkyun Kim

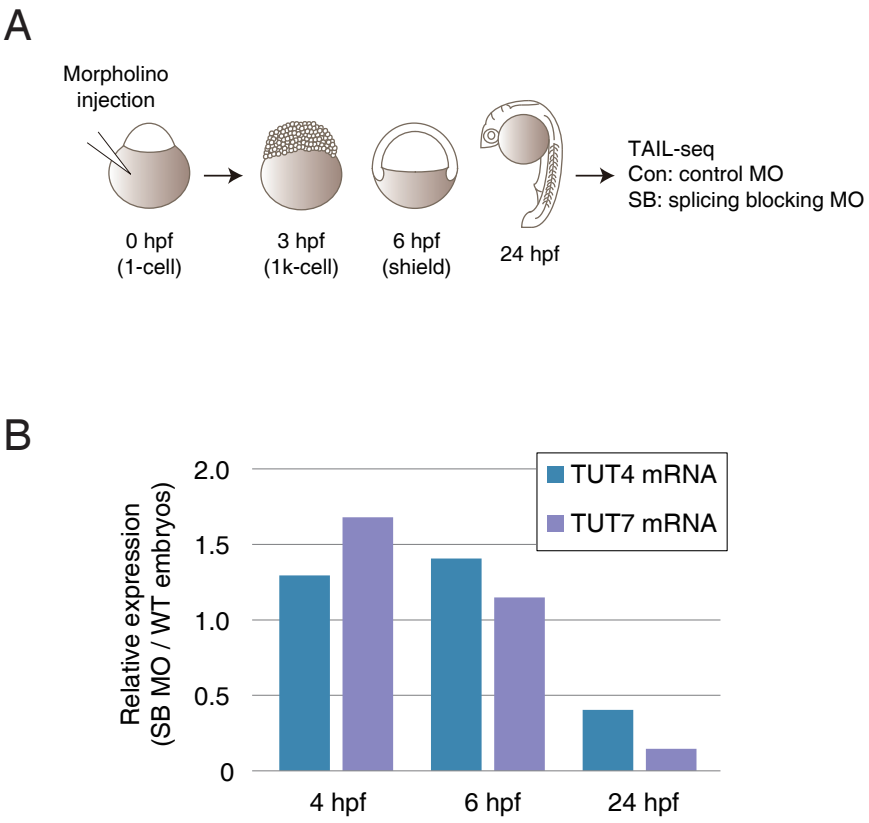

Figure 20. TUT4/7 splicing blocking (SB) MO injection in zebrafish. (A) The experimental scheme. Following TUT4/7 SB MOs injection into fertilized 1-cell embryos, TAIL-seq was performed from embryos at 3, 6 and 24 hpf. (B) The level of MO-targeting region of TUT4/7 mRNAs after injection of TUT4/7 SB MO in zebrafish embryos, measured by qRT-PCR.

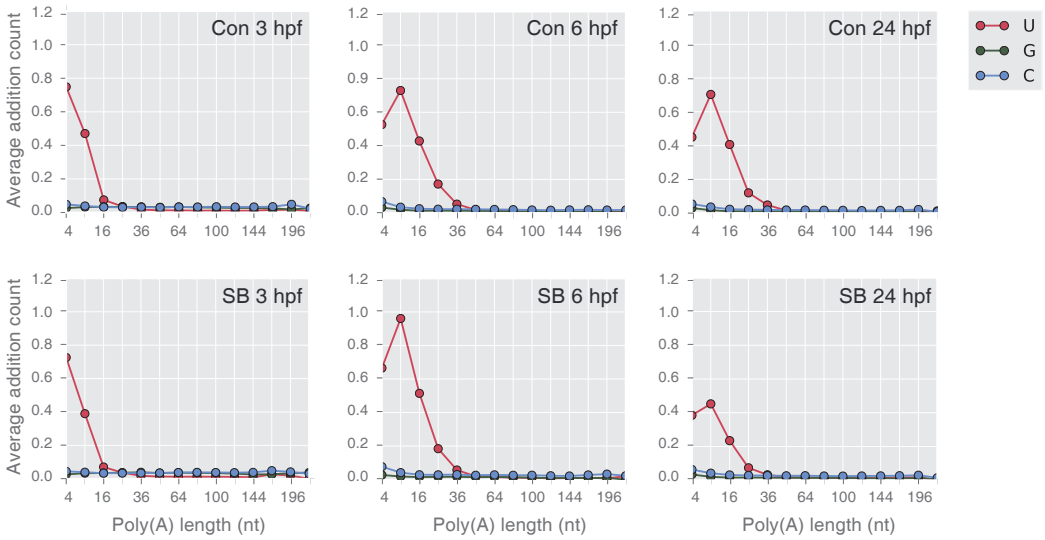

Figure 21. Average 3´ end modification measured by TAIL-seq following TUT4/7 SB MO injection. Uridylated short A tails greatly reduced at 24 hpf, while at 3 and 6 hpf, it remained nearly unaffected in TUT4/7 morphants compared to control morphants.

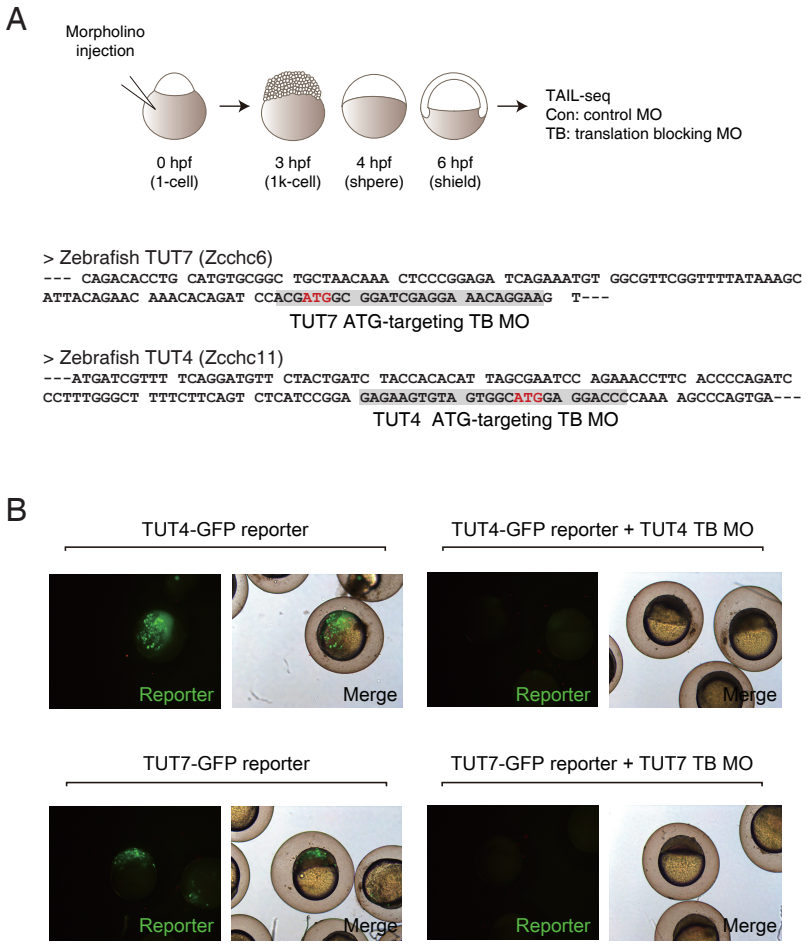

Figure 22. TUT4/7 translation blocking (TB) MO injection in zebrafish. (A) The experimental scheme (top) and design of TUT4 and TUT7 TB MOs that bind to start codon (AUG) region of TUT4 and TUT7, respectively (bottom). Following TUT4/7 TB MOs injection into fertilized 1-cell embryos, TAIL-seq was performed from embryos at 3, 4, and 6 hpf. (B) Validation of MO efficiency by co-injecting GFP reporters that include TB MO binding sites with TB MOs. When GFP reporter was co-injected with TUT4 and TUT7 TB MOs, respectively, GFP expressions were significantly reduced at 6 hpf, compared to TB MO only injected embryos.

efficiency of TB MOs using GFP reporters that have TUT4 or TUT7 TB MO binding site since there were no available antibodies against zebrafish TUT4 and TUT7 (Figure 22B). When embryos were co-injected with TUT4 and TUT7 TB MOs, average uridylation was significantly reduced between 3 and 6 hpf, compared to control morphants (Figure 23). This result indicates that maternal TUT4 or TUT7 mRNAs are required for mRNA uridylation during the MZT in zebrafish. I also performed knockdown of TUT4 and TUT7 with TB MOs in *Xenopus laevis* embryos[6]. Because *Xenopus laevis* genome, which is tetraploid, has two copies of genes encoded in long (L) or short (S) forms of chromosome (Bisbee et al., 1977; Session et al., 2016), I designed two types of AUG-targeting TB MOs against TUT4 (TUT4L and TUT4S) and TUT7 (TUT7L and TUT7S), respectively (Figure 24A). When I injected TUT4 and TUT7 TB MOs together into fertilized frog embryos, I found that uridylation was substantially reduced during the MZT in TUT4/7 morphants compared to control morphants (Figure 24B). Taken together, I concluded that maternally derived TUT4 or TUT7 transcripts are necessary for mRNA uridylation during the MZT in both zebrafish and *Xenopus* embryos.

2.5 Uridylation activity of TUT4 and/or TUT7 is required for the progression of early embryonic development

To investigate the role of TUT4 and TUT7 in the progression of early development, I analyzed morphological phenotype upon TUT4 and/or TUT7 knockdown in zebrafish embryos. Remarkably, I found that TUT4 and/or TUT7 TB MO treated zebrafish embryos showed delayed epiboly, a major cell movement during gastrulation (Figure 25) [7]. TUT7

[6] In collaboration with Dr. Hyunjun Kim
[7] In collaboration with Jungkyun Kim

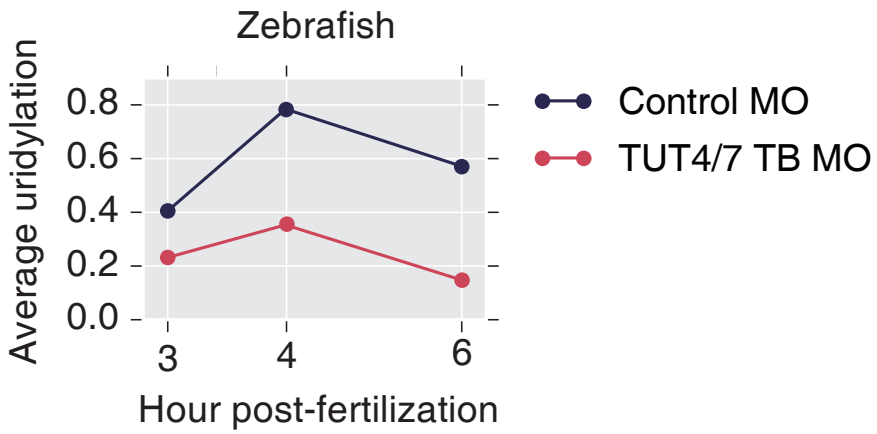

Figure 23. Average uridylation count upon TUT4/7 TB MO injection in zebrafish. Uridylation on short poly(A) tails (5-25 nt) was significantly reduced between 3 and 6 hpf upon TUT4/7 TB morphants, compared to control morphants.

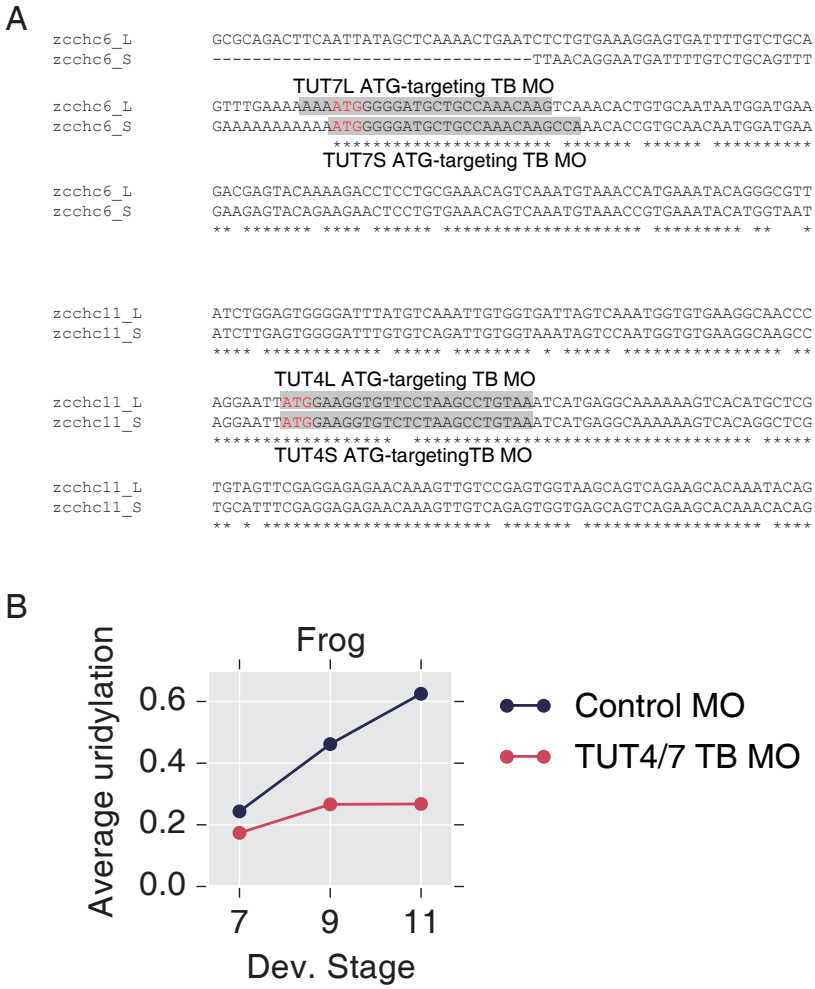

Figure 24. TUT4/7 TB MO injection in *Xenopus laevis*. (A) Design of *Xenopus* TUT4/7 AUG-targeting TB MOs (B) Average uridylation upon TUT4/7 knockdown. Following TUT4/7 TB MOs injection into fertilized 1-cell embryos, TAIL-seq was performed from embryos at stage 7, 9 and 11. Uridylation on short poly(A) tails (5-25 nt) was significantly reduced between stage 7 and 11 in TUT4/7 TB morphants, compared to control morphants.

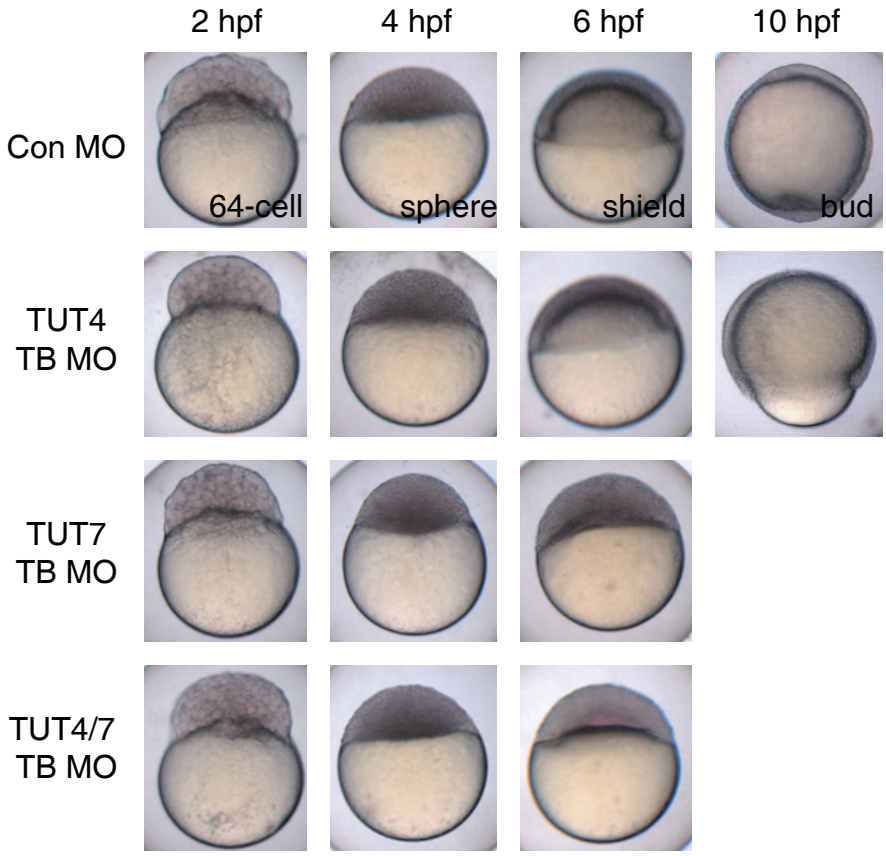

Figure 25. Developmental defects of TUT4 and TUT7 TB MOs at the indicated time points in zebrafish. TUT4 and TUT7 knockdown caused the epiboly block during late (~10 hpf) and early (~4 hpf) gastrulation, respectively.

single KD and TUT4/7 double KD resulted in developmental arrest at sphere stage (4 hpf) with 100% of the MO-injected embryos failing to initiate epiboly. This phenotype was highly reproducible in all experiments. From TAIL-seq result, I noticed that TUT4/7 double KD resulted in decreased level of uridylation at 1 k-cell (1,000-cell) stage (3 hpf) (Figure 23), preceding the morphological arrest at sphere stage (4 hpf). As compared with the defect of TUT7 MO, however, TUT4 MO caused milder phenotype in terms of timing of developmental arrest. Most TUT4 morphants were morphologically similar to control embryos until shield stage (6 hpf), but did not progress to late epiboly stage (Figure 25). In several experiments, I observed that TUT4 MO-injected embryos were developmentally delayed in late epiboly stage and eventually failed to complete the gastrulation. These results suggest that TUT4 and TUT7 may have different expression patterns or different functions in early embryos since they failed to compensate for the phenotypes of each other.

When I measured uridylation rate of TUT4 and/or TUT7 morphants at 4 hpf, I found that TUT7 single KD resulted in noticeable depletion of uridylation level while TUT4 morphants showed largely unchanged uridylation frequency at 4 hpf with only slightly decreased level compared to control (Figure 26). This result indicates that TUT7 may act dominantly in mRNA uridylation before 4 hpf and the degree of depleted uridyltaion level may be related with the associated phenotype caused by MOs. Nevertheless, uridylation was more clearly depleted in TUT4/7 double morphants than TUT7 single morphants, suggesting that TUT4 has an additive role in uridylation with TUT7 during the MZT.

To determine whether the developmental defect is caused by the impaired uridylation activity, I performed a rescue experiment by co-injecting TUT4 or TUT7 mRNAs with TUT4 or TUT7 TB MOs, respectively. Previous report revealed that a C-terminal half of TUT7, which contains an active catalytic motif, is sufficient for the catalytic activity

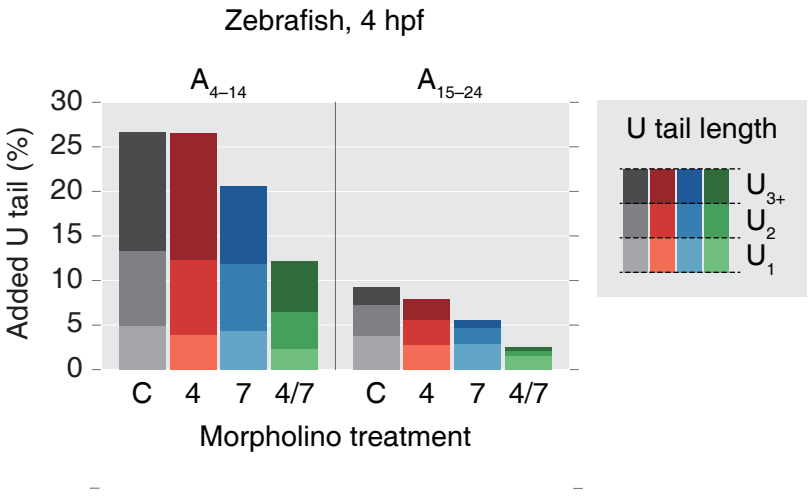

Figure 26. Uridylation frequency measured by TAIL-seq following TUT4/7 double and individual KD at 4 hpf in zebrafish embryos. Frequency of added U tail (y-axis) is the fraction of uridylated reads among the total number of mRNA reads with short (15-24 nt) and very short poly(A) tail (4-14 nt). Combination of TUT4 and TUT7 TB MO has a synergistic effect on the inhibition of uridylation activity although TUT7 acts dominantly in mRNA uridylation before 4 hpf in zebrafish.

(Lapointe & Wickens, 2013; Lim et al., 2014). Accordingly, I generated C-terminal half TUT4 and TUT7 mRNAs that lack the MO-binding site by in-vitro transcription and co-injected them with the TB MOs into 1-cell embryos (Figure 27). Zebrafish TUT4 and TUT7 mRNAs could only partially rescue developmental defects of TUT4 and TUT7 MO, respectively. Comparing to 100% occurrence of developmental defect by TUT4 or TUT7 MO alone, co-injection with TUT4 or TUT7 mRNA slightly rescued the epiboly defect by 16 or 19%, respectively. Unfortunately, the embryos that are rescued with TUT7 mRNAs failed to complete the gastrulation and eventually died although they could initiate the epiboly movement.

To further validate the role of TUT4 and TUT7 in early embryonic development, I analyzed morphological phenotype upon injection of TUT4 and TUT7 AUG-targeting TB MOs into *Xenopus* embryos. Compared with control embryos, TUT4/7 double morphants showed typical gastrulation defective phenotypes such as failure in blastopore closure (Figures 28A and B) and convergent extension defects (Figures 28C and D)[8]. Embryos with severe gastrulation defect often died at the onset of neurulation at stage 14 (data not shown), while most of the surviving morphants showed kinked and shortened axis that are the hallmarks of convergent extension defect during gastrulation (Figure 28C and D). In individual KD experiments of TUT4 and TUT7, both TUT7L and TUT7S MO caused gastrulation defects while TUT4 morphants were normally developed (Figure 29A). In addition, TUT4/7 double KD caused less blastopore closure defect compared to TUT7 single KD (Figure 29B), suggesting that the gastrulation defects caused by TUT4/7 knockdown is mainly due to the loss of TUT7 function.

To examine whether the degree of depleted uridylation level correlated with the associated phenotype caused by MOs in *Xenopus*, I measured uridylation frequency in the

[8] In collaboration with Dr. Hyunjun Kim

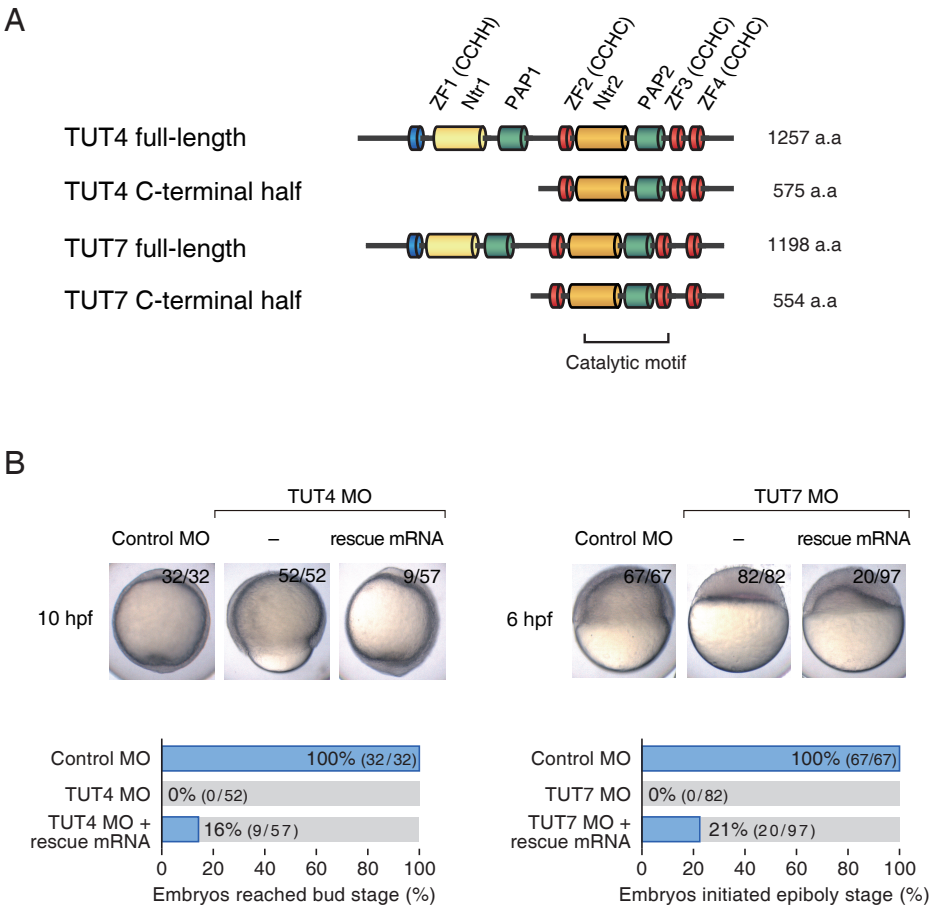

Figure 27. TUT4 and TUT7 mRNA partially rescue epiboly defects caused by TUT4 and TUT7, respectively. (A) Domain organization of full-length and C-terminal half of zebrafish TUT4 and TUT7. Yellow, nucleotidyl transferase domain; green, PAP-associated domain; light yellow, inactive nucleotidyl domain due to sequence variations; blue, C2H2 zinc finger; red, CCHC zinc finger domain. (B) Rescue of the phenotype by exogenous C-terminal half of TUT4 and TUT7 mRNAs (top) and quantification of phenotypes (bottom) in zebrafish. The percentage of embryos in the same morphological class is indicated in each panel.

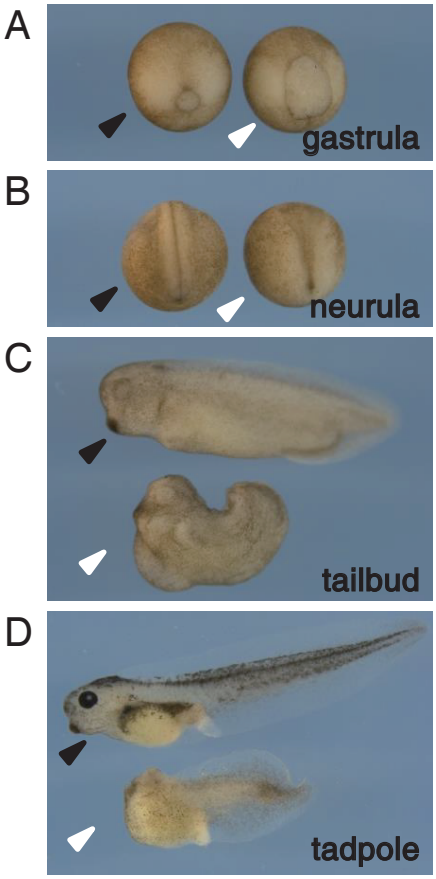

Figure 28. Developmental defects of TUT4/7 TB MOs in *Xenopus laevis* (black arrowhead, control morphants; white arrowhead, TUT4/7 morphants). Knockdown of both TUT4 and TUT7 using the TB MOs resulted in conventional gastrulation defective phenotypes such as failure in blastopore closure at stage 12 or 14 (A and B), and convergent extension defects at tailbud or tadpole stages (C and D).

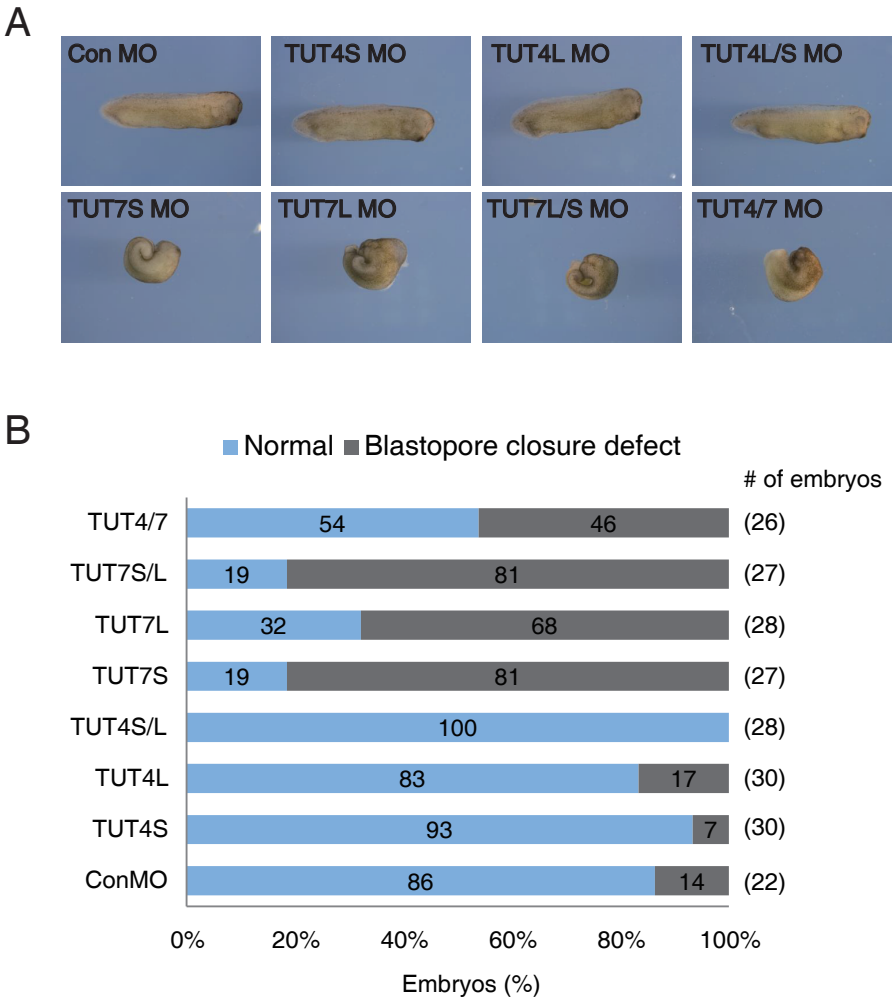

Figure 29. Convergent extension defects caused by TUT4/7 knockdown are mainly due to the loss of TUT7 function. (A) Developmental defects of TUT4 and TUT7 TB MOs in *Xenopus laevis*. Both TUT7L and TUT7S MO caused gastrulation defects while TUT4 morphants were normally developed and TUT4/7 double KD caused less blastopore closure defect compared to TUT7 single KD. (B) Quantification of figure 29A.

morphant embryos at stage 12 by performing TAIL-seq (Figure 30). I found that TUT7 single KD resulted in noticeable reduction of uridylation rate while TUT4 morphants showed nearly unchanged level of uridylation compared to control. Coherent with the associated phenotype, the combination of TUT4 and TUT7 MO did not have an additive effect on the depletion of uridylation activity, but rather resulted in slighter decrease of uridylation than that of TUT7 morphants. This result suggests that the severity of the developmental defect has a positive correlation with the reduction of uridylation in the TUT4/7 morphants. Taken together, given that the phenotypes of *Xenopus* TUT7 are equivalent to the epiboly block of zebrafish TUT7 morphants, uridylation by TUT7 but not TUT4 has a conserved role in early vertebrate development. However, I cannot rule out another possibility that *Xenopus* TUT4 MO has low knockdown efficiency compared to TUT7 MO since I could not quantify the KD efficiency of MOs due to the lack of effective antibodies.

To get a hint of the expression patterns of TUT4 and TUT7 proteins in early embryo, I searched previously published *Xenopus* proteomics data (Peshkin et al., 2015). Interestingly, I found that the level of TUT7 protein gradually increased soon after fertilization while TUT4 proteins were not detected at early embryonic stages (data not shown). Therefore, I consider that protein expressions of TUT4 and TUT7 may be differentially regulated during early embryonic development, leading to different developmental phenotype of TUT4 and TUT7 MOs. In other word, TUT4 and TUT7 may have distinctive spatiotemporal expression at early embryonic stages and thus cannot completely compensate for the loss of each other in early embryos.

I confirmed the phenotypes of TUT7-depleted embryos using different TB MOs against *Xenopus* TUT7, which are complementary to the 5′ UTR region of TUT7 mRNAs encoded in long or short forms of chromosome (TUT7L and TUT7S, respectively) (Figure

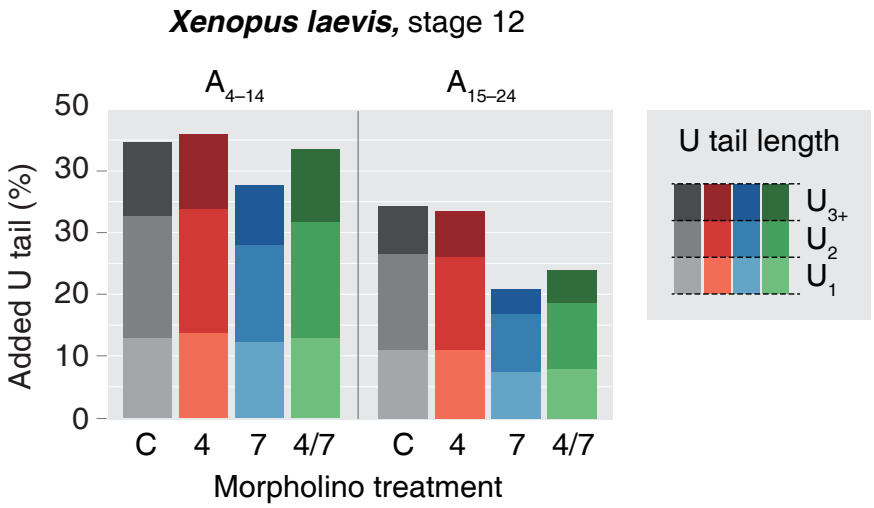

Figure 30. Uridylation frequency measured by TAIL-seq following TUT4/7 double and individual KD at stage 12 in *Xenopus laevis*. TUT7 single KD resulted in noticeable reduction of uridylation frequency while TUT4 morphants showed nearly unchanged level of uridylation compared to control and the combination of TUT4 and TUT7 MO resulted in slighter decrease of uridylation than that of TUT7 morphants.

31A). In consistent with AUG-targeting MOs of TUT7, both types of 5′ UTR-targeting MOs caused growth defects and morphological abnormalities during gastrulation. To accurately quantify the defects during gastrulation, I classified the gastrulation defects into three subtypes (normal, mild, severe) based on the degree of blastopore closure at stage 12 (Figure 31B). A combination of TUT7L and TUT7S 5′ UTR MOs showed the most severe on the gastrulation defects. When control embryos complete the blastopore closure at stage 12, most of TUT7L/S double KD embryos slowed down the gastrulation process and showed defective conversion extension with a shortened axial body structure, in agreement with the phenotype of TUT7 AUG-targeting MOs. Hence, these results reveal that the observed gastrulation defect is not caused by the potential off-target effects of TUT7 MOs but specific to TUT7 depletion.

To further verify that the developmental defects caused by TUT7 MOs are TUT7 specific, I tried rescue experiments in *Xenopus* by using wild type (WT) TUT7 or catalytically dead mutant (DADA) that has point mutations at 770 and 772 residues (aspartate to alanine) in the catalytic domain (Benoit et al., 2008; Martin and Keller, 1996). By using in-vitro transcription, I generated C-terminal half TUT7 mRNAs and C-terminal half TUT7 DADA mRNAs, and then co-injected them with control or TUT7 AUG-targeting TB MOs into *Xenopus* embryos. WT TUT7 could reproducibly rescue gastrulation defects caused by TUT7 MOs, increasing the number of normal embryos by over 2-fold compared to TUT4/7 morphants while TUT7 DADA showed no effect (Figure 32). Comparing to 78% occurrence of both mild and severe blastopore closure defects by TUT7 MO alone, co-injection with TUT7 WT mRNA rescued the gastrulation defects by 28%. In contrast, co-injection of a catalytically inactive TUT7 mRNA produced almost the same phenotype with TUT7 morphants. To examine whether the effect of TUT7 MOs is mediated by uridylation activity, the level of uridylation was measured in the TUT7 morphants at stage

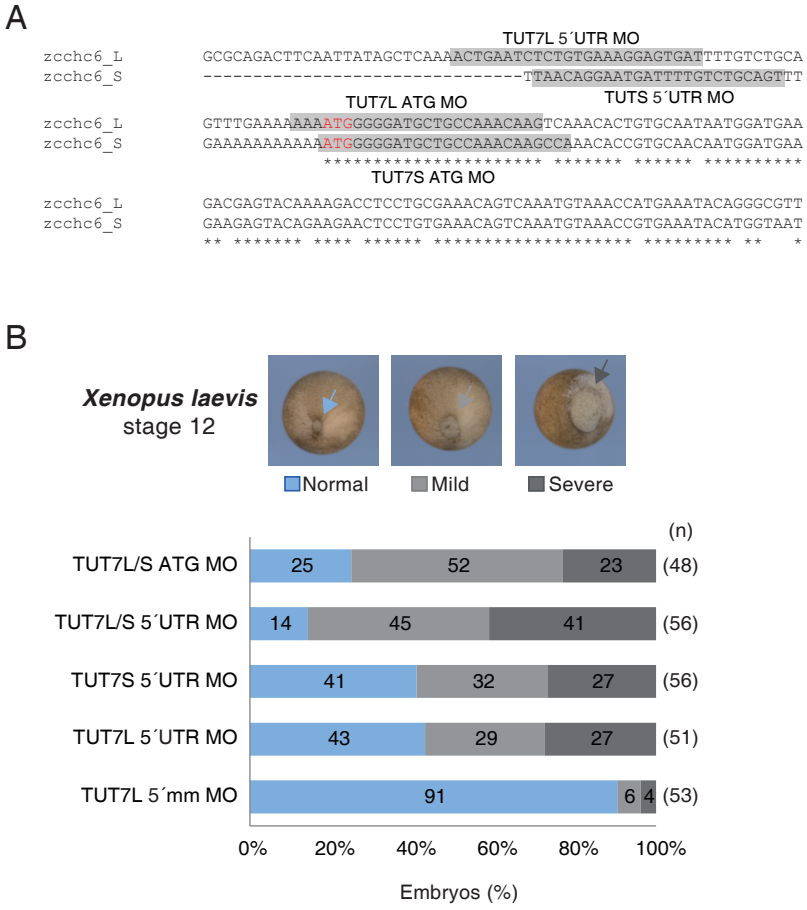

Figure 31. Gastrulation defective phenotypes of TUT7L/S 5´ UTR TB MOs in *Xenopus laevis*. (A) Design of TUT7 5´ UTR TB MOs. (B) Both TUT7L and TUT7S 5´ UTR TB MO caused gastrulation defects analogous to those observed in TUT7 ATG targeting TB morphants, characterized by a failure in blastopore closure at stage 12.

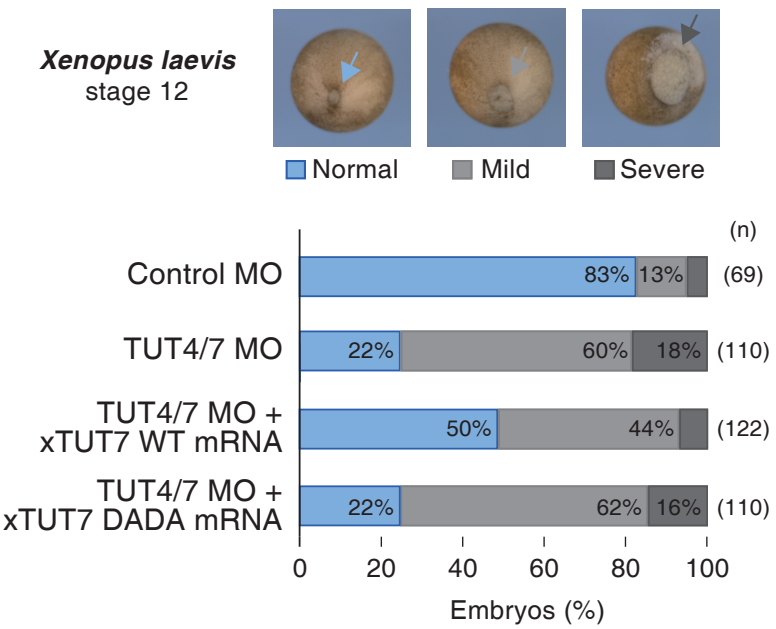

Figure 32. Rescue of the phenotypes by TUT7 WT and DADA mutant mRNAs in *Xenopus* (top) and quantification of phenotypes (bottom). Blastopore closure defects by TUT7 MOs could be rescued by WT TUT7 mRNA, but not by the catalytic mutant TUT7 mRNA. Catalytically inactive TUT7 (DADA) has point mutations at 770 and 772 residues (aspartate to alanine) in the catalytic domain.

9 and 12. TUT7 morphants showed a reduction of uridylation over ~40% compared with that of control morphants, which could be rescued by WT TUT7 mRNA, but not by the catalytic mutant TUT7 mRNA, confirming that the nucleotidyl transferase domain of TUT7 directs the mRNA uridylation (Figure 33). Collectively, these results indicate that the phenotype of TUT7 MOs is specific and due to the loss of uridylation activity of TUT7.

2.6 Maternal mRNAs with short poly(A) tails are uridylated and degraded during the MZT

In mammalian somatic cells, deadenylation generally triggers mRNA decapping and degradation. On the contrary, in early embryos, deadenylation is not immediately followed by mRNA destabilization, and decay of deadenylated mRNAs is delayed until the onset of ZGA. Considering that uridylation serves as a decay mark for deadenylated mRNAs in mRNA decay pathway (Lim et al., 2014) and increases simultaneously with maternal mRNA decay in my TAIL-seq analysis, induced uridylation may play a role for temporal regulation of maternal mRNA clearance during the MZT.

To investigate how depletion of uridylation activity affects maternal mRNA clearance, I carried out RNA sequencing from TUT4/7 TB MO-injected zebrafish embryos at 2, 4 and 6 hpf (Figure 34A). In a principle component analysis (PCA) of gene expression profiles, the PC1 appeared to reflect developmental status of the embryos (Figures 25 and 34B). Embryos with similar morphology had very similar values of PC1, suggesting that gene expression profiles of the morphants correlated strongly with their delayed morphology in embryonic development. The most severe delay happened between 4 and 6 hpf in TUT4/7 double morphants and this developmental delay was also reflected in PC1 of global mRNA

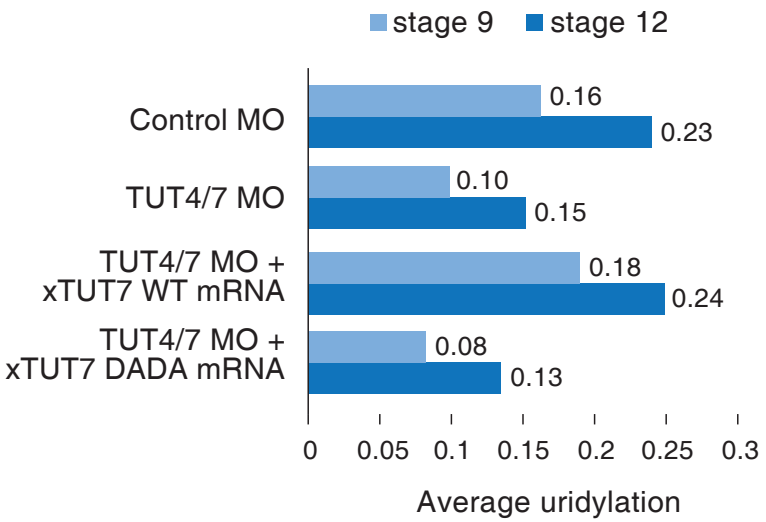

Figure 33. Rescue of the uridylation by TUT7 WT and DADA mutant mRNAs in *Xenopus*. Following TUT4/7 ATG TB MOs injection into fertilized 1-cell embryos, uridylation frequency from stage 9 and 12 embryos was measured by TAIL-seq. TUT7 morphants showed a significant reduction of uridylation compared with that of control morphants, which could be rescued by WT TUT7 mRNA, but not by the catalytic mutant TUT7 mRNA.

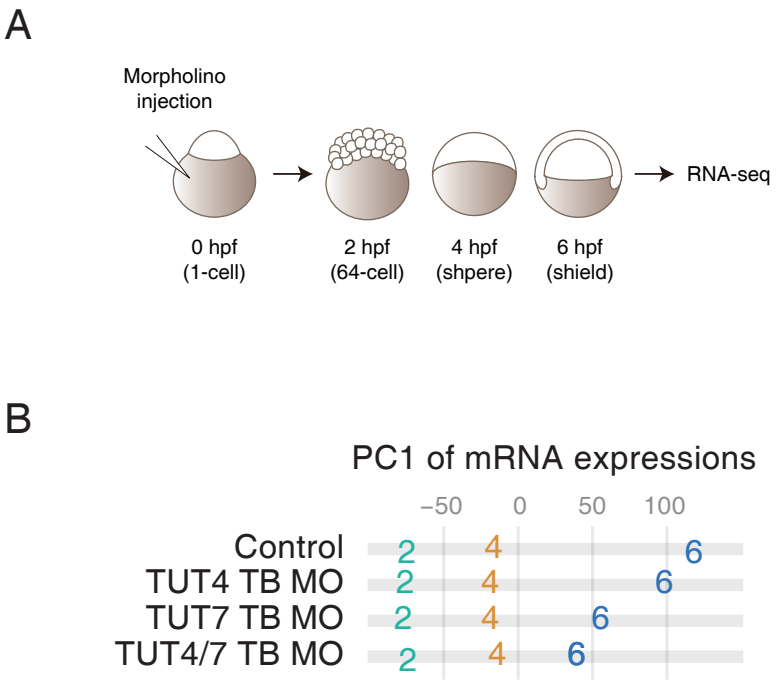

Figure 34. RNA sequencing from TUT4/7 TB MO-injected zebrafish embryos at 2, 4, and 6 hpf. (A) The experimental scheme. Following TUT4/7 TB MOs injection into fertilized 1-cell embryos, RNA-seq was performed from embryos at 2, 4, and 6 hpf. (B) Principle component analysis (PCA) of the gene expression profiles. The PC1 from the PCA reflects developmental status ofthe embryos. Embryos with similar morphology had very similar PC1 values. The most severe delay happened for TUT4/7 double knockdown embryos.

landscape. Consistently, mRNA expression between 2 and 4 hpf are not globally affected by TUT4 and/or TUT7 MO, while zygotic gene expression as well as maternal mRNA clearance are significantly delayed between 4 and 6 hpf in TUT4/7 morphants, indicating that TUT4/7 MO resulted in overall delay of development between 4 and 6 hpf (Figure 35) (Harvey et al., 2013).

Since it is difficult to distinguish the defect of maternal mRNA clearance from the general delay in embryonic development at later stage, I focused on the expression profiles between 2 and 4 hpf. Interestingly, I found that a large fraction of maternal genes was increased between 2 and 4 hpf in TUT4/7 morphants compared to control, indicating loss of maternal mRNA degradation (Figure 36A, The full list of mRNA fold change between 2 and 4 hpf are shown in Table 2). I confirmed several individual genes whose decay rates already slowed down at 4 hpf in TUT4/7 morphants compared with control embryos (Figure 36B). In contrast, zygotic gene expression was nearly unchanged until 4 hpf but it was significantly delayed at 6 hpf, suggesting that first wave of zygotic transcription was initiated normally, while additional zygotic transcription was severely damaged at later stages (Figure 37A). I checked several individual genes that were previously known as first-wave genes including mapk12b, sox19a and asb11 (Lee et al., 2013), which showed normal expressions by 4 hpf in both TUT4/7 morphants and control embryos (Figure 37B). Together, I conclude that the defect of maternal mRNA degradation precedes both the delay of zygotic gene expression and the arrest of morphological development in TUT4/7 morphants.

To verify that the imparied maternal mRNA clearance is not caused by developmental delay, I compared mRNA profiling of TUT4/7 morphants with that of α-amanitin-injected embryos that is previously published (Lee et al., 2013). In the previous study, α-amanitin, as a transcription inhibitor, resulted in development arrest at sphere stage, which is sim-

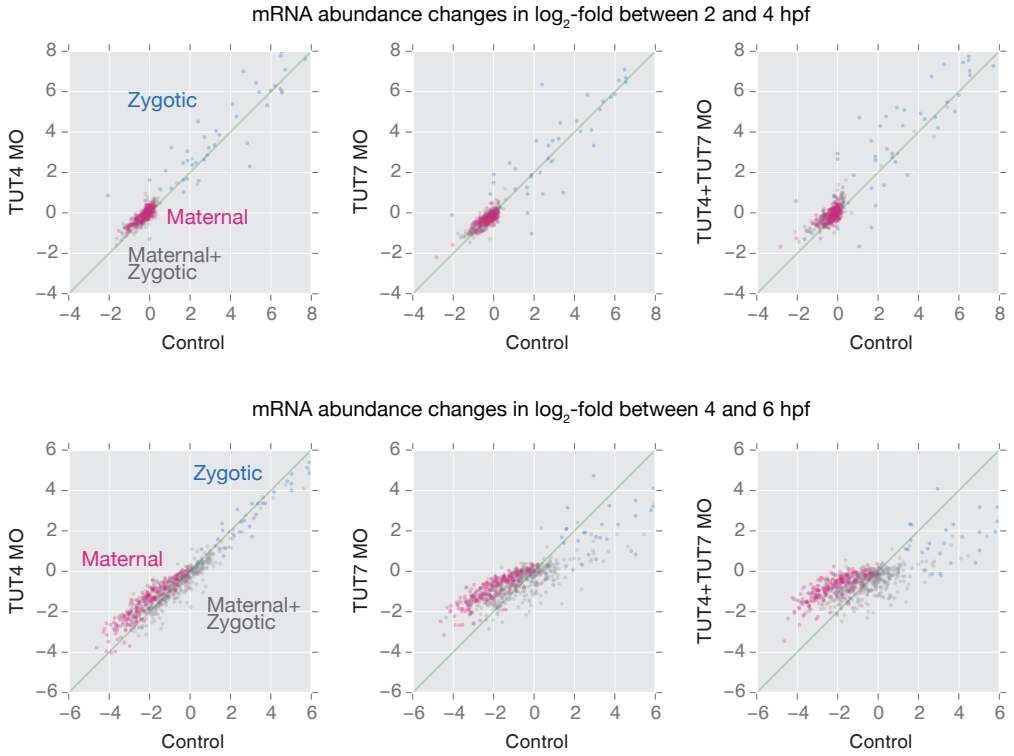

Figure 35. mRNA abundance changes upon TUT4/7 knockdown. mRNA abundance between 2 and 4 hpf are not globally affected by TUT4/7 MO, while zygotic gene expression as well as maternal mRNA clearance are significantly delayed between 4 and 6 hpf. mRNAs are classified into 3 groups based on the published data: maternal-only genes (pink), maternal-zygotic genes (grey), and zygotic-only genes (blue) (Harvey et al., 2013).

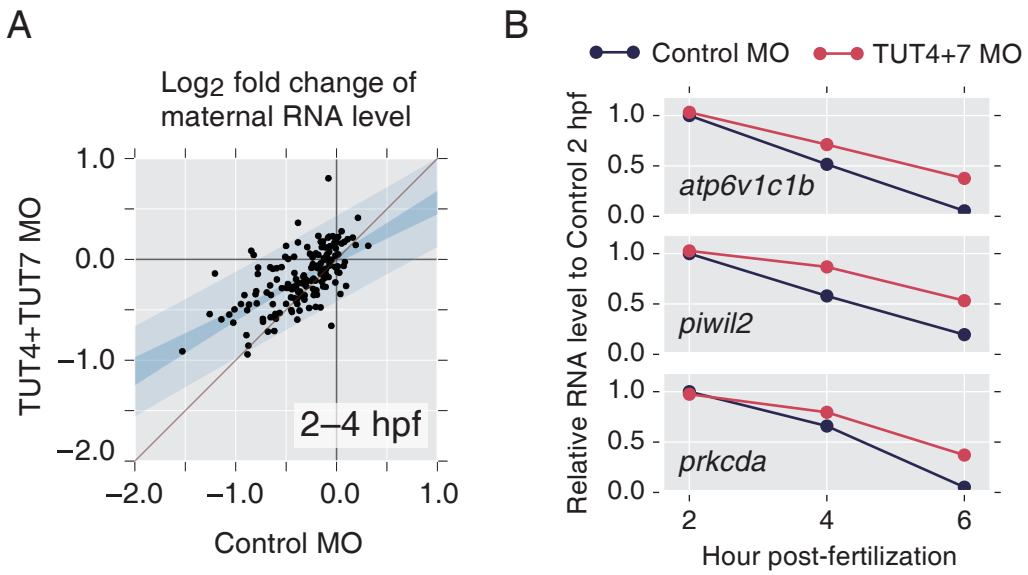

Figure 36. TUT4/7 KD caused the defect of maternal mRNA clearance. (A) Abundance change of maternal genes between 2 and 4 hpf. Light blue shade represents the 95% prediction interval and dark blue shade represents the 95% confidence interval. (B) Validation ofindividual maternal genes.

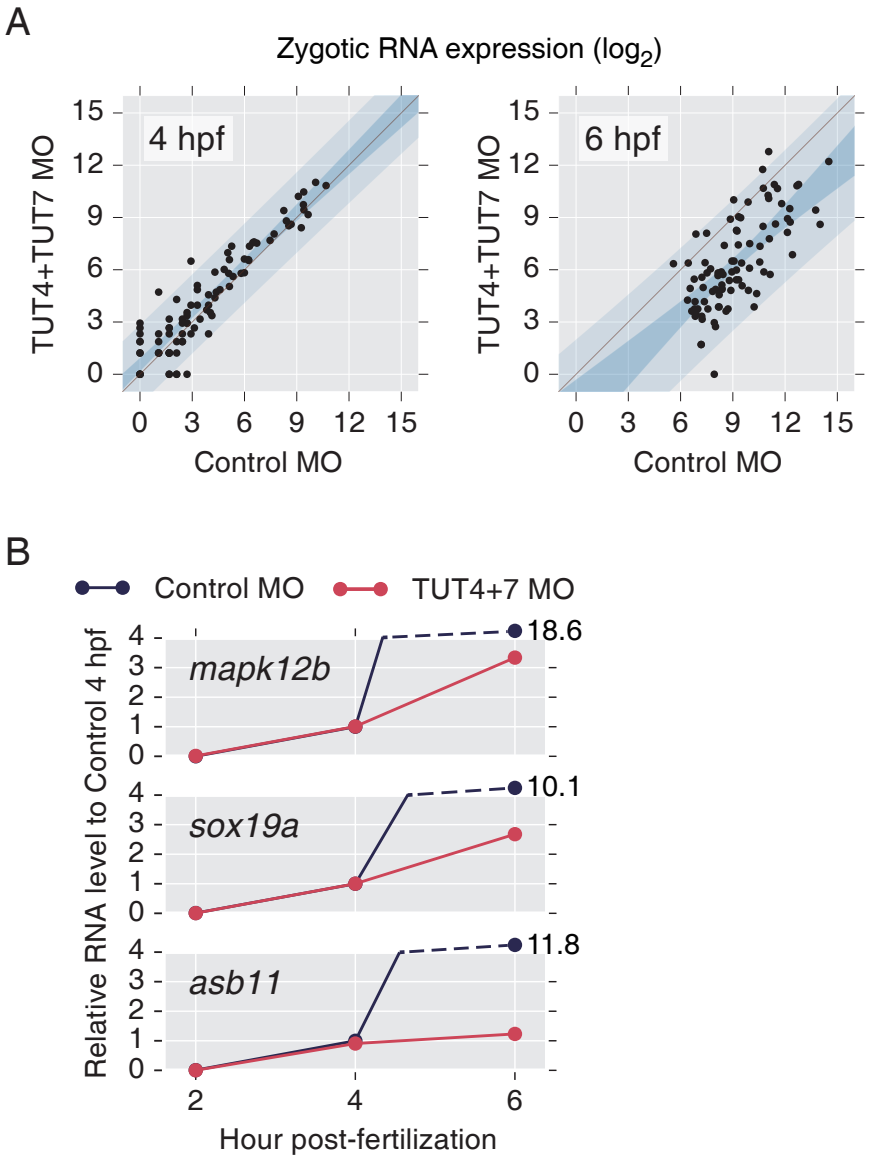

Figure 37. Zygotic gene expression was nearly unchanged until 4 hpf but it was significantly delayed at 6 hpf. (A) Global RNA expression of zygotic genes. Light blue shade represents the 95% prediction interval and dark blue shade represents the 95% confidence interval. (B) Validation ofindividual zygotic genes.

ilar phenotype with that of TUT4/7 morpholino in my experiments; disturbed zygotic transcription but not maternal mRNA decay between 2 and 4 hpf in zebrafish embryos. Compared with α-amanitin treated embryos, the expression of zygotic genes was correctly initiated, while decay of maternal transcripts is impaired between 2 and 4 hpf in TUT4/7 morphants. The resulting indicated that the defect of maternal mRNA degradation was followed by the delay of zygotic transcription in TUT4/7 morphants (Figure 38).

Next, I confirmed that TUT4/7 prefer short poly(A) mRNAs in early embryos, as described in mammalian cells (Lim et al., 2014). Expectedly, maternal transcripts with shorter poly(A) tails were more affected than longer poly(A) mRNAs by TUT4/7 depletion in their uridylation levels, indicating that maternal RNAs with high deadenylation or low cytoplasmic polyadenylation activity would be selectively targeted by TUT4/7-mediated uridylation in early embryo (Figure 39A). Consistently, TUT4/7 KD followed by TAIL-seq revealed that the depletion of uridylation resulted in the significant accumulation of short poly(A) mRNAs in TUT4/7 morphants compared to control morphants (Figure 39B), suggesting that TUT4/7-mediated uridylation is required for the degradation of these mRNAs. Taken together, these results demonstrate that mRNA uridylation has an essential role in the progression of the MZT by promoting the decay of deadenylated maternal mRNAs.

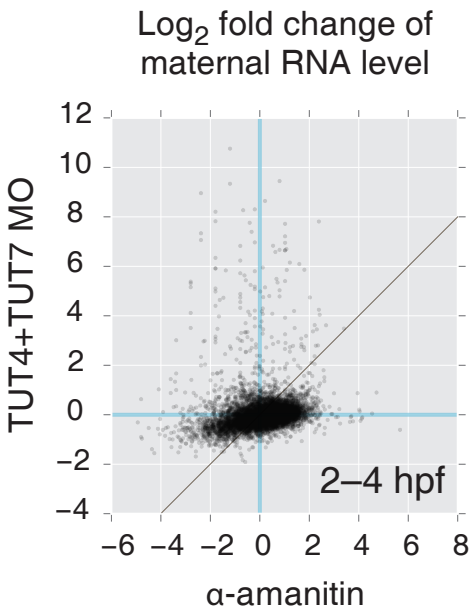

Figure 38. Comparison of mRNA fold changes (4 hpf / 2 hpf) between TUT4/7 morphants and α-amanitin-treated zebrafish embryos. In the previouis study, α-amanitin disturbed zygotic transcription but not maternal mRNA clearance between 2 and 4 hpf in zebrafish embryos. (Lee et al., 2013).

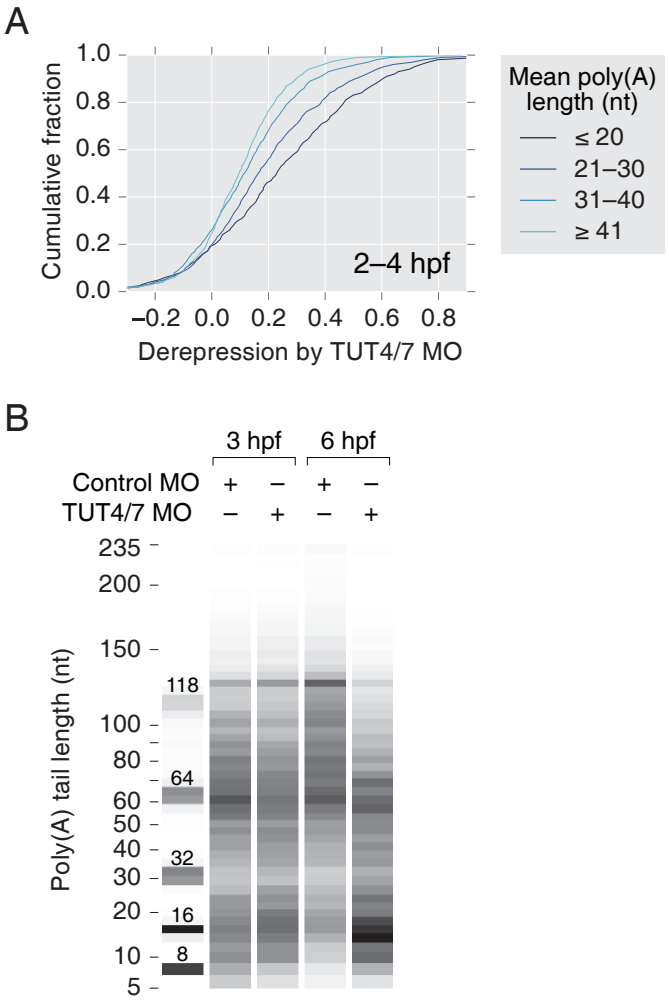

Figure 39. Uridylation is required for the selective decay of short poly(A) tailed mRNAs. (A) Cumulative distribution plot for derepression levels between 2 and 4 hpf according to the poly(A) tail length. Maternal transcripts with shorter poly(A) tails were more affected than longer poly(A) mRNAs by TUT4/7 depletion in their uridylation levels. (B) Virtual gel image of poly(A) tail length distribution. Global poly(A) tail distribution shows that TUT4/7 TB MO causes the significant accumulation of short poly(A) mRNAs. The total intensity of each bin (intensity multiplied by area) is proportional to read counts and normalized by each lane.

3. Conclusion

In this study, I investigated the regulation of mRNA tailing during the MZT and discovered a conserved role of mRNA uridylation in promoting maternal mRNA clearance in vertebrate embryos. During the MZT, maternal mRNAs are massively uridylated and degraded. Maternally deposited TUT7 (Zcchc6) is responsible for mRNA uridylation independently of ZGA in both zebrafish and *Xenopus*. Uridylation is required for the selective and precise clearance of maternal transcripts with short poly(A) tails (Figure 40). Depletion of uridylation activity causes impaired maternal mRNA clearance, resulting in the developmental delay during gastrulation. The use of multiple TUT7 MOs and rescue experiments with WT or catalytically inactive TUT7 confirmed the specificity of the developmental phenotype from the TUT7 MOs.

My current study using TAIL-seq provides accurate genome-wide profiles of poly(A) tails of maternal transcripts in early vertebrate embryos, revealing dynamic remodeling of poly(A) tail during early embryogenesis. Previous global analyses were performed by comparing the data from poly(A)+ RNA-seq with those from rRNA-depleted RNA-seq in frog embryos (Collart et al., 2014; Owens et al., 2016). But this approach was limited in the accuracy of the measurement of poly(A) tail length. Here, I employed TAIL-seq to examine the dynamic and temporal regulation of poly(A) tail length during the MZT in vertebrates. For temporal regulation of maternal gene expression, poly(A) tails of maternal transcripts undergo a dramatic remodeling resulting in the poly(A) tail lengthening or shortening. Specifically, I found that poly(A) tails of maternal mRNAs elongate globally soon after fertilization in a temporally coordinated manner, whereas

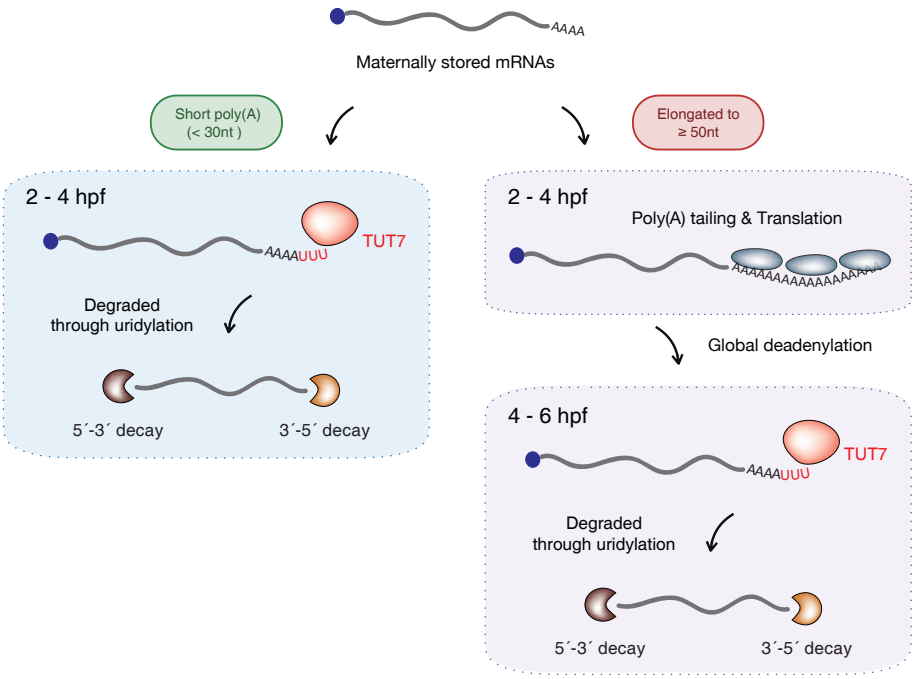

Figure 40. Selective mRNA decay during the MZT. Poly(A) tails of maternal mRNAs elongate globally after fertilization, whereas some subset of maternal transcripts remain unchanged or are rapidly deadenylated soon after fertilization. After the onset of ZGA, mRNA uridylation is dramatically induced. Such induction of uridylation is required for the selective and precise clearance of maternal transcripts with short poly(A) tails.

a subset of maternal transcripts are not subject to cytoplasmic polyadenylation (Figure 12). In zebrafish, for example, maternally supplied mRNAs, which have early embryonic function (e.g., sequence-specific transcription factors such as Nanog and Oct4), are highly polyadenylated following fertilization (Figure 14). In contrast, oocyte-specific maternal transcripts, whose aberrant expression may interfere with early embryonic development, remain unchanged in their short poly(A) tails or are rapidly deadenylated shortly after fertilization (Figure 15). Consistent with a previous report (Subtelny et al., 2014), poly(A) tail length correlates strongly with translation efficiency prior to gastrulation (6 hpf), indicating that early embryos (in cleavage and blastula stages) undergo dynamic poly(A) tailing for differential translation of maternal mRNAs during early development (Figure 16). It is unclear what confers the specificity to the differential regulation at these stages. Though previous studies have revealed that a combinatorial code of motifs in 3′ UTR governs the sequential polyadenylation and deadenylation of maternal mRNAs, they focused mainly on individual genes (Graindorge et al., 2008; Mendez & Richter, 2001; Pique et al., 2008). Therefore, further genome-wide motif analysis will have to be conducted in order to understand the mechanisms regulating the differential mRNA tailing during the MZT.

My study revealed that mRNA uridylation is necessary for maternal transcripts to be degraded at the right time, thereby directing the progression of the MZT. Uridylation barely detectable at pre-ZGA stages, but it increases drastically after the onset of ZGA, coinciding with global clearance of maternal mRNAs. This result suggests that maternal mRNA clearance is promoted by uridylation-dependent decay pathway in vertebrates. It is intriguing that deadenylation does not immediately induce mRNA degradation in early embryos and that short tailed mRNAs stay stable before the onset of uridylation of mRNAs (Figure 12B). For instance, in zebrafish, fertilization triggers selective deadenylation of a subset of maternal RNAs with long poly(A) such as sinup, uhrf1, and dnmt1. Subsequent

degradation is delayed until uridylation activity is induced. One of the possible mechanisms to explain these observations is that the capacity of the decay machinery could be insufficient due to the lack of components of the decay pathway during these early stages. My data show that uridylation activity operates at very low level in early embryos but subsequently increases at later stage. Upon the depletion of uridylation activity, maternal mRNA clearance is impaired, resulting in the delay of progression in early embryonic development. Therefore, these results collectively indicate that the induced uridylation activity is required for the timely clearance of maternal mRNAs during the MZT. I also found that maternal RNAs with shorter poly(A) tails are more affected by the depletion of uridylation, while longer poly(A) tails are less affected (Figure 39). Thus, the fate of maternally deposited mRNAs may be decided by the balance between cytoplasmic polyadenlyation and deadenylation activities following fertilization. It remains to be investigated how the selectivity of deadenylation is achieved and how deadeylation is mechanistically coupled to uridylation after the onset of ZGA.

In knockdown experiments in both zebrafish and *Xenopus* embryos, I discovered that TUT7 acts dominantly in mRNA uridylation during the MZT in both embryos, although TUT4 shows an additive effect on mRNA uridylation in zebrafish but not in *Xenopus* embryos. In both species, the TUT4 and TUT7 transcripts are maternally inherited. My TAIL-seq data indicate that TUT7 may be activated post-transcriptionally by cytoplasmic polyadenylation. A previously published *Xenopus* proteomics data (Peshkin et al., 2015) showed that the level of TUT7 protein gradually increases after fertilization while TUT4 protein is not detected at early embryonic stages. These results suggest that TUT4 and TUT7 may have distinctive temporal expression patterns during early embryonic stages, resulting in different developmental phenotype of TUT4 and TUT7 MOs. However, I cannot exclude another possibility that TUT4 TB MO has low KD efficiency compared to

TUT7 TB MO because KD efficiencies of MOs were not quantitatively assessed due to the lack of effective antibodies. In future studies, I will need to measure the translation rates of TUT4/7 by ribosome profiling analysis or high sensitive reporter assay (Kamachi et al., 2008).

Another critical contribution of my study is to provide important insights into the functional consequence of the maternal mRNA clearance during embryonic development. My work confirms that U-tail is a decay mark for deadenylated mRNAs, which is required for normal embryonic development. In zebrafish, inhibition of uridylation results in a slowdown of the decay of several hundred maternal transcripts that are normally destabilized by maternal decay pathway. TUT4/7 TB morphants failed to undergo cell movements during gastrulation and did not reach normal levels of zygotic transcription, implicating that maternal mRNA clearance is important for these development processes. However, it is currently unclear whether the developmental defects result directly from the de-repression of a selective group of maternal mRNAs. It will be interesting to identify the maternal genes that are down-regulated by uridylation during early development.

4. Methods and Materials

Embryo collection

Zebrafish embryos were obtained by natural mating of wild-type AB strain and grown in embryo medium at 28.5°C. The embryos were staged according to standard morphological criteria (Kimmel et al., 1995). A total of 300 wild-type zebrafish embryos at each stage were collected for TAIL-seq libraries. TAIL-seq libraries of MO-injected embryos were prepared using 100 embryos for each treatment group. Embryos of *Xenopus laevis* were obtained as described (Sive et al., 2007). Human chorionic gonadotropin was injected into a female frog 12 hour before collecting eggs. The eggs were obtained in 1X Marc's Modified Ringers (MMR) solution and in vitro fertilized using excised testes from a male frog. The fertilized embryos were staged according to Nieuwkoop and Faber stages (Nieuwkoop & Faber, 1994). Mouse embryos were obtained by natural mating of wild-type ICR strain (provided by Macrogen Inc.).

Plasmid construction

The coding sequences of C-terminal region of zebrafish TUT4 (681-1,257 aa) and TUT7 (641-1,196 aa) were cloned into the EcoRI and XbaI sites in the pCS2+-EGFP-C1 vector: pCS2+-GFP-drTUT4-half and pCS2+-GFP-drTUT7-half. To validate the efficiency of the TUT4/7 TB MOs, fragments of the zebrafish TUT4 (140 bp) and TUT7 (103 bp) mRNA containing TB MO target sequence were inserted into the SalI and XbaI sites in the pX-YFP

vector (Nguyen et al., 2015): pXY-drTUT4-short and pXY-drTUT7-short. The C-terminal coding region of *Xenopus laevis* TUT7 (887-1,518 aa) was cloned into the EcoRI and XbaI sites in the pCS2+-GFP vector: pCS2+-GFP-xTUT7-half. The catalytically inactive *Xenopus* TUT7 was generated by PCR-directed mutagenesis: pCS2+-GFP-DADA-xTUT7-half. Point mutations were introduced at 770 and 772 residues (aspartate to alanine) in conserved catalytic domain of *Xenopus laevis* TUT7 (Lapointe & Wickens, 2013). Capped mRNAs were synthesized from linearized plasmids using the mMessage mMachine SP6 kit (Ambion).

Microinjection

MOs were provided by Gene Tools LLC and are listed in Table 1. Approximately 1nl of solution containing of MOs was injected into wild-type zebrafish embryos at 1-cell stage. One-cell stage *Xenopus* embryos were injected with 2nl of MO solution. For validation of MO efficiency, the plasmid pXY-drTUT4-short and pXY-drTUT7-short were injected alone or co-injected with the TUT4 and TUT7 MO, respectively, into zebrafish 1-cell embryos. GFP fluorescence was detected at 6 hpf. For the rescue experiments, each mRNA was mixed with the TB MOs or control MOs and injected into 1-cell stage embryos. 50 or 150 pg of in-vitro transcribed mRNAs was injected into one-cell-stage zebrafish or *Xenopus* embryos, respectively.

Quantitative RT-PCR

For quantitative RT-PCR following SB MO injection, total RNA was extracted from zebrafish embryos using TRIzol (Invitrogen). 1-5 μg of total RNA was treated with DNase I

(Takara), and reverse-transcribed using SuperScript III (Thermo Scientific) and random hexamer. The levels of MO-targeting mRNA region were analyzed by SYBR green assay (Applied Biosystems) using ABI StepOne real-time PCR system. The following primers were used: zebrafish TUT4: forward, 5′-CAAAGCGTCATCCTCCAAAC-3′ and reverse, 5′-TAATTCCCTCCATCCGAAGC-3′; zebrafish TUT7: forward, 5′-ACATCTCGCCAGCTCTCAGT-3′ and reverse, 5′-GCACACAACTACAGGCATCC-3′.

Construction of TAIL-seq/mTAIL-seq library

TAIL-seq libraries were prepared as previously described (Chang et al., 2014). Briefly, 30~80 μg of total RNAs extracted from zebrafish or frog embryos were used as starting materials, which were treated with DNaseI (Takara), purified with RNeasy MiniElute column (Qiagen), and rRNA-depleted by using Ribo-Zero gold kit (Epicentre). The RNAs were ligated to the biotinylated 3′ adaptor using T4 RNA ligase 2 (truncated KQ, NEB), and partially digested by RNase T1 (Ambion). The ligated RNAs were precipitated with streptavidin beads (Invitrogen), phosphorylated at the 5′ end by PNK reaction (Takara), and subjected to size fractionation (500-1,000 nt). The purified RNAs were ligated to the 5′ adaptor, reverse-transcribed, and amplified by PCR. mTAIL-seq libraries were also prepared as described previously (Lim et al., 2016). Total RNAs were extracted from mouse embryo samples using TRIzol reagent (Invitrogen), and ligated to 3′ hairpin adaptor using T4 RNA ligase 2 (NEB) for overnight. The ligated RNAs were partially digested by RNase T1 (Ambion) and precipitated with streptavidin beads (Invitrogen). 5′ phosphorylation (PNK, Takara) and endonucleolytic cleavage reaction (APE1, NEB) were performed on beads. The eluted RNAs were gel purified (300-750 nt), ligated to 5′ adaptor, reverse-transcribed and amplified by PCR. The cDNA libraries were mixed with PhiX control library v3 (Illumina)

and spike-in mixture and then sequenced by paired-end run (51 x 251 cycles) on Illumina MiSeq or HiSeq 2500. Resulting data were processed as previously described (Chang et al., 2014; Lim et al., 2016). The spike-ins were synthesized by IDT ultramer service. Each spike-in was amplified and gel purified as in TAIL-seq library construction. To discriminate spike-ins of different length, they were barcoded and multiplexed in each sequencing. Sequencing samples are summarized in Table 2.

RNA-seq analysis

Zebrafish embryos were injected with 1nl of TUT4/7 TB MO or control MO at 1-cell stage. For each sample, 30 embryos were collected and total RNA was extracted with TRIzol (Invitrogen). The samples were spiked in with ERCC RNA Spike-In Mix (Ambion) for normalization purpose. The quality of total RNA was checked by Agilent 2100 Bioanalyzer. Ribosomal RNA was depleted from total RNA using Ribo-Zero Gold kit (Epicentre). RNA-seq libraries were constructed by DNALink Inc. using TruSeq stranded total RNA library prep kit (Illumina) and sequenced in Illumina Nextseq 500 v2 to yield paired-end 76 nt reads. The sequencing reads were aligned to GRCz10 genome assembly using STAR (Dobin et al., 2013). The reads were counted and normalized using RSEM (Li & Dewey, 2011). For analysis, transcripts with insufficient reads (<100 normalized reads in any library) were removed. mRNAs are classified into three groups based on the published data, which analyzed single nucleotide polymorphisms (SNPs) of embryos obtained from crosses of two different strains (Harvey et al., 2013). It discriminated the maternal and zygotic transcriptomes, thereby categorizing mRNAs as maternal-only genes, maternal-zygotic genes, and zygotic-only genes.

Ribosome profiling analysis

Ribosome profiling (RPF) and RNA-seq data were downloaded from a publicly available database (GSE52809) (Subtelny et al., 2014). Sequencing reads were trimmed into 28-nt-long sequences. The reads were aligned to GRCz10 genome assembly using STAR (Dobin et al., 2013). Reads mapped to each transcript were counted using BEDTools multicov (Quinlan & Hall, 2010). The trimmed mean of M-values (TMM) normalization method was applied to RPF and RNA-seq data (Robinson & Oshlack, 2010). Translational effiecienty (TE) was calculated by the normalized ratio of RPF to RNA-seq. Genes with ≥100 reads in RNA-seq data were included in the analysis.

Phylogenetic analysis of TUTase homologs

The SwissProt and TrEMBL databases were downloaded and they were reduced to contain only proteins from species of interest: *H. sapiens, G. gallus, X. tropicalis, D. rerio, S. purpuratus, D.melanogaster, C. elegans, S. pombe, S. cerevisiae,* and *E. nidulans* (the teleomorph form of *A.nidulans*). TUT homologs were searched by blastp using seven human TUTs, *S. pombe* Cid-1, and *C. elegans* Cid-1 as seed sequences. The sequences were aligned using PROMALS (Pei & Grishin, 2007). Using Gblocks preprocessor, nonconserved regions of the multiple sequence alignment (MSA) from PROMALS were removed (Castresana, 2000). As both close and distant homologs are aligned together, I set the parameters very generous to pass most weakly conserved positions. The main phylogenetic analysis was performed using PhyML (Guindon et al., 2010). The phylogenetic tree was optimized to maximize likelihood with Jones-Taylor-Thornton substitution model.

Name	Sequence (5'-3')	targeting region	Dose	species
TUT4 SB	GTGAGTTTGTGTCCAGTTACCTTGA	splicing junjction		zebrafish
TUT7 SB	TGTGCGGTTACACACCTGGAAGAAC	splicing junjction		zebrafish
TUT4 TB	GGTCCTCCATGCCACTACACTTCTC	start codon		zebrafish
TUT7 TB	CTTCCTGTTTCCTCGATCCGCCATC	start codon		zebrafish
xTUT4S TB	TTACAGGCTTAGAGACACCTTCCAT	start codon		Xenopus laevis
xTUT4L TB	TTACAGGCTTAGGAACACCTTCCAT	start codon		Xenopus laevis
xTUT7S TB	TGGCTTGTTTGGCAGCATCCCCCAT	start codon		Xenopus laevis
xTUT7L TB	CTTGTTTGGCAGCATCCCCCATTTT	start codon		Xenopus laevis
xTUT7L_TB_5mm	CTTcTTTcGCAcCATCgCgCATTTT	5 base pair mismatch		Xenopus laevis
xTUT7S 5´ UTR	ACTGCAGACAAAATCATTCCTGTTA	5´ UTR region		Xenopus laevis
xTUT7L 5´ UTR	ATCACTCCTTTCACAGAGATTCAGT	5´ UTR region		Xenopus laevis
Control	CCTCTTACCTCAGTTACAATTTATA			

Table 1. Lists of morpholinos used in this study.

		Fold change (RNA-seq)		Mean of polyA length (nt)						Average U length of shortA tails (5-25 nt)					
Gene ID	Gene name	Con MO	TUT4/7 MO	0h	1h	2h	4h	6h	8h	0h	1h	2h	4h	6h	8h
ENSDARG00000068992	hspa8	0.22	0.24	21.6	22.0	23.6	25.3	24.5	23.0	0.11	0.14	0.23	0.39	0.33	0.43
ENSDARG00000039007	eno3	-0.24	-0.13	8.9	9.3	10.0	10.5	11.7	14.7	0.35	0.44	0.59	1.65	2.66	2.70
ENSDARG00000006580	cldnd	-1.51	0.06	25.5	20.3	17.7	20.7	16.9	16.8	0.12	0.03	0.07	0.08	0.40	0.39
ENSDARG00000029722	hmgb2a	0.51	0.23	56.6	47.6	50.3	46.1	52.8	49.1	0.13	0.15	0.12	0.34	0.16	1.16
ENSDARG00000045514	atp5c1	-1.30	0.16	8.8	9.6	10.5	13.4	17.4	20.9	0.06	0.08	0.10	0.38	0.72	0.88
ENSDARG00000098739	phc2b	-1.22	-0.35	40.9	29.1	28.3	23.7	14.8	13.8	0.22	0.15	0.14	0.09	0.32	1.26
ENSDARG00000017163	sinup	-1.53	0.85	33.4	27.6	23.8	24.7	20.6	22.4	0.06	0.01	0.03	0.01	0.21	0.24
ENSDARG00000015551	fth1a	-0.04	0.00	11.8	12.8	14.5	20.9	27.8	36.7	0.16	0.18	0.29	0.68	1.14	1.57
ENSDARG00000029150	hsp90ab1	0.17	0.18	15.0	16.1	19.9	29.3	32.1	39.4	0.15	0.29	0.45	1.87	1.64	0.77
ENSDARG00000004757	ybx1	0.30	0.47	39.2	33.7	39.3	43.2	44.3	50.3	0.05	0.38	0.29	0.78	0.44	0.37
ENSDARG00000020504	h3f3a	0.46	0.24	19.9	23.1	33.9	64.0	60.9	38.9	0.05	0.03	0.12	0.44	0.21	0.52
ENSDARG00000071583	gtf3ab	-0.58	-0.26	13.2	16.4	21.1	32.3	22.4	22.8	0.07	0.03	0.06	0.14	0.26	0.48
ENSDARG00000035400	btf3	-0.48	0.35	15.6	14.8	15.5	19.5	24.6	28.0	0.13	0.27	0.33	0.48	0.15	0.05
ENSDARG00000076568	sec61b	0.03	0.33	18.1	21.0	22.6	37.1	39.4	37.5	0.18	0.07	0.07	0.17	0.12	0.28
ENSDARG00000093176	zgc:77118	-0.74	-0.18	50.9	33.9	28.4	30.5	22.0	22.3	0.14	0.14	0.10	0.11	0.65	0.97
ENSDARG00000019763	acp5a	-0.62	-0.17	9.7	10.6	14.5	34.8	27.2	22.8	0.19	0.20	0.15	0.31	0.16	0.80
ENSDARG00000035622	xbp1	-0.59	0.37	7.0	7.8	8.9	12.6	15.8	15.5	0.19	0.35	0.41	0.86	0.62	0.55
ENSDARG00000021124	cfl1	-0.19	-0.04	12.2	14.1	19.1	34.8	35.8	34.9	0.04	0.04	0.09	0.28	0.14	0.31
ENSDARG00000036044	rps20	-0.38	0.25	21.0	20.6	21.4	24.1	29.0	33.3	0.17	0.27	0.39	0.99	0.22	0.22
ENSDARG00000011094	ccna2	-0.06	-0.06	29.2	41.6	48.6	51.7	43.9	26.1	0.11	0.12	0.18	0.47	0.48	0.79
ENSDARG00000036629	rps14	0.14	0.26	25.6	25.1	24.5	29.9	31.3	30.4	0.09	0.14	0.18	0.22	0.21	0.25
ENSDARG00000009212	ppiaa	-0.06	0.36	16.2	17.7	20.3	31.6	34.1	30.8	0.01	0.08	0.08	0.32	0.34	0.48
ENSDARG00000104068	gstp1	-1.11	0.06	16.6	16.0	18.5	24.5	23.0	26.9	0.06	0.08	0.09	0.16	0.25	0.74
ENSDARG00000035957	gmnn	-0.03	0.12	13.5	18.0	27.3	45.6	24.4	30.4	0.09	0.13	0.21	0.30	0.49	0.70
ENSDARG00000040534	epcam	-0.88	0.29	34.0	27.5	26.4	26.5	27.4	25.6	0.14	0.07	0.13	0.12	0.15	0.44
ENSDARG00000100003	glulb	0.21	0.17	27.0	20.5	21.7	24.6	21.5	21.3	0.41	0.69	0.63	0.89	0.71	1.06
ENSDARG00000043137	cdca8	-0.79	-0.01	8.1	9.3	11.9	24.6	22.1	20.0	0.12	0.04	0.06	0.26	0.33	0.47
ENSDARG00000103791	nme2b.1	-0.20	0.48	23.8	19.5	19.3	23.8	18.7	19.9	0.23	0.41	0.71	1.70	1.85	3.27
ENSDARG00000099380	rpl13	-0.50	0.15	13.2	13.5	13.5	16.5	22.5	24.3	1.65	1.54	1.50	1.71	1.44	0.86
ENSDARG00000041619	gnb2l1	0.05	0.18	20.8	19.4	19.9	27.7	28.4	29.7	0.29	0.14	0.30	0.57	0.36	0.36
ENSDARG00000004169	stmn1a	-0.65	0.24	11.3	11.7	12.9	21.6	25.4	26.5	0.24	0.23	0.29	0.46	0.50	0.80
ENSDARG00000076474	org	-2.81	0.15	21.2	14.2	12.4	14.2	15.0	15.7	0.08	0.05	0.03	0.13	0.53	0.76
ENSDARG00000102892	h1m	-0.22	-0.19	28.2	22.4	25.4	23.5	18.3	21.4	0.21	0.14	0.12	0.17	0.52	1.13
ENSDARG00000038066	kpna2	-2.25	0.19	14.0	12.5	13.4	15.0	28.6	24.9	0.09	0.01	0.06	0.31	0.60	1.86
ENSDARG00000003701	cldng	-1.50	0.06	25.4	19.9	20.2	25.6	19.8	14.4	0.27	0.23	0.18	0.20	0.17	2.06
ENSDARG00000099865	hnrnpabb	0.28	0.20	38.2	38.4	40.8	36.8	43.5	32.9	0.07	0.07	0.27	0.26	0.20	0.59
ENSDARG00000057026	ran	0.03	0.36	22.2	20.0	18.4	17.7	29.0	27.8	0.20	0.28	0.36	0.88	0.60	0.67
ENSDARG00000043509	rpl11	-0.23	0.13	32.9	31.7	30.2	33.0	40.9	50.1	0.05	0.17	0.21	0.44	0.59	0.17
ENSDARG00000042905	rpl10a	-0.28	0.24	15.9	16.5	15.6	17.1	23.5	37.0	0.26	0.14	0.23	0.93	1.25	0.57
ENSDARG00000043257	ckbb	-0.40	-0.17	8.3	9.0	9.4	10.5	12.7	17.5	0.35	0.91	1.56	2.83	3.04	2.18
ENSDARG00000092553	slc25a5	0.00	0.27	20.8	18.7	21.6	33.5	41.2	42.2	0.02	0.13	0.14	0.75	0.66	0.40
ENSDARG00000028295	mkrn4	-0.15	-0.41	15.7	17.0	24.6	38.3	27.1	24.3	0.09	0.06	0.07	0.45	0.29	0.22
ENSDARG00000026871	uchl1	-0.47	-0.08	13.2	11.9	14.5	20.5	18.1	16.7	0.06	0.09	0.04	0.14	0.21	0.71
ENSDARG00000036161	hnrnpa0l	0.44	0.19	42.0	43.7	46.4	44.1	48.1	36.3	0.19	0.11	0.15	0.15	0.09	0.40
ENSDARG00000043236	ccna1	-0.10	-0.17	21.4	22.3	25.2	27.7	20.1	16.0	0.07	0.08	0.09	0.11	0.40	0.29
ENSDARG00000103846	hspa5	-0.56	-0.20	9.0	9.6	11.1	16.5	16.4	21.1	0.76	0.71	0.68	1.10	0.93	1.71
ENSDARG00000051783	rplp0	-0.50	0.40	13.3	12.9	13.4	14.1	24.2	42.4	0.13	0.23	0.43	1.89	2.35	0.93
ENSDARG00000077291	rps2	-0.31	0.36	15.0	14.0	14.7	14.7	23.7	40.9	0.17	0.51	0.99	3.24	3.20	0.94
ENSDARG00000092693	tpt1	0.06	0.22	17.7	17.1	16.0	17.2	29.0	38.7	0.13	0.13	0.43	0.74	0.44	0.47
ENSDARG00000057738	hells	-1.33	0.74	13.1	14.2	15.2	21.1	19.4	19.1	0.04	0.03	0.02	0.09	0.49	0.81
ENSDARG00000077664	zgc:110239	-0.70	-0.07	38.8	23.8	20.6	20.5	33.7	25.8	0.07	0.03	0.02	0.08	0.19	0.38
ENSDARG00000076667	ccng1	0.04	0.03	33.6	36.0	36.5	38.7	40.5	39.6	0.07	0.07	0.08	0.25	0.03	0.10
ENSDARG00000002344	tubb4b	-1.05	0.18	12.3	12.5	12.6	14.4	14.6	14.8	0.05	0.09	0.11	0.28	0.62	0.60
ENSDARG00000042864	rpl7l1	-0.80	0.46	7.4	7.6	8.6	17.4	23.0	26.9	0.11	0.10	0.13	0.36	0.44	0.51
ENSDARG00000102632	ubc	-0.09	0.12	23.6	16.6	16.3	25.1	28.1	24.2	0.16	0.27	0.23	0.70	0.43	1.54
ENSDARG00000056515	spsb1	-0.48	0.40	24.1	21.4	22.9	27.8	17.9	16.8	0.04	0.08	0.04	0.07	0.16	0.60
ENSDARG00000029445	EIF1B	0.19	0.23	24.5	23.8	27.7	37.2	33.6	31.9	0.03	0.07	0.06	0.06	0.10	0.24
ENSDARG00000095743	sox11b	0.21	-0.13	12.2	20.1	30.6	50.8	30.0	22.6	0.03	0.05	0.11	0.36	0.24	0.96
ENSDARG00000043457	gapdh	-0.24	-0.38	9.9	10.5	10.5	11.5	14.3	17.8	0.28	0.54	0.67	1.41	1.55	2.07
ENSDARG00000100558	slbp	-1.21	0.62	16.8	17.4	18.1	25.5	31.4	22.6	0.04	0.06	0.08	0.06	0.29	0.40
ENSDARG00000031495	seta	0.25	0.33	23.4	22.8	27.2	37.4	40.9	37.0	0.01	0.08	0.08	0.20	0.09	0.09
ENSDARG00000055120	ctsba	-0.36	-0.05	23.6	18.0	19.0	27.9	28.5	35.7	0.08	0.14	0.06	0.22	0.33	0.49
ENSDARG00000099664	sep15	0.04	0.01	22.0	24.4	25.5	31.8	32.2	28.4	0.05	0.08	0.08	0.13	0.04	0.29
ENSDARG00000058451	rpl6	-0.25	0.30	12.3	11.7	11.7	13.5	16.9	28.5	0.01	0.04	0.08	0.35	0.63	0.41
ENSDARG00000031044	lipg	-1.74	-0.31	18.9	13.4	14.2	17.6	14.4	16.7	0.01	0.03	0.02	0.13	0.18	0.00
ENSDARG00000055996	rps8a	-0.36	0.06	14.8	12.0	12.2	18.4	28.1	42.5	0.07	0.10	0.09	0.50	0.77	0.33
ENSDARG00000035993	sumo3b	0.14	0.12	36.6	45.0	37.1	37.8	45.3	33.6	0.05	0.19	0.06	0.06	0.29	0.47
ENSDARG00000014208	zgc:55413	-0.92	0.13	44.4	24.0	20.1	25.1	24.9	22.5	0.16	0.08	0.08	0.16	0.94	0.93
ENSDARG00000070545	top1l	0.03	0.24	10.8	16.1	24.2	48.8	47.2	37.1	0.38	0.17	0.16	0.48	0.45	0.57

ENSDARG00000014817	ranbp1	-0.08	0.07	11.3	12.2	15.7	22.2	37.8	30.1	0.07	0.13	0.19	0.80	0.31	0.56
ENSDARG00000070822	cnp	0.03	-0.01	17.2	18.2	18.2	20.4	18.8	17.5	0.20	0.34	0.38	0.77	1.10	1.93
ENSDARG00000013946	ivns1abpb	-0.02	0.01	15.8	17.9	22.8	27.1	21.0	20.8	0.04	0.02	0.01	0.18	0.28	0.62
ENSDARG00000042566	rps7	-0.04	0.24	20.4	19.0	17.2	24.6	27.0	32.5	0.23	0.45	0.58	1.23	1.18	0.98
ENSDARG00000006316	rpl23a	-0.38	0.38	23.1	18.9	18.6	23.7	28.2	33.1	0.19	0.25	0.28	0.86	0.41	0.36
ENSDARG00000058306	prpf18	-0.61	0.40	13.7	15.0	18.2	25.5	21.2	22.4	0.04	0.01	0.02	0.02	0.22	0.16
ENSDARG00000037640	aurkb	-1.75	0.33	20.2	11.9	11.2	12.8	15.0	16.6	0.03	0.02	0.05	0.23	0.20	0.40
ENSDARG00000013475	cct4	-0.54	0.13	9.6	10.1	10.9	15.6	17.4	20.0	0.02	0.06	0.10	0.65	0.27	0.54
ENSDARG00000018145	mid1ip1l	-0.83	-0.07	13.3	13.1	16.7	29.8	15.3	17.2	0.08	0.09	0.12	0.07	0.31	0.20
ENSDARG00000035324	hnrpl	-0.02	0.28	20.5	20.4	22.6	26.1	23.5	25.5	0.06	0.09	0.23	0.14	0.09	0.18
ENSDARG00000037746	actb1	-0.28	0.02	9.1	8.5	9.2	10.7	15.8	25.5	0.07	0.14	0.18	0.46	0.66	0.69
ENSDARG00000099148	bzw1b	-0.03	0.25	13.0	15.8	22.6	31.4	32.1	25.5	0.15	0.09	0.18	0.30	0.20	0.59
ENSDARG00000041623	mt2	-2.39	-0.10	13.1	13.1	15.4	19.2	20.5	25.2	0.03	0.03	0.04	0.03	0.14	0.37
ENSDARG00000013307	rpl19	-0.86	0.14	10.9	11.4	11.4	14.2	20.0	30.5	0.14	0.20	0.35	1.29	1.20	0.49
ENSDARG00000010246	prmt1	0.14	0.22	47.3	31.7	28.7	37.7	36.5	34.7	0.12	0.05	0.02	0.30	0.31	0.50
ENSDARG00000018637	sec61g	-0.75	0.49	11.5	9.8	9.7	13.8	29.5	34.4	0.07	0.08	0.19	0.41	0.09	0.14
ENSDARG00000020482	nono	0.02	0.28	34.0	40.2	40.7	43.7	37.2	35.2	0.26	0.25	0.41	0.35	0.68	0.38
ENSDARG00000009779	mcl1a	-0.71	0.44	14.5	14.2	17.4	21.4	16.5	17.6	0.06	0.09	0.09	0.28	0.19	0.32
ENSDARG00000101472	pop4	-0.54	0.72	20.7	22.6	29.2	37.4	21.3	33.7	0.03	0.03	0.04	0.03	0.23	0.00
ENSDARG00000099439	serp1	-0.31	0.04	13.7	15.6	18.6	30.6	29.1	28.7	0.09	0.11	0.09	0.30	0.11	0.48
ENSDARG00000027187	kat8	-0.50	0.39	13.5	13.1	14.7	19.7	19.7	20.1	0.02	0.02	0.01	0.05	0.13	0.31
ENSDARG00000053291	pnrc2	0.65	0.27	9.3	10.7	13.7	19.8	17.3	15.4	0.44	0.44	0.64	0.70	0.57	0.28
ENSDARG00000057234	chtopa	-0.03	0.08	19.8	21.8	31.8	55.1	59.4	42.1	0.10	0.15	0.30	0.38	0.49	0.70
ENSDARG00000017219	pabpc1a	-0.01	0.38	21.3	21.6	20.4	40.0	42.4	38.2	0.81	0.85	0.59	0.88	0.98	0.67
ENSDARG00000103672	cirbpa	0.23	0.31	39.6	33.8	35.2	43.1	36.3	42.0	0.00	0.04	0.22	0.16	0.08	0.21
ENSDARG00000031776	zgc:92066	-0.28	0.01	10.4	10.6	10.8	16.4	21.6	26.6	0.14	0.39	0.41	1.07	1.17	1.74
ENSDARG00000015862	rpl5b	-0.10	0.36	18.9	20.3	23.1	26.8	34.8	37.1	0.26	0.25	0.26	0.50	0.49	0.30
ENSDARG00000035018	thy1	-1.89	-0.22	36.6	26.0	22.2	22.1	21.1	18.9	0.24	0.25	0.12	0.12	0.36	0.17
ENSDARG00000018904	cstf3	0.06	0.16	22.5	29.3	35.1	39.2	44.6	29.3	0.21	0.12	0.11	0.05	0.33	1.03
ENSDARG00000035771	MEPCE	0.10	0.18	13.6	16.9	22.7	31.8	22.1	22.6	0.02	0.03	0.09	0.67	0.49	0.54
ENSDARG00000038785	abcf2a	0.13	0.50	25.6	27.5	25.4	28.1	21.8	19.9	0.39	0.17	0.19	0.18	0.53	0.95
ENSDARG00000010149	atp5a1	-0.15	-0.15	10.1	10.8	12.4	16.8	19.3	18.6	0.13	0.12	0.14	0.66	0.80	1.35
ENSDARG00000021864	rplp1	-0.51	0.47	13.2	12.4	13.1	14.8	25.2	25.8	0.15	0.15	0.18	0.55	0.63	0.14
ENSDARG00000101362	mibp	-0.51	0.42	17.8	22.6	29.2	41.3	22.9	26.4	0.02	0.02	0.02	0.00	0.29	0.36
ENSDARG00000053058	rps11	-0.21	0.14	19.9	18.8	18.0	19.4	26.2	36.3	0.89	0.88	1.09	1.48	1.47	1.36
ENSDARG00000015978	zgc:86599	-0.94	0.24	9.2	9.3	11.0	19.5	19.9	22.9	0.34	0.27	0.26	0.42	0.89	0.86
ENSDARG00000014867	rpl8	-0.29	0.17	12.7	10.5	13.0	21.1	31.0	37.1	0.07	0.13	0.08	0.65	0.80	0.30
ENSDARG00000102452	eif3ha	-0.23	0.26	10.4	9.9	11.6	16.1	19.4	23.5	0.03	0.12	0.13	0.38	0.72	0.64
ENSDARG00000010481	bzw1a	0.12	0.10	39.3	40.0	36.6	36.6	53.1	38.0	0.17	0.31	0.46	0.46	0.23	0.61
ENSDARG00000012432	fam76b	0.12	0.27	19.0	25.3	36.2	33.5	22.1	22.8	0.16	0.11	0.17	0.22	0.30	0.52
ENSDARG00000002271	zfand5b	-0.01	0.22	15.0	18.4	26.0	31.8	22.2	17.3	0.16	0.14	0.08	0.37	0.29	0.63
ENSDARG00000051923	ccnb1	-0.12	0.55	22.0	20.0	24.4	26.1	17.4	18.7	0.36	0.15	0.31	0.29	0.53	0.73
ENSDARG00000003860	cbx3a	-0.13	0.19	30.0	23.4	23.9	25.0	27.2	22.8	0.00	0.04	0.04	0.06	0.17	0.13
ENSDARG00000037870	actb2	0.04	0.22	12.5	13.5	16.5	26.5	36.8	34.6	0.06	0.07	0.30	0.68	0.55	0.53
ENSDARG00000039208	nasp	-1.45	0.53	16.4	17.9	17.5	17.4	21.5	22.5	0.14	0.29	0.29	0.61	1.26	1.74
ENSDARG00000075421	pttg1	-0.04	-0.11	29.5	25.7	25.6	24.2	19.7	19.9	0.03	0.02	0.09	0.03	0.17	0.39
ENSDARG00000053217	cox7a2a	-1.76	0.45	8.6	8.8	10.0	15.2	20.6	34.0	0.08	0.07	0.09	0.19	0.05	0.05
ENSDARG00000098622	ccne1	0.12	-0.08	47.6	31.8	31.4	32.6	35.3	26.4	0.07	0.23	0.35	0.33	0.18	0.16
ENSDARG00000054155	pcna	-0.11	0.09	14.0	12.9	16.2	25.1	28.7	25.1	0.09	0.23	0.20	0.95	0.53	0.82
ENSDARG00000041811	rps25	-0.16	0.39	21.8	18.3	18.0	20.8	29.6	41.1	0.33	0.47	0.62	0.74	0.49	0.41
ENSDARG00000102076	zgc:158852	-0.25	0.08	37.5	37.5	36.1	38.4	20.7	21.9	0.06	0.02	0.04	0.14	0.34	0.62
ENSDARG00000007320	rpl7	-0.33	0.39	14.7	17.0	15.5	13.9	25.6	44.0	0.97	1.43	1.65	2.68	2.45	0.69
ENSDARG00000020850	eef1a1l1	0.30	0.38	19.2	21.8	20.8	28.9	39.2	32.7	0.29	0.11	0.50	0.82	0.56	0.73
ENSDARG00000055655	birc5b	-2.44	0.49	13.5	10.6	11.8	15.2	18.4	11.1	0.81	0.48	0.36	0.51	0.41	1.36
ENSDARG00000026766	bcl2l10	-0.79	0.88	13.4	11.5	14.2	22.6	17.4	18.0	0.18	0.07	0.09	0.20	0.37	0.66
ENSDARG00000006691	rpl12	0.12	0.31	47.5	41.3	42.3	37.6	44.3	43.1	0.76	0.95	0.76	1.09	0.79	0.81
ENSDARG00000023330	anp32b	0.26	0.48	25.7	22.2	19.4	16.5	18.1	24.0	0.14	0.40	0.27	0.31	0.20	0.29
ENSDARG00000038635	magoh	0.11	0.14	22.0	20.3	23.0	26.6	26.0	25.4	0.02	0.01	0.06	0.00	0.07	0.22
ENSDARG00000013968	psap	0.08	0.13	21.5	23.6	31.4	31.1	32.0	29.3	0.01	0.09	0.40	0.42	0.28	0.40
ENSDARG00000056119	eef1g	-0.39	0.30	12.0	11.7	12.1	13.2	20.2	24.2	0.59	1.16	1.59	4.39	2.19	2.02
ENSDARG00000100392	rps18	0.06	0.27	29.9	28.1	29.0	37.6	50.0	47.9	0.04	0.17	0.13	0.33	0.33	0.09
ENSDARG00000057912	eif1axb	-0.30	0.30	10.3	11.4	12.9	21.2	32.7	28.9	0.02	0.09	0.10	0.15	0.10	0.38
ENSDARG00000092798	ppib	-0.17	0.01	11.4	13.1	15.0	25.2	34.3	35.6	0.03	0.03	0.09	0.22	0.23	0.26
ENSDARG00000036180	ccnb2	-0.09	0.16	22.2	24.8	28.2	28.9	17.9	13.2	0.16	0.15	0.26	0.20	0.44	1.50
ENSDARG00000103598	siva1	-0.63	0.18	16.4	15.9	17.2	18.9	18.9	14.3	0.28	0.16	0.14	0.27	0.46	0.93
ENSDARG00000100371	eef2b	0.17	0.21	16.0	13.5	14.5	16.4	24.4	24.5	0.20	0.41	0.29	2.03	1.87	1.28
ENSDARG00000007836	ctsla	0.22	0.04	24.3	21.9	17.6	21.8	21.4	20.4	0.08	0.00	0.10	0.20	0.05	0.41
ENSDARG00000056008	atp5g1	-0.88	0.09	13.4	12.1	14.0	25.9	31.5	26.5	0.06	0.11	0.14	0.39	0.21	0.17
ENSDARG00000052856	khdrbs1a	0.35	0.42	23.9	22.7	25.6	24.0	26.6	30.1	0.09	0.13	0.15	0.42	0.38	0.44
ENSDARG00000008363	mcl1b	-0.20	0.98	22.1	24.1	31.7	36.8	29.1	28.5	0.41	0.33	0.29	0.14	0.35	0.34
ENSDARG00000053990	hmgb2b	-0.20	0.30	25.0	23.9	28.9	37.8	42.4	38.3	0.48	0.15	0.33	0.46	0.36	0.66

ENSDARG00000036678	TRMT10A	-1.10	-0.04	13.7	17.2	22.6	32.2	26.0	29.5	0.05	0.11	0.03	0.09	0.05	0.17
ENSDARG00000020261	rab2a	-1.25	0.25	13.6	14.0	15.6	21.4	26.6	29.2	0.06	0.08	0.06	0.20	0.09	0.37
ENSDARG00000056517	thoc3	-0.62	-0.11	10.2	11.4	15.3	25.4	25.3	23.3	0.08	0.19	0.14	0.17	0.30	0.74
ENSDARG00000026476	tia1l	-0.03	0.07	19.6	29.7	36.5	42.1	55.0	34.8	0.12	0.09	0.17	0.57	0.18	0.81
ENSDARG00000003681	eif5	-0.03	0.59	16.9	16.1	20.7	26.6	22.7	25.0	0.00	0.05	0.03	0.16	0.28	0.47
ENSDARG00000101844	mibp2	-0.15	0.12	9.1	10.1	11.3	15.8	20.0	25.0	0.15	0.09	0.10	0.58	0.83	1.82
ENSDARG00000044562	cycsb	-0.88	0.56	20.1	18.5	26.0	31.6	35.5	32.0	0.02	0.03	0.09	0.00	0.24	0.52
ENSDARG00000074849	rac1a	0.04	-0.11	19.8	30.1	36.8	48.7	37.2	31.3	0.03	0.20	0.42	0.43	0.23	0.66
ENSDARG00000101813	nap1l1	0.02	0.17	17.7	15.0	17.0	22.8	19.9	21.3	0.15	0.19	0.07	0.45	0.58	0.66
ENSDARG00000102624	kif22	0.02	0.54	40.8	44.9	44.7	51.6	28.4	37.5	0.35	0.05	0.09	0.33	0.20	0.18
ENSDARG00000031775	ube2s	-0.60	0.72	15.1	17.3	20.7	26.2	22.0	24.4	0.05	0.03	0.06	0.06	0.11	0.50
ENSDARG00000099612	zgc:66483	0.02	-0.49	16.3	19.6	26.4	34.0	20.3	17.4	0.05	0.05	0.11	0.21	0.26	0.50
ENSDARG00000054818	rpl32	-0.05	0.14	19.2	20.4	19.0	30.1	36.4	37.4	0.09	0.12	0.20	0.24	0.08	0.23
ENSDARG00000068123	gkap1	0.22	0.35	25.8	27.1	26.7	26.6	22.7	21.9	0.02	0.03	0.04	0.07	0.23	0.80
ENSDARG00000012682	pfn2l	-0.03	0.52	15.3	18.6	27.2	29.7	33.0	31.9	0.09	0.15	0.07	0.30	0.24	0.77
ENSDARG00000008049	si:dkey-42i9.4	0.01	0.22	27.4	27.5	28.5	28.7	22.2	16.7	0.09	0.14	0.09	0.28	0.42	0.90
ENSDARG00000004713	mad2l1	-1.50	0.68	17.0	12.0	13.6	18.5	16.9	19.2	0.02	0.14	0.09	0.19	0.15	0.83
ENSDARG00000014047	cldn7b	0.41	0.44	46.3	44.7	42.1	43.5	29.1	27.7	0.10	0.62	0.38	0.85	0.61	1.54
ENSDARG00000037009	banf1	-0.14	0.04	21.0	21.5	26.1	42.0	53.2	38.2	0.53	0.46	0.33	0.54	0.05	0.37
ENSDARG00000044601	rtn4a	-0.28	0.27	19.1	18.0	21.2	29.4	33.1	32.3	0.12	0.05	0.18	0.44	0.26	0.38
ENSDARG00000062002	adnpa	0.05	0.22	19.8	23.8	31.1	37.6	23.2	22.9	0.02	0.03	0.31	0.53	0.38	0.56
ENSDARG00000001788	atp5o	-1.71	0.03	15.1	11.1	10.8	12.9	24.2	27.2	0.06	0.04	0.02	0.07	0.53	0.91
ENSDARG00000057328	cth1	-0.85	-0.02	42.2	36.1	33.4	30.7	19.2	13.5	0.00	0.19	0.06	0.22	0.29	0.83
ENSDARG00000020289	pif1	-0.51	0.23	32.4	21.2	27.4	26.5	16.2	16.8	0.08	0.23	0.15	0.20	0.16	0.10
ENSDARG00000071555	zgc:153675	-0.60	-0.04	17.3	15.5	18.7	31.3	29.4	18.3	0.03	0.12	0.04	0.15	0.41	1.82
ENSDARG00000078473	nucks1a	0.15	0.24	19.4	25.9	24.5	25.8	26.7	31.0	0.21	0.22	0.43	0.34	0.28	0.20
ENSDARG00000074624	si:ch211-198a12.6	0.01	-0.02	13.9	16.6	24.3	34.0	30.7	23.1	0.12	0.14	0.47	0.50	0.45	1.06
ENSDARG00000063100	psmd14	-0.36	0.13	13.6	13.8	14.9	18.2	25.2	26.9	0.05	0.11	0.19	0.54	0.30	0.91
ENSDARG00000052674	csnk1a1	0.13	0.15	18.8	25.2	29.2	35.9	30.3	29.4	0.09	0.18	0.05	0.44	0.28	0.60
ENSDARG00000055753	suv39h1b	-0.19	-0.08	18.4	19.7	25.7	42.0	24.5	21.8	0.05	0.09	0.07	0.09	0.17	0.26
ENSDARG00000044628	dtd1	-1.06	0.23	13.2	13.3	13.2	15.2	20.1	22.5	0.38	0.41	0.37	0.48	0.38	1.22
ENSDARG00000058471	plk1	-0.99	0.44	28.2	17.2	18.3	24.1	20.4	22.4	0.04	0.19	0.21	0.26	0.66	1.21
ENSDARG00000033364	zgc:158387	-0.33	-0.13	16.5	16.0	19.9	32.2	26.7	26.5	0.02	0.09	0.13	0.43	0.21	0.15
ENSDARG00000012505	u2af2a	0.20	0.21	25.5	25.6	29.3	31.3	39.0	28.6	0.06	0.16	0.29	0.34	0.16	0.62
ENSDARG00000103994	ppiab	-0.79	0.25	7.5	7.1	7.6	7.7	9.9	16.8	0.05	0.19	0.39	1.11	1.91	1.13
ENSDARG00000056410	fdx1	-0.14	-0.04	19.8	22.8	27.8	37.7	31.5	23.0	0.02	0.05	0.04	0.07	0.09	0.39
ENSDARG00000005699	ddx19	-0.03	0.20	17.5	18.2	24.8	44.1	40.1	29.4	0.13	0.12	0.23	0.62	0.15	0.79
ENSDARG00000053912	fbl	0.06	0.27	14.0	20.3	29.5	40.6	46.1	41.0	0.00	0.10	0.19	0.45	0.40	0.90
ENSDARG00000104353	nop58	-0.05	0.10	8.7	13.8	22.4	24.7	25.4	24.8	0.22	0.15	0.49	1.00	0.38	1.19
ENSDARG00000036625	polr2f	-0.87	0.66	11.5	12.4	15.5	26.0	27.2	24.1	0.00	0.03	0.11	0.16	0.85	1.59
ENSDARG00000002613	rpa3	-0.14	0.18	29.9	26.0	32.0	39.1	31.1	31.2	0.08	0.23	0.23	0.27	0.22	0.47
ENSDARG00000029003	eif1axa	-1.45	0.31	12.8	10.9	11.6	21.6	18.6	17.5	0.28	0.18	0.10	0.11	0.38	0.60
ENSDARG00000036316	rpl39	-0.80	0.09	12.7	10.2	12.0	21.1	30.0	43.3	0.28	0.31	0.28	0.96	1.43	0.86
ENSDARG00000032849	ndrg1a	0.01	-0.13	20.1	23.6	31.3	53.3	45.3	33.3	0.00	0.14	0.01	0.10	0.47	1.00
ENSDARG00000030871	siah1	-1.83	0.17	17.5	16.0	17.8	18.5	19.5	22.6	0.03	0.01	0.02	0.10	0.11	0.04
ENSDARG00000043631	bcas2	-0.71	0.09	36.1	29.5	35.8	34.8	33.7	33.4	0.08	0.04	0.11	0.02	0.07	0.12
ENSDARG00000058454	dynll1	0.30	0.35	10.8	15.0	17.2	23.2	33.5	27.3	0.17	0.11	0.32	0.00	0.30	0.37
ENSDARG00000008480	trmt61a	-0.17	-0.24	13.4	16.9	24.7	35.8	25.3	20.9	0.02	0.03	0.05	0.44	0.30	0.54
ENSDARG00000041182	rpl4	-0.48	0.16	13.7	13.4	16.8	22.8	27.8	39.9	0.14	0.12	0.15	0.61	0.74	0.25
ENSDARG00000002403	nusap1	-0.65	0.71	9.4	12.3	15.5	24.6	20.2	21.2	0.11	0.19	0.15	0.30	0.20	0.31
ENSDARG00000019644	ldhba	-0.42	-0.15	12.5	13.3	13.4	22.3	33.3	30.3	0.05	0.16	0.19	0.89	0.54	1.90
ENSDARG00000043177	lsm1	-1.09	0.43	15.0	16.2	23.6	31.1	23.8	22.4	0.04	0.06	0.02	0.08	0.19	0.67
ENSDARG00000032725	rps27a	-0.51	0.36	13.3	14.9	13.9	16.9	37.3	52.3	0.11	0.13	0.06	0.19	0.38	0.42
ENSDARG00000004735	hnrnpub	0.17	0.22	13.0	21.3	21.9	25.2	24.7	22.1	0.03	0.23	0.40	0.78	0.51	1.22
ENSDARG00000087869	si:ch211-11k18.4	-0.42	-0.28	18.7	20.0	22.5	27.5	18.0	24.0	0.12	0.10	0.08	0.25	0.73	1.22
ENSDARG00000103007	rps3	-0.33	0.34	12.1	11.6	13.3	13.9	17.0	21.1	0.21	0.24	0.20	0.87	1.04	0.42
ENSDARG00000005254	kdelr2a	-0.09	0.14	16.3	19.7	27.6	38.5	39.9	26.8	0.17	0.08	0.18	0.32	0.32	0.31
ENSDARG00000057854	sap18	0.07	0.21	16.5	19.0	23.7	27.1	26.8	25.9	0.07	0.03	0.08	0.26	0.15	0.31
ENSDARG00000020711	rrm2	0.17	0.34	34.2	36.1	34.3	33.7	23.0	16.9	0.40	0.46	0.15	0.55	0.66	0.86
ENSDARG00000092919	zp3c	-0.93	-0.51	9.3	10.8	13.5	20.8	22.2	19.6	0.08	0.08	0.24	0.71	1.00	0.55
ENSDARG00000098453	pank4	-0.16	-0.30	11.9	18.3	25.0	45.5	37.0	18.5	0.05	0.01	0.05	0.19	0.00	0.48
ENSDARG00000007960	hnrnpaba	0.86	-0.19	42.9	33.6	33.5	30.0	35.7	35.6	0.17	0.08	0.22	0.30	0.15	0.38
ENSDARG00000016318	med7	-0.36	0.14	9.0	11.2	17.6	38.8	26.5	25.0	0.00	0.05	0.05	0.30	0.49	0.31
ENSDARG00000038900	acadm	-0.81	-0.48	10.4	8.5	11.2	17.3	25.0	21.4	0.07	0.24	0.29	0.76	0.81	1.41
ENSDARG00000043960	rpf2	-0.33	-0.08	7.8	10.4	11.9	18.0	22.1	24.6	0.41	0.34	0.61	1.48	1.47	1.70
ENSDARG00000033597	api5	0.04	0.10	20.6	31.5	45.5	60.6	52.5	35.4	0.03	0.11	0.03	0.54	0.40	0.67
ENSDARG00000007377	odc1	0.00	0.03	28.7	33.4	30.2	31.2	28.4	25.3	0.00	0.10	0.00	0.05	0.34	0.46
ENSDARG00000056186	eif5a2	-0.20	0.31	16.6	14.3	15.6	19.9	32.5	42.1	0.13	0.16	0.20	0.82	0.72	0.43
ENSDARG00000036675	hnrnpa1b	0.99	-0.03	23.1	22.8	20.9	20.4	20.8	23.4	0.24	0.11	0.04	0.11	0.16	0.37
ENSDARG00000011373	mknk2a	-0.39	-0.27	24.0	18.8	20.3	25.1	17.7	15.6	0.13	0.28	0.17	0.40	0.48	0.75
ENSDARG00000029856	cnn3b	-0.03	0.21	41.4	28.2	30.5	39.6	25.0	24.1	0.00	0.15	0.19	0.27	0.75	0.88

ENSDARG00000104011	rps17	0.23	0.29	32.1	30.5	32.8	30.7	36.0	34.9	0.12	0.11	0.24	0.24	0.17	0.48
ENSDARG00000100741	cdc20	0.00	0.35	25.1	26.1	28.2	32.7	22.0	20.2	0.10	0.17	0.17	0.20	0.66	1.36
ENSDARG00000052334	ociad1	-0.69	-0.05	18.0	16.2	19.3	24.3	29.1	26.5	0.04	0.08	0.09	0.31	0.24	1.00
ENSDARG00000037188	rpa2	-0.36	0.25	9.6	11.0	12.5	21.8	27.7	27.7	0.03	0.07	0.04	0.21	0.27	0.41
ENSDARG00000073787	si:ch73-303b9.1	-0.88	0.15	20.5	14.0	13.8	18.1	20.4	21.1	0.09	0.23	0.17	0.34	0.39	0.67
ENSDARG00000100528	map1lc3c	-1.45	0.17	14.6	12.0	14.5	23.9	19.4	19.1	0.17	0.09	0.13	0.16	0.55	1.40
ENSDARG00000019230	rpl7a	-0.24	0.34	13.1	10.3	11.7	10.1	18.1	32.2	0.14	0.35	0.45	0.55	0.61	0.50
ENSDARG00000021669	sec61a1	0.04	0.15	14.1	15.8	18.3	22.3	24.5	26.0	0.04	0.18	0.10	0.33	0.30	0.37
ENSDARG00000014770	usp4	-0.26	0.09	16.2	15.2	17.7	22.6	23.2	21.7	0.00	0.11	0.15	0.18	0.33	0.81
ENSDARG00000010487	sae1	0.05	0.17	16.8	21.7	25.2	36.8	33.0	30.0	0.10	0.11	0.06	0.32	0.10	0.28
ENSDARG00000005772	tsr2	-0.42	-0.14	11.1	10.7	12.7	21.0	24.2	23.5	0.06	0.04	0.10	0.06	0.16	0.29
ENSDARG00000017230	fbxw11b	-0.84	0.07	10.3	11.9	16.4	28.4	22.3	25.4	0.16	0.07	0.21	0.52	1.14	0.69
ENSDARG00000018890	snrpa	0.05	0.27	29.5	32.0	38.4	45.0	42.4	27.8	0.08	0.19	0.02	0.13	0.13	0.47
ENSDARG00000020465	ewsr1b	0.13	0.69	49.8	45.5	54.4	50.2	47.0	34.4	0.00	1.14	0.50	0.12	0.21	0.36
ENSDARG00000100918	prc1a	-0.10	-0.27	18.0	26.5	33.5	37.7	30.9	26.9	0.13	0.10	0.08	0.28	0.29	0.85
ENSDARG00000101624	lmnb2	-0.14	0.63	15.0	21.3	21.4	24.7	24.2	22.7	1.04	0.05	0.46	0.85	0.84	0.75
ENSDARG00000104227	nop10	-0.23	0.16	12.7	12.3	16.0	25.6	24.1	25.9	0.06	0.04	0.12	0.11	0.10	0.29
ENSDARG00000039880	arpp19b	-0.23	1.01	18.7	20.9	24.8	26.7	25.2	31.8	0.00	0.01	0.01	0.12	0.09	0.56
ENSDARG00000089922	DSN1	-0.34	-0.34	9.9	12.2	18.9	34.1	20.6	25.1	0.07	0.11	0.11	0.29	0.27	0.84
ENSDARG00000041607	eif4ebp3l	0.11	0.15	26.4	33.3	32.9	36.7	33.9	29.3	0.00	0.06	0.28	0.14	0.13	0.29
ENSDARG00000020008	vcp	-0.05	0.11	14.8	16.0	17.2	16.9	23.9	35.6	2.04	1.82	1.51	1.27	1.40	1.80
ENSDARG00000055973	zar1l	-2.03	-0.36	11.7	8.2	8.0	9.7	10.2	10.4	0.00	0.01	0.06	0.22	0.33	0.00
ENSDARG00000044521	eef1b2	-0.42	0.13	11.9	12.9	12.3	16.4	17.0	18.1	0.08	0.06	0.17	0.68	0.65	0.95
ENSDARG00000023298	rps27.1	-0.20	0.45	20.8	21.1	20.1	23.3	27.7	26.1	0.06	0.51	1.08	1.27	0.81	0.18
ENSDARG00000093931	fam101b	-0.28	-0.01	25.7	25.9	30.4	35.9	22.8	22.7	0.00	0.11	0.21	0.14	0.00	0.00
ENSDARG00000028106	glrx	-0.85	-0.16	5.6	6.1	7.9	19.7	22.9	23.9	0.87	0.74	0.62	0.56	0.25	0.14
ENSDARG00000070437	rpl22	-0.32	0.18	16.2	15.5	15.8	20.8	28.5	38.5	0.11	0.25	0.34	0.55	0.86	0.30
ENSDARG00000063021	rpain	-1.39	0.42	49.6	15.2	13.1	16.6	15.2	17.6	0.14	0.01	0.02	0.09	0.13	0.38
ENSDARG00000019181	rpsa	-0.51	0.34	11.7	9.6	10.1	11.3	16.8	36.1	0.75	1.15	1.37	2.93	3.46	1.91
ENSDARG00000031435	zgc:56493	-0.42	-0.01	10.4	11.5	14.7	29.3	34.1	31.8	0.00	0.05	0.10	0.19	0.10	0.66
ENSDARG00000037995	gdf3	-0.19	-0.29	19.0	22.6	31.7	39.5	24.3	15.0	0.04	0.02	0.08	0.08	0.11	1.00
ENSDARG00000036875	rps12	-0.27	0.34	19.6	14.3	13.9	14.8	17.9	21.1	0.73	0.82	0.76	1.78	1.03	0.95
ENSDARG00000004937	skp2	-0.29	0.54	16.0	18.2	24.6	31.1	25.9	20.8	0.00	0.06	0.31	0.73	0.42	0.98
ENSDARG00000042539	ywhaqa	-0.39	0.31	10.6	12.6	16.1	30.1	28.7	26.6	0.12	0.16	0.20	0.61	0.14	0.45
ENSDARG00000046030	zgc:110339	-1.07	0.15	10.0	10.6	13.1	18.1	20.8	25.4	0.07	0.30	0.40	1.04	0.69	1.58
ENSDARG00000061963	vrtn	0.08	0.52	26.1	37.1	44.6	52.4	44.9	34.7	0.09	0.13	0.07	0.15	0.16	0.91
ENSDARG00000087647	sept7a	0.14	-0.07	50.1	61.4	68.8	80.9	61.2	36.5	0.18	0.06	0.08	0.40	0.00	0.43
ENSDARG00000035625	snrnp27	-0.11	0.13	24.2	19.7	26.8	45.7	40.4	33.5	0.04	0.04	0.00	0.03	0.08	0.85
ENSDARG00000025566	slc25a3b	-0.45	0.44	12.5	12.9	14.8	20.0	24.5	28.1	0.17	0.05	0.02	0.42	0.52	0.20
ENSDARG00000090768	zp3.2	-1.33	-0.47	10.2	10.6	12.5	18.7	27.0	27.0	0.25	0.24	0.31	0.88	2.58	2.46
ENSDARG00000053457	rpl23	-0.05	0.17	18.8	16.7	20.3	27.6	32.3	35.9	0.07	0.17	0.13	0.91	0.28	0.51
ENSDARG00000025073	rpl18a	-0.38	0.34	19.8	19.8	19.1	18.0	28.7	28.0	0.12	0.24	0.24	1.12	0.68	0.19
ENSDARG00000054804	anp32e	0.25	0.39	37.1	25.9	29.6	33.0	38.6	42.7	0.00	0.26	0.00	0.33	0.09	0.23
ENSDARG00000070849	rps15	-0.07	0.29	18.8	16.9	17.1	20.5	24.8	33.7	0.04	0.19	0.46	0.92	1.15	0.16
ENSDARG00000052518	stx4	-0.46	-0.13	18.3	18.1	27.4	31.2	22.5	18.9	0.02	0.10	0.14	0.29	0.26	0.58
ENSDARG00000036190	txnl4a	0.04	0.30	23.6	17.3	26.0	37.6	27.4	28.8	0.03	0.07	0.14	0.19	0.13	0.37
ENSDARG00000070828	actl6a	0.02	0.23	16.8	20.4	25.5	37.7	32.5	27.1	0.05	0.04	0.17	0.20	0.24	0.17
ENSDARG00000009447	atp5g3b	-0.76	0.24	10.7	9.3	9.6	13.1	16.9	23.2	0.06	0.10	0.10	0.12	0.36	0.43
ENSDARG00000012718	wee2	-0.13	-0.55	30.8	28.7	24.9	27.5	16.5	17.7	0.07	0.40	0.40	0.29	0.41	1.00
ENSDARG00000012820	nop56	0.04	0.21	9.1	13.9	21.6	39.5	35.9	29.5	0.19	0.21	0.17	0.31	0.74	1.14
ENSDARG00000004405	snx10a	-1.33	0.40	12.2	12.2	15.1	23.0	16.1	22.4	0.06	0.11	0.11	0.18	0.21	0.36
ENSDARG00000075795	nol7	-0.49	0.22	10.7	11.8	17.2	37.0	30.6	32.6	0.05	0.05	0.05	0.21	0.13	0.24
ENSDARG00000105036	arl6ip4	-0.15	0.23	11.8	17.1	23.5	36.4	28.0	28.0	0.02	0.01	0.04	0.06	0.18	0.15
ENSDARG00000014329	npm1a	0.09	0.26	20.5	24.6	26.5	40.4	38.5	38.3	0.06	0.03	0.06	0.17	0.14	0.63
ENSDARG00000001940	dnajc1	0.02	-0.07	22.6	24.8	26.2	31.8	29.2	25.0	0.21	0.13	0.21	0.41	0.46	0.51
ENSDARG00000038239	tnpo2	0.05	0.27	20.6	18.6	20.2	22.5	25.2	22.1	0.29	0.37	0.46	1.32	0.64	0.43
ENSDARG00000035871	rpl30	0.22	0.13	19.6	17.0	18.4	23.1	29.1	36.8	0.00	0.12	0.26	0.68	0.53	0.19
ENSDARG00000075445	psmb5	-0.15	0.18	17.5	17.4	19.7	30.7	24.5	24.0	0.06	0.07	0.10	0.08	0.49	0.69
ENSDARG00000011405	rps9	0.07	0.14	16.1	17.6	17.8	22.0	27.6	30.4	0.12	0.11	0.09	0.41	0.53	0.21
ENSDARG00000076439	ppp4cb	0.11	0.21	22.0	24.6	24.4	23.4	18.9	20.8	0.08	0.19	0.02	0.09	0.11	0.58
ENSDARG00000002710	ncl	0.10	0.23	9.9	13.3	18.0	22.9	24.8	23.5	0.04	0.14	0.18	0.42	0.20	0.53
ENSDARG00000035570	zgc:101016	-0.52	-0.16	9.9	11.0	14.9	25.9	27.9	20.4	0.43	0.29	0.29	0.42	0.83	1.23
ENSDARG00000068820	h2afva	-0.16	0.14	26.0	26.0	30.0	33.8	33.5	27.3	0.00	0.16	0.06	0.02	0.37	1.03
ENSDARG00000077732	alyref	0.12	0.05	17.4	26.0	36.9	45.9	43.7	38.7	0.06	0.09	0.00	0.43	0.05	0.25
ENSDARG00000008803	marcksb	0.21	0.14	69.9	48.2	51.0	36.1	59.8	55.5	0.00	0.22	0.06	0.36	0.15	0.23
ENSDARG00000090912	npc2	-0.09	-0.25	40.9	26.8	29.7	39.8	28.1	33.5	0.67	0.25	0.29	0.51	0.33	1.04
ENSDARG00000099039	pcbp2	-0.09	0.15	19.0	29.6	41.4	51.0	55.0	35.1	0.00	0.04	0.03	0.44	0.59	0.33
ENSDARG00000007438	ube2ib	-0.63	0.23	37.3	27.6	29.1	22.7	22.0	26.1	0.00	0.07	0.29	0.15	0.61	1.39
ENSDARG00000038068	ddx5	0.84	0.73	35.2	35.0	42.8	23.4	29.1	23.6	0.00	0.69	0.21	0.38	0.26	0.55
ENSDARG00000051854	cdt1	-0.15	0.04	10.5	14.9	24.7	32.5	23.5	17.5	0.22	0.16	0.17	0.43	0.50	0.64
ENSDARG00000040510	ca15b	-1.11	0.14	10.7	10.0	12.9	17.4	17.0	13.8	0.32	0.19	0.24	0.39	0.85	0.55

ENSDARG00000015543	s100a1	-0.79	-0.04	11.4	14.5	16.7	36.7	40.4	36.4	0.22	0.09	0.29	0.18	0.11	0.78
ENSDARG00000013931	eif3m	-0.11	0.32	18.5	16.0	17.3	27.5	27.6	31.6	0.02	0.09	0.11	0.19	0.19	0.19
ENSDARG00000025391	pfdn2	-0.61	0.17	19.2	18.9	23.2	26.6	28.4	27.6	0.02	0.13	0.17	0.17	0.21	0.37
ENSDARG00000074242	serbp1a	-0.05	0.17	9.8	11.7	14.9	23.6	46.5	44.5	0.76	0.51	0.92	1.49	0.44	0.58
ENSDARG00000057556	rpl17	-0.32	0.16	17.0	20.4	19.6	26.1	29.4	37.1	0.00	0.06	0.20	0.71	0.41	0.44
ENSDARG00000037283	plrg1	-0.19	0.13	17.3	22.4	27.3	41.4	39.9	26.6	0.11	0.07	0.15	0.14	0.38	0.51
ENSDARG00000102291	eef1da	-0.19	-0.12	14.4	13.1	13.2	14.8	20.2	22.9	0.18	0.09	0.31	1.11	1.04	0.88
ENSDARG00000101037	asf1ba	-1.97	0.06	16.6	18.2	20.9	29.3	30.5	29.8	0.01	0.02	0.04	0.15	0.03	1.24
ENSDARG00000014571	ctnnb1	0.20	0.21	23.1	31.4	34.3	33.0	29.9	36.1	0.19	0.16	0.56	1.17	0.44	0.18
ENSDARG00000024681	pane1	-0.92	0.25	14.4	12.3	14.3	20.3	17.0	15.9	0.00	0.01	0.02	0.13	0.33	0.37
ENSDARG00000037559	uba1	0.11	0.54	16.1	23.4	33.9	47.1	18.4	17.9	0.11	0.18	0.33	0.86	1.21	2.17
ENSDARG00000003952	pfn2	0.00	0.13	8.7	12.3	16.0	21.7	19.0	20.3	0.16	0.13	0.20	0.45	0.38	0.65
ENSDARG00000077620	cdca7a	0.01	0.08	25.7	27.6	33.2	34.0	26.4	30.6	0.03	0.12	0.32	0.52	0.42	0.62
ENSDARG00000059461	mepce	0.10	0.18	19.1	22.0	28.5	34.9	19.9	22.4	0.29	0.07	0.20	0.33	0.40	0.00
ENSDARG00000044774	pou5f3	0.08	0.29	23.1	28.1	37.0	36.2	38.7	21.5	0.22	0.15	0.23	0.82	0.42	0.70
ENSDARG00000001558	kifc1	-0.13	0.36	14.6	15.9	20.5	31.6	18.3	19.7	0.10	0.08	0.19	0.13	0.85	1.08
ENSDARG00000042063	si:ch211-145c1.1	-1.21	-0.26	10.2	9.4	11.9	20.5	16.1	18.2	0.50	0.25	0.20	0.47	0.17	1.90
ENSDARG00000101766	ptmab	0.24	0.05	11.9	13.7	19.6	25.6	37.9	33.5	0.09	0.26	0.39	0.47	0.43	0.53
ENSDARG00000010332	zgc:56231	-1.13	-0.04	33.7	21.5	21.5	23.9	17.7	22.9	0.19	0.06	0.14	0.16	1.08	0.00
ENSDARG00000077870	taf9	-0.44	0.00	15.0	14.2	16.7	41.6	28.2	30.6	0.06	0.15	0.13	0.23	0.33	1.12
ENSDARG00000011125	snrpb	-0.07	0.17	19.7	17.0	16.8	17.5	18.4	22.7	0.11	0.16	0.22	0.24	0.44	0.46
ENSDARG00000019778	rps6	-0.57	0.41	16.3	14.4	14.8	18.6	19.5	21.8	0.20	0.46	0.30	0.78	0.47	0.26
ENSDARG00000020298	btg2	0.01	-0.07	12.9	18.6	27.3	32.5	21.0	15.4	0.03	0.19	0.23	0.33	1.02	1.52
ENSDARG00000023394	slc37a2	0.03	-0.14	14.6	21.2	30.8	47.1	45.9	27.9	0.12	0.05	0.05	0.42	0.24	0.41
ENSDARG00000057691	srsf1a	0.17	0.15	38.8	33.7	26.6	32.6	33.6	31.0	0.00	0.00	0.15	0.16	0.02	0.06
ENSDARG00000017659	sps2	0.10	0.11	24.1	25.4	31.5	31.2	38.7	27.3	0.31	0.13	0.05	0.21	0.18	1.16
ENSDARG00000021838	rps23	-0.24	0.73	20.9	20.5	20.4	22.0	33.3	42.6	0.07	0.06	0.19	0.38	0.51	0.34
ENSDARG00000038720	si:ch211-14a17.7	-1.22	-0.03	8.6	8.3	9.1	11.4	14.0	14.7	0.39	0.32	0.56	1.66	2.38	1.71
ENSDARG00000038768	mrpl12	-1.38	0.28	9.7	10.8	12.7	18.6	16.6	21.1	0.11	0.17	0.16	0.38	0.42	0.61
ENSDARG00000099366	supt4h1	0.09	-0.01	24.1	17.9	17.9	20.0	21.4	20.0	0.04	0.00	0.01	0.00	0.00	0.21
ENSDARG00000010516	rpl21	-0.47	0.23	14.4	11.2	12.8	13.6	23.5	36.8	0.13	0.44	0.57	1.58	0.90	0.80
ENSDARG00000003570	hsp90b1	-0.62	-0.37	10.3	10.8	12.2	15.5	20.6	19.3	1.02	1.30	1.19	2.36	1.27	1.71
ENSDARG00000007755	wdr61	-0.22	0.19	12.4	12.9	15.5	19.8	20.9	19.6	0.03	0.01	0.01	0.08	0.21	0.35
ENSDARG00000091831	ddx27	-0.04	0.47	9.5	10.0	13.5	29.9	19.9	24.9	0.25	0.18	0.32	0.70	0.66	0.67
ENSDARG00000070959	si:ch211-288g17.3	0.01	0.14	14.0	23.5	35.4	56.3	57.3	48.9	0.02	0.05	0.13	0.20	0.19	0.50
ENSDARG00000045075	tmem106a	-0.22	-0.18	14.7	13.7	21.6	35.1	28.4	37.1	0.02	0.10	0.07	0.54	0.49	0.21
ENSDARG00000056509	pdik1l	0.09	-0.59	16.0	23.5	33.0	45.2	24.1	28.9	0.02	0.00	0.24	0.25	0.51	0.14
ENSDARG00000046048	vapal	-0.95	0.08	14.0	14.0	16.0	21.5	23.2	23.4	0.09	0.20	0.18	0.22	0.41	1.61
ENSDARG00000071566	ppp1cab	0.16	0.18	25.6	31.4	21.9	24.8	26.7	23.6	0.03	0.18	0.03	0.11	0.04	0.11
ENSDARG00000008936	sec11a	-0.09	-0.02	14.5	22.4	30.5	38.4	33.6	29.0	0.05	0.05	0.07	0.04	0.08	0.23
ENSDARG00000025581	rpl10	-0.35	0.24	27.1	28.2	27.6	31.0	33.8	35.1	0.00	0.15	0.29	1.53	0.15	0.46
ENSDARG00000102750	cdh1	0.41	-0.10	37.9	37.4	33.1	36.9	32.9	34.3	0.06	0.62	0.43	1.24	1.76	1.16
ENSDARG00000014244	rbmx	0.27	0.28	56.4	25.6	27.8	35.1	40.3	29.0	0.00	0.13	0.00	0.04	0.12	0.41
ENSDARG00000042927	mapre1a	0.02	0.16	17.7	19.8	23.6	33.3	19.0	15.9	0.04	0.07	0.07	0.28	0.42	0.39
ENSDARG00000043453	rps5	-0.65	0.00	22.7	22.6	23.1	26.1	33.1	44.1	0.00	0.06	0.14	0.69	1.41	0.13
ENSDARG00000005355	larp6	-0.19	-0.07	9.3	10.1	12.5	12.2	13.6	13.1	0.02	0.16	0.23	0.87	1.20	3.04
ENSDARG00000007795	cst3	3.00	0.73	15.5	14.4	17.2	43.2	42.1	39.8	0.18	0.06	0.21	0.71	0.62	0.36
ENSDARG00000101009	cited4b	0.59	0.07	9.4	10.1	11.2	16.3	17.1	19.3	0.18	0.16	0.18	0.30	0.25	0.59
ENSDARG00000058729	akirin2	0.01	0.23	34.4	33.6	38.2	41.0	28.2	31.6	0.00	0.06	0.03	0.36	0.29	0.09
ENSDARG00000043976	etf1b	-0.11	-0.26	10.3	11.2	14.5	22.8	26.0	24.8	0.22	0.05	0.31	1.05	0.77	0.78
ENSDARG00000105116	p4hb	0.06	0.01	21.3	22.4	25.6	28.5	29.4	35.4	0.08	0.31	0.19	0.63	0.48	1.05
ENSDARG00000002267	dcaf13	-0.08	0.08	10.3	12.7	14.1	36.2	31.8	34.7	0.42	0.46	0.27	0.61	0.63	1.45
ENSDARG00000099579	aldh18a1	-0.30	-0.19	17.8	16.1	18.7	29.9	33.5	23.5	0.09	0.14	0.20	0.60	0.41	1.03
ENSDARG00000058354	selt1a	-0.64	0.20	13.0	14.6	17.8	24.8	21.3	21.0	0.22	0.10	0.05	0.16	0.29	1.33
ENSDARG00000029533	rpl18	0.00	0.42	21.3	18.9	22.6	36.0	36.2	40.7	0.00	0.22	0.38	0.29	0.05	0.24
ENSDARG00000043848	sod1	-0.76	0.11	14.6	16.0	20.9	25.9	17.2	25.8	0.30	0.45	0.39	0.64	0.77	1.20
ENSDARG00000012672	gtf2e2	-0.07	0.26	10.8	13.7	22.2	39.6	31.7	22.5	0.05	0.04	0.04	0.17	0.31	0.48
ENSDARG00000071478	lnx2b	0.06	0.15	26.8	25.5	29.3	31.1	19.2	22.7	0.04	0.11	0.14	0.01	0.10	0.19
ENSDARG00000012369	rdh10b	-1.36	0.62	9.2	9.3	10.1	10.9	17.4	24.8	0.19	0.20	0.22	1.35	0.73	1.68
ENSDARG00000019444	ssr4	-0.39	0.05	11.8	16.1	21.9	34.5	31.9	36.5	0.27	0.15	0.11	0.34	0.41	0.58
ENSDARG00000019293	tfdp1a	-0.23	0.04	13.5	17.1	24.2	39.9	36.1	31.4	0.09	0.07	0.07	0.28	0.28	0.46
ENSDARG00000086425	prpf3	0.04	0.21	13.8	22.3	25.2	38.2	33.2	28.2	0.11	0.04	0.25	0.15	0.42	1.02
ENSDARG00000088091	pfn1	-0.22	0.84	24.6	20.8	23.5	26.8	40.2	40.1	0.05	0.19	0.21	0.66	0.38	0.92
ENSDARG00000087528	snip1	-0.12	0.10	12.3	15.5	20.3	48.5	31.0	28.8	0.27	0.13	0.07	0.29	0.64	1.45
ENSDARG00000091150	mki67	0.16	0.34	13.5	20.5	30.0	39.0	33.9	21.2	0.27	0.09	0.14	0.41	0.31	1.56
ENSDARG00000012222	nup35	0.04	0.28	23.9	25.0	34.9	40.6	19.1	19.9	0.11	0.07	0.22	0.29	0.63	1.32
ENSDARG00000015128	rpl27	-0.40	0.21	14.4	17.5	18.6	18.8	31.4	45.1	0.11	0.04	0.04	0.21	0.13	0.27
ENSDARG00000029071	creld2	-0.87	0.17	22.0	20.7	22.0	28.2	18.0	34.0	0.00	0.01	0.04	0.06	0.20	0.00
ENSDARG00000031317	ppdpfb	-1.09	0.34	43.2	34.7	33.9	34.1	28.0	30.4	0.00	0.34	0.07	0.20	0.13	0.85
ENSDARG00000026908	tmed2	-0.23	-0.01	17.6	18.2	21.0	44.6	38.7	30.0	0.06	0.07	0.10	0.29	0.66	0.76
ENSDARG00000019137	tram1	-0.11	-0.11	9.6	13.7	25.0	44.6	28.2	39.1	0.09	0.12	0.16	0.34	0.46	0.25

ENSDARG00000014017	rrm1	-0.74	0.45	18.1	17.4	20.3	22.2	24.8	23.8	0.13	0.20	0.14	0.47	0.55	0.83
ENSDARG00000014013	lbr	-0.04	-0.25	15.3	21.1	26.3	36.3	29.4	24.8	0.17	0.05	0.03	0.03	0.16	0.51
ENSDARG00000005791	rpl28	-0.16	0.12	23.8	23.5	23.4	27.7	30.1	39.5	0.00	0.13	0.00	0.35	0.03	0.17
ENSDARG00000044093	rpl13a	-0.74	0.61	8.8	10.0	10.2	12.7	17.1	21.4	0.76	0.39	0.65	1.21	0.72	0.59
ENSDARG00000075008	pask	-0.43	-0.01	13.3	13.6	20.8	29.1	15.1	14.5	0.34	0.44	0.35	0.16	0.38	0.75
ENSDARG00000088130	si:dkey-30c15.10	-1.13	-0.05	15.7	14.4	15.5	19.2	23.5	23.2	0.00	0.01	0.02	0.10	0.21	0.36
ENSDARG00000006225	ddx39aa	0.12	0.35	24.5	10.4	10.3	16.2	17.0	19.3	0.75	0.86	0.91	0.64	0.71	0.90
ENSDARG00000087402	TPM1	-1.09	0.01	31.2	22.4	22.3	27.8	20.8	19.2	0.00	0.04	0.09	0.06	0.43	0.33
ENSDARG00000015239	prp19	0.12	0.25	54.7	35.3	31.4	37.4	36.2	27.1	0.25	0.23	0.07	0.09	0.04	0.32
ENSDARG00000039969	akirin1	0.14	0.02	32.8	40.4	46.1	52.5	41.6	37.9	0.00	0.19	0.08	0.00	0.15	0.35
ENSDARG00000070475	khdrbs1b	0.04	0.29	17.4	19.6	27.3	34.8	50.1	33.3	0.03	0.08	0.28	0.38	0.32	0.23
ENSDARG00000035678	zgc:91910	-0.13	0.15	20.2	22.5	28.4	42.7	40.7	32.4	0.25	0.11	0.09	0.13	0.24	0.64
ENSDARG00000070570	ppp4ca	0.08	0.11	15.9	17.5	21.5	43.7	19.6	27.8	0.08	0.05	0.10	0.06	0.10	0.23
ENSDARG00000096095	buc	-0.88	-0.14	9.6	11.1	15.6	25.5	15.1	12.7	0.20	0.24	0.35	0.53	0.11	0.00
ENSDARG00000040184	syncrip	-0.18	0.20	14.9	11.5	15.3	28.3	29.8	27.1	0.21	0.18	0.28	0.55	0.34	0.91
ENSDARG00000062472	sin3b	-0.36	0.20	10.9	13.7	18.5	25.5	21.1	18.6	0.05	0.02	0.12	0.58	0.13	0.40
ENSDARG00000057497	stk35l	0.24	0.06	23.6	23.2	23.3	26.3	19.3	22.0	0.32	0.32	0.24	0.51	0.53	0.48
ENSDARG00000035171	btg4	-1.81	0.63	11.9	10.6	11.8	15.3	12.6	36.0	0.04	0.08	0.05	0.09	0.00	
ENSDARG00000020232	eif6	-0.49	0.19	12.2	12.8	14.6	21.2	18.1	22.8	0.07	0.25	0.36	0.70	0.60	0.85
ENSDARG00000045940	lsm12b	-0.48	-0.31	11.3	11.3	12.4	26.9	20.6	23.0	0.14	0.24	0.25	0.24	0.49	0.58
ENSDARG00000045776	cnbpa	-0.08	0.23	9.3	13.1	18.9	44.4	46.7	35.4	0.19	0.16	0.38	0.53	0.76	1.35
ENSDARG00000040513	zgc:92313	-1.30	0.47	20.0	13.6	15.3	21.6	20.5	17.4	0.47	0.20	0.21	0.28	0.17	0.59
ENSDARG00000040725	zgc:114130	0.07	-0.10	18.9	21.5	21.8	24.3	18.3	18.2	0.06	0.03	0.12	0.28	0.29	0.13
ENSDARG00000015998	wdhd1	-0.39	0.15	22.7	16.8	14.3	13.1	16.6	13.8	0.08	0.31	0.27	0.44	1.60	2.06
ENSDARG00000009753	sf3b6	0.19	0.16	26.8	29.0	33.6	45.9	36.6	29.6	0.13	0.04	0.09	0.05	0.31	0.60
ENSDARG00000026842	acin1b	0.04	0.49	9.4	11.9	13.9	23.9	23.3	21.0	0.64	0.27	0.25	0.80	0.83	1.31
ENSDARG00000038754	plk3	-0.86	0.23	15.1	14.2	16.7	20.3	16.4	18.7	0.18	0.16	0.16	0.30	0.46	0.19
ENSDARG00000105293	srsf4	0.04	0.30	19.6	29.1	37.9	58.9	57.6	34.5	0.00	0.07	0.17	0.17	0.10	0.25
ENSDARG00000101332	uba2	-0.32	0.06	9.1	9.6	12.1	19.6	25.9	23.3	0.07	0.08	0.20	0.52	0.78	1.15
ENSDARG00000003035	hspa9	-0.47	-0.15	10.8	13.0	18.2	32.0	31.0	28.8	0.04	0.31	0.20	0.53	0.63	1.11
ENSDARG00000044298	phax	-0.79	-0.28	13.2	14.5	15.7	17.9	26.0	17.0	0.12	0.14	0.23	0.49	0.50	1.93
ENSDARG00000036060	exosc6	-0.75	0.30	9.6	10.7	12.7	18.5	21.4	17.9	0.00	0.04	0.01	0.16	0.15	0.51
ENSDARG00000092115	eif4a1a	0.09	0.26	22.9	19.6	18.6	25.9	27.4	25.6	0.16	0.52	0.21	0.20	0.40	0.68
ENSDARG00000024844	max	-0.06	0.35	11.4	14.7	20.4	37.6	31.8	23.2	0.11	0.08	0.08	0.60	0.58	1.06
ENSDARG00000008859	mylipa	-0.71	0.32	15.9	19.7	26.3	30.0	18.2	12.5	0.02	0.13	0.07	0.05	0.65	0.78
ENSDARG00000039830	gng5	0.03	0.34	33.6	34.5	44.4	55.1	45.3	37.3	0.00	0.02	0.25	0.05	0.22	0.23
ENSDARG00000003757	cnpy1	-0.59	-0.12	19.4	20.1	20.6	35.1	24.0	30.8	0.35	0.43	0.24	0.34	0.32	0.85
ENSDARG00000026448	med29	-2.40	0.67	17.1	15.3	16.7	20.9	20.9	23.6	0.03	0.00	0.14	0.07	0.89	0.37
ENSDARG00000039345	drg1	-0.22	-0.06	9.7	12.7	15.8	34.4	39.0	26.5	0.15	0.09	0.14	0.34	0.33	0.78
ENSDARG00000026185	ccdc94	-0.09	0.24	11.9	14.0	18.4	33.6	21.9	21.7	0.07	0.04	0.03	0.57	0.40	0.54
ENSDARG00000103409	uhrf1	0.03	0.21	28.0	21.5	20.6	22.2	20.5	16.3	0.44	0.34	0.26	0.86	0.55	1.78
ENSDARG00000014324	sh2d5	-0.85	-0.50	34.2	30.0	29.2	18.2	15.9	9.5	0.33	0.08	0.29	0.06	0.20	0.00
ENSDARG00000086309	erlec1	0.05	-0.14	12.4	15.5	21.8	30.8	20.5	18.6	0.03	0.03	0.05	0.00	0.39	0.94
ENSDARG00000075314	zgc:174906	-0.34	0.67	12.7	16.3	20.5	30.8	17.7	22.5	0.00	0.04	0.05	0.05	0.00	0.43
ENSDARG00000026072	pdcd5	-0.18	0.09	14.4	14.9	19.4	38.4	30.5	27.3	0.00	0.04	0.06	0.18	0.48	1.26
ENSDARG00000104702	cat	-0.96	-0.24	19.6	11.6	12.8	19.2	25.8	23.7	0.13	0.02	0.11	0.54	0.56	1.00
ENSDARG00000016484	dkc1	-0.07	0.12	12.4	13.1	19.5	44.3	43.5	31.6	0.04	0.03	0.06	0.95	0.52	1.50
ENSDARG00000042484	tle2	0.06	-0.01	20.9	21.0	28.5	41.2	36.1	34.0	0.00	0.00	0.03	0.23	0.80	0.65
ENSDARG00000019195	vps9d1	-0.55	0.31	10.9	14.9	19.6	33.9	18.1	30.3	0.68	0.07	0.08	0.52	1.18	0.86
ENSDARG00000058212	ndnl2	-0.17	0.23	13.2	16.4	21.4	36.8	21.4	24.2	0.00	0.02	0.01	0.00	0.16	0.44
ENSDARG00000010948	kif11	-1.04	0.89	19.3	11.4	12.7	11.9	24.1	21.1	0.84	0.50	0.73	1.86	0.78	1.47
ENSDARG00000017891	tcp1	-0.33	0.09	14.8	15.7	18.2	23.2	25.3	23.3	0.00	0.07	0.28	0.34	0.53	0.62
ENSDARG00000039424	snrpb2	-0.07	0.03	15.3	21.4	30.0	49.4	34.5	26.7	0.02	0.10	0.00	0.24	0.23	1.08
ENSDARG00000053070	gosr2	-0.17	0.28	7.9	9.7	13.1	26.9	18.7	25.8	0.08	0.38	0.22	0.72	0.53	0.80
ENSDARG00000099104	rpl24	-0.38	0.03	17.7	19.4	18.6	22.5	31.5	35.5	0.03	0.09	0.02	0.50	0.56	0.65
ENSDARG00000058292	sephs1	0.18	0.37	23.0	28.5	36.5	44.5	39.4	29.2	0.25	0.02	0.00	0.00	0.03	0.24
ENSDARG00000039347	rps24	-0.43	0.35	11.7	12.5	13.8	17.8	26.5	37.5	0.21	0.17	0.33	1.10	0.86	0.37
ENSDARG00000037560	mtm1	-0.66	0.22	14.9	15.8	18.2	23.4	15.9	17.3	0.00	0.02	0.02	0.12	0.31	0.34
ENSDARG00000069790	dynll2a	-0.52	-0.04	9.4	13.0	16.2	25.5	34.2	28.3	0.36	0.34	0.24	0.25	0.47	0.43
ENSDARG00000103337	rrp1	-0.22	-0.02	9.5	9.9	12.1	15.6	19.6	25.1	0.27	0.29	0.44	1.61	1.49	1.24
ENSDARG00000038639	elovl6l	-2.03	0.34	12.2	10.3	13.1	19.6	29.2	22.2	0.17	0.15	0.13	0.29	0.72	1.14
ENSDARG00000029291	ipmkb	-0.13	-0.46	17.0	15.8	23.4	38.9	29.3	28.4	0.00	0.02	0.05	0.19	0.40	1.00
ENSDARG00000013729	srsf6a	0.01	-0.07	32.9	40.4	50.0	61.8	51.6	29.5	0.00	0.00	0.21	0.47	0.10	0.25
ENSDARG00000015657	zgc:77112	-0.63	-0.18	10.6	11.2	14.4	18.2	11.9	18.9	0.19	0.12	0.10	0.34	0.95	0.00
ENSDARG00000042252	eif4h	0.11	0.14	15.0	18.3	27.0	41.3	39.0	26.5	0.03	0.10	0.02	0.03	0.00	0.55
ENSDARG00000093007	mphosph6	0.01	-0.46	12.5	16.5	24.9	47.4	36.8	30.6	0.12	0.13	0.10	0.32	0.75	0.46
ENSDARG00000045914	si:ch211-51e12.7	0.08	0.15	18.1	25.0	42.1	85.3	56.5	38.6	0.00	0.05	0.10	0.11	0.41	1.65
ENSDARG00000071426	lrrc59	-0.61	0.41	7.6	7.6	8.8	14.6	17.6	13.6	0.58	0.41	0.48	0.89	1.50	0.93
ENSDARG00000067639	prpf4	0.09	0.34	18.4	18.5	24.7	32.3	25.9	25.2	0.09	0.05	0.09	0.18	0.64	1.42
ENSDARG00000004046	phf6	-0.43	0.07	8.8	10.6	14.6	27.9	20.7	29.9	0.02	0.11	0.21	0.23	0.27	1.13
ENSDARG00000104835	map3k4	0.00	-0.06	14.6	18.5	21.4	30.1	21.1	20.5	0.04	0.13	0.04	0.14	0.91	1.09

ENSDARG00000105098	dr1	0.12	0.44	24.8	29.0	29.5	31.9	25.7	27.9	0.27	0.36	0.40	0.51	0.29	0.45
ENSDARG00000013800	snrpd3	0.09	0.30	45.1	29.7	37.2	40.3	37.4	27.8	0.10	0.14	0.12	0.05	0.10	0.26
ENSDARG00000069422	nhp2	-0.24	0.17	11.1	14.1	19.4	52.1	44.5	28.3	0.06	0.07	0.04	0.11	0.55	0.75
ENSDARG00000070472	ARF5	-0.01	0.15	12.6	15.0	22.4	27.3	35.7	28.2	0.16	0.09	0.15	0.40	0.72	1.00
ENSDARG00000102195	zc3h7a	-0.09	-0.06	23.0	26.5	22.2	35.5	31.9	24.5	0.20	0.12	0.22	0.27	0.29	0.69
ENSDARG00000010572	slc25a25a	-0.70	-0.08	13.3	13.6	15.9	28.6	17.5	18.9	1.00	0.76	0.43	0.26	0.70	0.00
ENSDARG00000014591	ilf2	0.13	0.39	34.4	40.1	34.4	29.6	30.8	30.1	0.00	0.05	0.23	0.02	0.25	0.11
ENSDARG00000056695	phc2a	-0.28	0.16	10.4	12.8	18.4	30.4	17.3	20.4	0.25	0.16	0.32	0.55	0.97	1.63
ENSDARG00000029252	ssb	0.25	0.26	20.5	25.7	16.3	28.3	33.2	27.7	0.15	0.16	0.19	0.50	0.41	0.68
ENSDARG00000079467	si:ch73-15b2.5	-0.75	-0.08	16.0	14.6	19.7	28.9	17.0	25.4	0.07	0.12	0.13	0.08	0.77	0.25
ENSDARG00000028335	hmga1a	0.56	0.80	32.1	21.5	18.2	24.3	24.2	32.6	0.00	0.22	0.07	0.24	0.14	0.17
ENSDARG00000021120	ndc1	-0.03	-0.04	14.7	21.9	33.3	41.1	34.5	29.2	0.00	0.05	0.06	0.00	0.04	0.91
ENSDARG00000011201	rplp2l	0.09	0.47	25.0	21.4	21.2	25.0	24.7	28.1	0.46	0.42	0.47	0.87	0.71	0.57
ENSDARG00000007279	yipf5	-0.21	-0.09	11.3	14.3	19.0	25.3	25.4	16.9	0.29	0.26	0.36	0.62	0.32	0.80
ENSDARG00000053810	hnrnpc	-0.93	0.44	20.7	18.6	20.5	21.2	19.6	18.1	0.28	0.12	0.10	0.19	0.22	0.23
ENSDARG00000024109	naa40	-0.14	-0.01	23.4	22.9	27.2	39.9	35.2	26.7	0.05	0.05	0.02	0.23	0.31	1.48
ENSDARG00000006399	ywhae1	0.08	0.53	38.9	33.0	39.2	48.8	43.1	33.8	0.00	0.00	0.09	0.00	0.42	0.49
ENSDARG00000070061	gfer	-0.80	-0.29	10.7	12.3	16.1	24.8	18.3	16.9	0.16	0.11	0.19	0.20	1.47	0.87
ENSDARG00000078917	zgc:195245	-2.82	0.10	8.1	10.5	12.3	26.8	30.7	31.8	0.11	0.06	0.06	0.17	0.19	1.40
ENSDARG00000009830	hdlbpa	-0.14	-0.04	9.3	8.8	13.4	28.9	51.4	52.0	0.29	0.46	0.31	0.76	0.42	0.28
ENSDARG00000013776	thop1	-0.26	0.18	11.2	10.5	11.9	17.9	19.5	15.8	0.47	0.66	0.69	1.90	1.68	2.17
ENSDARG00000038695	elavl1	0.16	0.27	23.3	21.9	21.6	22.5	32.3	29.5	0.00	0.17	0.32	0.71	0.33	0.26
ENSDARG00000020730	smpd4	0.14	0.89	30.7	46.5	41.2	47.6	22.1	28.4	0.53	0.63	0.79	0.27	0.55	1.75
ENSDARG00000016903	wdr5	-0.10	0.09	14.9	18.0	24.9	29.5	30.5	26.9	0.33	0.11	0.23	0.06	0.53	1.23
ENSDARG00000043797	cdc5l	-0.04	0.09	9.7	12.3	18.8	28.3	21.3	16.6	0.11	0.18	0.18	1.17	0.75	1.75
ENSDARG00000025850	rps21	-0.16	0.30	21.7	21.1	24.2	35.2	40.6	57.3	0.04	0.08	0.12	0.19	1.00	0.16
ENSDARG00000017084	bud31	0.06	0.07	41.6	36.5	37.1	40.7	36.3	34.9	0.20	0.00	0.03	0.14	0.39	0.86
ENSDARG00000091902	b3gnt2b	-0.15	0.32	21.9	23.5	24.0	33.4	32.2	27.3	0.05	0.00	0.12	0.10	0.20	0.25
ENSDARG00000017703	paqr3a	0.01	-0.25	24.8	30.4	38.2	41.0	34.4	27.0	0.03	0.05	0.09	0.21	0.09	0.00
ENSDARG00000041232	rps29	0.03	0.25	37.0	27.2	28.7	39.5	44.7	50.1	0.00	0.12	0.35	0.00	0.00	0.21
ENSDARG00000036510	ccnt2b	0.03	-0.06	13.5	18.6	25.1	38.8	26.4	25.8	0.20	0.15	0.37	0.79	0.93	0.92
ENSDARG00000035692	rps3a	-0.43	0.26	20.4	17.6	17.7	19.1	36.7	46.0	0.09	0.25	0.38	1.32	1.19	0.35
ENSDARG00000028848	lsm12a	-0.14	-0.36	29.0	22.7	26.9	36.6	25.1	27.1	0.07	0.16	0.63	0.20	0.49	0.75
ENSDARG00000020123	adck3	-0.60	-0.39	7.5	7.8	9.6	23.8	19.9	15.5	5.50	5.05	4.24	2.81	1.35	1.54
ENSDARG00000039217	orc1	-0.52	-0.10	33.7	22.7	28.7	35.5	20.5	17.4	0.19	0.24	0.14	0.29	0.77	3.70
ENSDARG00000014222	zgc:86598	-0.32	0.09	14.3	17.9	19.3	23.3	20.3	19.2	0.03	0.20	0.20	0.38	0.67	1.08
ENSDARG00000095904	prpf31	-0.08	0.13	14.6	20.5	31.1	34.7	41.3	26.3	0.19	0.38	0.36	0.29	0.19	1.53
ENSDARG00000062326	zgc:158409	-0.06	0.60	10.9	14.3	20.8	39.4	54.5	49.2	0.05	0.02	0.10	0.18	0.07	0.06
ENSDARG00000033126	prkrip1	-0.44	0.58	10.6	12.9	18.2	35.2	32.6	22.6	0.21	0.18	0.21	0.83	0.80	1.03
ENSDARG00000007216	abce1	-0.15	0.36	12.5	15.1	13.6	23.0	26.2	26.7	0.38	0.36	0.53	0.65	0.85	1.07
ENSDARG00000010437	fam46c	-0.16	-0.40	12.7	14.9	16.4	21.6	20.8	16.8	0.50	0.34	0.41	0.98	1.00	1.22
ENSDARG00000068755	exosc8	-0.26	0.19	29.7	28.5	33.2	39.6	25.5	26.7	0.07	0.13	0.00	0.00	0.12	0.30
ENSDARG00000004173	copa	-0.85	-0.11	10.4	14.1	15.6	24.5	17.4	28.2	0.37	0.10	0.19	0.70	1.11	0.66
ENSDARG00000078069	rrm2	0.17	0.34	32.7	32.8	30.5	35.2	23.5	20.7	0.35	0.71	0.39	0.83	0.68	1.33
ENSDARG00000036489	MAF1	-0.04	0.20	21.7	32.9	42.0	44.3	33.4	27.2	0.07	0.23	0.08	0.40	0.80	1.50
ENSDARG00000102320	mob1a	-1.21	0.61	18.3	17.0	18.4	23.2	20.9	28.6	0.26	0.49	0.47	0.51	0.74	0.44
ENSDARG00000021849	si:dkey-256h2.1	-0.04	0.03	18.5	17.9	25.0	25.3	16.7	15.9	0.11	0.17	0.33	0.75	0.86	0.43
ENSDARG00000025350	prdx2	-0.37	-0.21	16.4	14.0	16.4	19.3	17.8	21.9	0.14	0.18	0.25	0.56	0.67	1.26
ENSDARG00000009285	rpl15	-0.25	0.24	17.3	16.7	19.4	26.4	30.4	35.5	0.04	0.16	0.09	0.56	0.18	0.29
ENSDARG00000077226	smarca4a	0.23	0.23	20.6	21.7	26.3	22.5	33.8	24.9	0.10	0.24	0.46	1.34	0.82	1.70
ENSDARG00000003531	tcea1	-0.04	0.12	20.2	29.6	45.0	68.6	48.9	31.9	0.71	0.05	0.08	0.30	0.07	0.71
ENSDARG00000040072	scpep1	-0.67	-0.30	21.3	20.0	21.7	25.7	30.2	28.8	0.15	0.04	0.05	0.24	0.41	0.00
ENSDARG00000099060	zgc:111868	-0.85	-0.10	7.9	9.5	11.7	16.2	21.4	18.6	0.53	0.28	0.39	1.19	1.35	2.33
ENSDARG00000040988	tpi1b	-0.29	-0.11	10.5	12.1	16.5	28.4	37.6	31.4	0.16	0.27	0.11	0.65	0.63	0.37
ENSDARG00000069373	crcp	-1.66	0.34	12.9	14.1	16.9	26.8	33.6	33.6	0.04	0.04	0.01	0.02	0.14	0.00
ENSDARG00000017093	emc8	-0.30	0.06	12.8	13.4	17.2	26.9	26.3	14.7	0.34	0.23	0.48	1.12	0.66	0.96
ENSDARG00000101260	GPATCH2	-0.06	0.08	25.2	25.4	35.9	35.0	30.2	32.2	0.00	0.46	0.52	1.00	0.43	1.48
ENSDARG00000099241	ppp2cb	-1.15	0.20	10.4	11.7	12.5	21.4	31.9	37.1	0.53	0.16	0.31	0.59	0.84	0.40
ENSDARG00000017781	hsd17b10	-0.09	0.02	19.9	18.4	23.2	36.9	36.2	28.6	0.03	0.05	0.06	0.03	0.07	0.38
ENSDARG00000087393	prr11	-0.65	-0.43	22.9	15.7	19.3	28.7	28.6	38.7	0.00	0.08	0.06	0.07	0.12	0.25
ENSDARG00000079686	naa30	-0.07	0.01	19.0	16.9	19.9	30.7	19.2	21.9	0.06	0.08	0.11	0.18	0.59	0.31
ENSDARG00000015427	hdac1	0.12	0.20	29.0	19.6	19.9	30.3	32.6	28.3	0.25	0.17	0.25	0.96	0.67	0.90
ENSDARG00000006074	uck2a	-0.12	-0.29	11.6	14.1	19.6	37.7	33.3	19.5	0.98	0.77	0.74	0.41	0.71	0.22
ENSDARG00000057676	golga7	-0.45	0.20	45.1	29.9	33.6	31.0	30.6	24.2	0.40	0.26	0.30	0.31	0.43	1.00
ENSDARG00000056338	szrd1	0.08	-0.10	19.8	19.0	29.0	38.0	38.8	29.0	0.00	0.12	0.17	0.26	0.18	0.66
ENSDARG00000094616	zgc:113984	0.43	0.78	9.2	10.3	13.0	21.0	25.9	29.5	0.14	0.30	0.34	0.67	0.18	0.57
ENSDARG00000009023	ankrd28b	-0.45	-0.05	14.6	13.6	17.7	26.9	23.0	14.7	0.02	0.08	0.01	0.20	0.00	0.94
ENSDARG00000033738	zgc:153867	-0.49	0.46	28.3	25.8	26.2	21.2	25.8	31.3	0.24	0.05	0.10	0.30	0.60	0.12
ENSDARG00000016908	zgc:171779	-0.85	-0.71	11.9	11.4	12.2	17.9	30.9	34.5	0.10	0.46	0.36	1.61	1.57	2.43
ENSDARG00000063177	manf	-0.27	-0.06	11.2	14.4	18.2	31.3	16.8	18.8	0.10	0.14	0.24	0.34	0.09	1.33
ENSDARG00000004189	cbx1a	0.18	0.26	16.2	25.0	30.6	35.1	39.9	24.1	0.35	0.24	0.47	0.71	0.07	0.77

ENSDARG00000009336	aif1l	0.13	0.30	18.7	25.4	22.1	20.3	26.7	23.7	0.00	0.05	0.35	0.58	0.22	0.14
ENSDARG00000069279	elovl7a	-1.38	0.71	13.2	11.7	12.8	18.7	20.0	17.7	0.14	0.16	0.11	0.14	0.00	0.59
ENSDARG00000031427	calm2a	0.12	-0.03	31.0	28.4	33.0	32.1	32.2	23.6	0.11	0.24	0.00	0.03	0.04	0.17
ENSDARG00000013802	pcid2	-0.30	-0.14	11.3	11.3	15.6	30.8	29.2	25.1	0.03	0.17	0.07	0.56	0.12	0.50
ENSDARG00000012485	aurka	-1.10	0.41	11.1	10.8	12.1	15.8	14.6	19.9	0.03	0.15	0.16	0.24	0.59	1.26
ENSDARG00000099458	ddx46	0.14	-0.01	25.6	25.4	26.9	38.4	37.3	36.3	0.00	0.01	0.15	0.27	0.15	0.70
ENSDARG00000039150	lgmn	-0.08	-0.19	24.8	20.2	25.7	45.7	29.1	28.6	0.08	0.07	0.01	0.58	0.22	0.72
ENSDARG00000039650	itm2cb	-0.84	0.12	37.4	22.8	17.9	18.7	13.9	20.0	0.45	0.47	0.44	0.74	0.71	1.22
ENSDARG00000044760	gnaia	0.00	0.22	13.2	27.5	31.2	32.1	36.9	24.1	0.26	0.25	0.34	0.80	0.71	0.89
ENSDARG00000070108	dek	0.06	0.15	14.6	19.5	21.4	20.0	25.2	19.0	0.00	0.08	0.16	0.25	0.23	0.32
ENSDARG00000008447	fkbp4	0.10	0.18	16.4	23.8	31.6	64.9	20.5	26.4	0.00	0.01	0.04	0.26	0.80	1.74
ENSDARG00000063626	ddx21	-0.10	0.07	8.9	10.0	10.5	13.1	17.5	24.9	0.05	0.20	0.52	0.91	1.19	1.47
ENSDARG00000007387	irf2a	0.11	0.43	10.4	14.8	18.3	27.9	25.0	23.0	0.09	0.08	0.09	0.19	0.33	0.49
ENSDARG00000008732	zgc:66479	0.03	-0.15	14.8	20.9	28.1	34.2	32.3	26.0	0.00	0.11	0.04	0.57	0.08	0.45
ENSDARG00000002659	mapre1b	0.02	0.07	17.7	24.6	22.4	21.6	29.7	24.4	0.05	0.39	0.26	0.48	0.33	0.71
ENSDARG00000055566	mastl	-0.28	0.02	18.7	23.1	23.1	27.4	19.7	26.1	0.11	0.19	0.19	0.34	0.29	1.54
ENSDARG00000104837	nudc	-0.28	0.03	14.2	13.8	18.9	28.5	34.1	26.5	0.03	0.03	0.09	0.21	0.35	0.73
ENSDARG00000037291	dpf2l	-0.25	0.27	35.9	35.1	34.1	33.9	39.6	32.0	0.11	0.10	0.00	0.04	0.10	0.69
ENSDARG00000101900	xrn2	-0.06	0.04	14.9	17.0	21.6	22.4	25.2	22.8	0.13	0.34	0.49	1.07	0.92	1.43
ENSDARG00000056307	znf706	0.05	0.02	36.8	34.6	35.8	42.4	20.6	20.1	0.00	0.02	0.09	0.49	0.19	0.26
ENSDARG00000001969	txlng	0.20	0.41	22.7	24.4	27.2	31.9	19.8	17.4	1.03	1.91	1.91	3.09	1.43	1.11
ENSDARG00000090152	anapc10	-0.85	0.08	14.4	13.7	15.2	21.6	23.8	24.3	0.00	0.01	0.08	0.21	0.17	0.60
ENSDARG00000040440	snrpd2	-1.88	0.36	16.3	16.5	15.6	14.7	11.3	18.9	0.33	0.63	0.48	0.76	1.31	0.96
ENSDARG00000014499	nutf2l	-0.79	-0.12	7.9	8.8	10.2	18.3	22.7	40.1	0.08	0.08	0.05	0.29	0.18	0.25
ENSDARG00000038870	slu7	0.05	-0.11	11.3	16.1	20.9	30.7	19.6	20.6	0.10	0.06	0.07	0.17	0.27	0.80
ENSDARG00000007385	cct7	0.00	0.05	11.2	13.8	16.7	28.0	30.1	33.2	0.00	0.12	0.21	0.82	0.37	1.05
ENSDARG00000054578	arl6ip1	-2.18	-0.48	24.1	14.9	12.0	16.6	20.0	23.0	0.04	0.08	0.06	1.67	1.00	0.29
ENSDARG00000061187	cbx5	0.21	0.14	19.6	24.2	30.5	35.7	29.5	30.4	0.14	0.08	0.05	0.39	0.46	0.74
ENSDARG00000028119	sumo3a	-0.04	0.80	34.8	20.9	29.9	33.8	35.0	36.7	0.00	0.03	0.12	0.24	0.08	0.40
ENSDARG00000005108	oclna	-0.08	0.02	35.7	24.1	19.7	20.5	21.5	18.1	0.00	0.34	0.23	0.06	0.13	0.59
ENSDARG00000057707	zgc:66443	0.01	0.14	12.0	16.4	24.9	46.8	19.5	19.7	0.21	0.15	0.31	0.15	0.60	0.42
ENSDARG00000012274	eif4e1c	-0.13	-0.05	17.0	22.9	25.3	32.5	26.8	27.2	0.13	0.14	0.08	0.32	0.59	0.09
ENSDARG00000102333	fcf1	-0.41	0.34	12.1	11.1	12.5	21.3	25.4	24.6	0.00	0.16	0.15	0.44	0.20	0.66
ENSDARG00000070358	smim12	-0.27	-0.20	13.1	15.5	20.0	41.5	32.8	33.2	0.04	0.07	0.01	0.18	0.12	0.50
ENSDARG00000055383	zgc:66160	-0.06	0.50	11.8	14.0	16.3	24.1	19.5	21.6	0.18	0.18	0.11	0.17	0.06	0.14
ENSDARG00000009871	snrpc	-0.05	0.19	32.5	37.9	51.1	67.0	49.3	34.9	0.00	0.24	0.00	0.00	0.04	0.96
ENSDARG00000035146	polr2j	-0.42	-0.01	13.8	11.2	17.1	25.7	25.5	21.4	1.25	0.64	0.69	0.51	0.76	0.87
ENSDARG00000043608	eif4ebp1	0.00	-0.10	19.5	18.4	18.3	22.6	36.8	37.3	0.00	0.01	0.05	0.03	0.57	0.81
ENSDARG00000069980	lman1	-0.18	-0.33	11.9	10.3	15.6	30.9	29.4	31.5	0.05	0.05	0.11	0.33	0.04	1.20
ENSDARG00000037158	rcc1	0.16	-0.05	30.2	36.1	45.9	32.1	34.3	23.4	0.00	0.15	0.58	0.34	0.65	1.49
ENSDARG00000077530	ahctf1	-0.32	0.39	15.9	12.6	13.6	20.0	18.7	17.0	0.07	0.19	0.20	0.69	0.32	1.14
ENSDARG00000070404	fam212ab	-1.30	0.71	9.8	8.9	9.0	10.5	15.0	15.4	0.02	0.06	0.05	0.10	0.08	0.31
ENSDARG00000070834	taf13	0.21	0.05	21.2	28.3	35.4	37.6	31.4	22.8	0.00	0.00	0.05	0.00	0.10	0.56
ENSDARG00000008383	arpc1a	-0.43	-0.09	11.4	12.1	17.7	30.6	22.8	24.6	0.11	0.08	0.08	0.19	0.93	0.31
ENSDARG00000059725	hypk	0.14	0.05	28.0	29.1	28.7	41.9	45.9	37.6	0.00	0.02	0.03	0.09	0.08	0.36
ENSDARG00000007099	cx43.4	0.58	-0.01	39.7	32.3	28.4	38.8	43.3	34.0	0.13	0.25	0.75	0.58	0.42	0.72
ENSDARG00000041081	suv420h1	-0.34	0.60	10.2	12.0	17.5	21.6	15.3	14.8	0.03	0.22	0.26	0.55	0.47	1.20
ENSDARG00000039363	dnajb12a	-0.40	-0.01	16.6	17.9	25.8	36.7	25.1	18.9	0.14	0.24	0.22	0.59	0.25	0.60
ENSDARG00000009740	ppp1r7	-0.03	0.14	21.9	21.1	21.8	27.0	27.4	21.4	0.36	0.14	0.06	0.17	0.46	1.30
ENSDARG00000008022	kif18a	-0.04	0.94	16.2	19.4	21.9	34.9	24.3	21.4	0.07	0.00	0.10	0.00	0.19	0.46
ENSDARG00000100114	sf3a3	-0.10	0.10	14.2	22.1	28.1	49.0	36.4	25.1	0.12	0.11	0.29	0.80	0.70	0.98
ENSDARG00000024488	top2a	-0.93	0.89	38.4	17.4	11.3	9.6	27.9	16.6	0.12	0.13	0.17	0.80	0.18	2.96
ENSDARG00000057167	eif4g2b	0.04	0.28	16.5	19.0	23.4	34.3	27.0	28.9	0.00	0.25	0.08	0.75	0.18	1.16
ENSDARG00000062650	rif1	0.31	-0.03	21.3	21.7	19.3	18.7	15.9	13.2	0.45	0.15	0.20	0.17	0.18	0.60
ENSDARG00000086840	si:ch211-266k8.4	-0.40	0.16	29.9	28.5	24.1	22.6	16.1	12.8	0.30	0.02	0.07	0.10	0.36	0.00
ENSDARG00000041435	uba52	-1.06	0.35	14.0	13.2	14.0	15.9	33.7	41.5	0.32	0.17	0.46	1.06	0.00	0.20
ENSDARG00000100515	dusp1	-1.07	0.04	16.7	12.0	14.3	16.6	11.4	14.3	0.04	0.11	0.19	0.20	0.21	0.42
ENSDARG00000017844	copz1	-0.46	-0.04	10.4	12.6	16.5	26.2	35.3	28.3	0.16	0.18	0.07	0.19	0.33	0.06
ENSDARG00000056099	gtf2h5	-0.53	-0.10	12.8	13.1	18.7	53.4	51.7	34.3	0.00	0.01	0.03	0.23	0.00	0.92
ENSDARG00000044339	rp2	-0.17	-0.31	13.7	20.1	30.5	47.2	31.4	18.8	0.21	0.31	0.18	0.88	0.58	1.68
ENSDARG00000030602	rps19	0.01	0.27	25.5	22.4	21.3	29.3	30.1	40.4	0.88	0.76	0.90	1.71	0.92	1.31
ENSDARG00000004251	dhfr	-0.20	0.21	14.6	15.3	20.3	26.5	25.7	26.3	0.08	0.05	0.09	0.07	0.08	0.37
ENSDARG00000015709	hsd17b12a	0.03	0.37	15.7	24.6	29.3	39.0	41.1	34.5	0.84	0.57	0.31	0.71	0.07	0.54
ENSDARG00000058346	sass6	-0.65	0.40	16.4	12.1	14.6	19.2	15.0	10.4	0.05	0.08	0.08	0.18	0.11	0.33
ENSDARG00000060199	mrpl18	-1.59	0.93	18.2	14.2	14.4	18.8	19.9	20.7	0.08	0.11	0.15	0.12	0.11	0.92
ENSDARG00000052617	raver1	-0.01	0.35	38.0	40.7	34.5	26.6	16.5	21.8	0.00	0.03	0.06	0.19	0.40	0.57
ENSDARG00000078457	si:ch211-250e5.16	-1.55	-0.73	7.2	7.8	8.4	10.5	16.7	19.6	0.30	0.92	0.82	1.62	1.20	1.50
ENSDARG00000024184	narf	-0.34	-0.01	10.0	10.6	16.7	32.6	20.6	34.0	0.28	0.12	0.19	0.47	0.96	1.43
ENSDARG00000062612	dhx37	-0.29	0.32	10.3	11.0	14.0	20.7	16.1	22.1	0.07	0.11	0.10	0.43	0.56	0.97
ENSDARG00000042876	abracl	-0.18	0.08	10.4	11.2	15.4	28.0	42.6	25.3	0.07	0.15	0.12	0.37	0.50	0.21
ENSDARG00000017741	g3bp1	-0.31	0.47	16.3	15.1	19.4	33.9	30.3	23.4	0.32	0.37	0.16	0.88	0.77	2.35

ENSDARG00000079508	fam114a2	-0.78	-0.32	11.8	12.1	16.3	24.6	15.9	19.8	0.08	0.10	0.13	0.51	0.58	0.77
ENSDARG00000058425	rab35b	-0.54	-0.05	11.4	10.0	12.6	21.2	18.7	22.2	0.28	0.23	0.41	1.17	1.05	1.10
ENSDARG00000023290	fabp3	-0.51	-0.28	12.0	10.8	12.5	15.8	20.6	15.9	0.07	0.18	0.18	0.60	0.69	0.15
ENSDARG00000008395	snupn	-0.21	0.73	53.6	30.5	22.8	25.4	17.6	16.8	0.00	0.56	0.24	0.05	0.16	0.65
ENSDARG00000046157	RPS17	0.23	0.29	11.4	11.2	11.8	14.5	22.3	39.1	0.13	0.36	0.52	1.10	0.92	0.16
ENSDARG00000003920	setb	0.21	0.12	18.2	18.5	24.6	28.5	27.9	32.0	0.52	0.33	0.32	1.58	0.44	0.68
ENSDARG00000098250	cox7b	-1.71	0.48	9.6	8.3	9.1	10.6	18.8	27.5	0.39	0.37	0.41	0.55	0.08	0.66
ENSDARG00000056557	copb1	-0.26	-0.03	10.4	12.5	12.8	29.2	23.0	17.2	0.00	0.01	0.10	0.33	0.48	1.59
ENSDARG00000098443	zfand6	-1.37	0.22	14.5	13.3	13.9	20.9	20.5	21.8	0.37	0.33	0.48	0.46	0.44	0.29
ENSDARG00000035776	n6amt1	-1.04	0.18	14.5	14.9	18.5	29.7	22.8	24.0	0.00	0.01	0.06	0.14	0.13	0.08
ENSDARG00000027813	nus1	0.00	-0.05	14.9	16.4	19.1	25.6	17.4	29.7	0.06	0.11	0.29	0.58	0.33	0.60
ENSDARG00000031770	kat7b	-0.20	-0.10	10.2	14.7	27.3	39.7	23.1	25.1	0.04	0.12	0.43	0.14	0.41	0.70
ENSDARG00000003153	cpsf5	-0.27	0.07	15.3	17.0	24.6	34.0	35.2	28.6	0.29	0.14	0.06	0.29	0.14	0.28
ENSDARG00000020334	ptpn11a	0.09	-0.05	19.5	29.3	34.9	34.9	46.3	32.1	0.06	0.23	0.28	0.33	0.87	0.58
ENSDARG00000018491	pdia4	-0.90	0.23	9.5	12.8	17.7	24.0	18.3	12.8	0.72	0.47	0.37	0.45	0.67	1.60
ENSDARG00000021483	cdc14b	-0.20	0.03	13.7	17.7	25.1	39.9	23.3	20.2	0.10	0.05	0.31	0.13	0.45	1.50
ENSDARG00000053047	eif2s2	-0.14	0.04	10.3	9.3	12.2	15.2	21.6	32.2	0.44	0.42	0.53	0.87	0.85	1.56
ENSDARG00000005230	ssr2	-0.97	0.04	10.5	12.0	15.0	26.9	28.0	54.6	0.08	0.08	0.35	0.42	1.36	0.00
ENSDARG00000044691	ppp1r3b	0.01	0.12	12.0	14.8	21.3	29.0	27.5	19.1	0.35	0.24	0.11	0.40	0.62	0.85
ENSDARG00000070043	dars	-0.10	0.07	12.1	17.5	20.6	26.6	30.4	21.1	0.28	0.11	0.29	0.67	0.50	0.83
ENSDARG00000103433	rpl14	-0.17	0.41	16.7	19.0	16.5	22.1	29.9	36.6	0.00	0.03	0.17	0.13	0.26	0.11
ENSDARG00000100374	txnrd1	-0.62	0.31	14.1	21.8	21.3	23.4	18.9	18.1	0.00	0.24	0.42	0.37	0.50	1.07
ENSDARG00000070426	chac1	-0.77	-0.02	22.9	24.7	27.5	35.7	29.3	22.0	0.32	0.21	0.56	0.41	0.54	0.79
ENSDARG00000037071	rps26	0.09	0.47	25.1	17.4	15.1	20.0	24.5	21.0	1.06	1.18	1.29	1.36	1.48	1.75
ENSDARG00000011312	stk3	-0.07	0.02	25.9	28.1	23.6	28.1	25.2	28.6	0.04	0.03	0.35	0.09	0.02	0.20
ENSDARG00000076815	eif3s10	0.08	0.22	18.6	21.2	35.0	30.0	36.1	25.9	0.05	0.13	0.36	1.24	0.62	1.12
ENSDARG00000010721	sept6	0.15	0.05	35.9	42.3	42.5	40.0	51.3	32.2	0.00	0.32	0.90	0.36	0.31	0.42
ENSDARG00000070657	pa2g4b	-0.10	0.24	9.5	10.7	11.4	15.0	22.2	32.3	0.11	0.36	0.57	1.27	1.42	1.33
ENSDARG00000021225	prkci	-0.08	-0.10	11.1	18.6	25.8	43.4	31.1	21.7	0.24	0.08	0.11	0.43	0.48	1.59
ENSDARG00000011613	rbm39a	0.21	0.27	17.2	26.2	38.9	47.6	36.2	28.5	0.08	0.00	0.09	0.00	0.15	1.08
ENSDARG00000055250	si:ch211-132b12.8	-1.22	-0.25	7.5	8.8	9.7	12.5	12.5	10.2	0.43	0.44	0.32	0.81	1.04	0.14
ENSDARG00000006527	brd3a	0.01	0.31	10.8	15.7	21.0	32.0	27.5	26.0	0.28	0.30	0.29	0.51	0.78	1.30
ENSDARG00000042623	acbd3	-0.12	0.06	16.5	17.7	23.2	27.5	23.4	22.1	0.15	0.10	0.13	0.32	0.23	0.52
ENSDARG00000005799	smim14	-0.59	0.10	17.6	15.1	20.6	24.5	22.4	19.3	0.15	0.13	0.09	0.25	0.22	0.43
ENSDARG00000037393	slc43a1a	-0.21	0.04	21.1	22.1	26.2	31.8	36.2	38.7	0.00	0.06	0.11	0.12	0.12	0.43
ENSDARG00000030949	srprb	-0.38	0.14	33.9	29.9	30.6	28.9	33.0	28.4	0.10	0.00	0.05	0.22	0.18	0.42
ENSDARG00000009950	edf1	-0.05	0.12	35.5	25.8	30.3	38.3	38.0	36.8	0.11	0.03	0.06	0.08	0.10	0.38
ENSDARG00000076836	gpx4b	-0.62	0.28	10.8	11.7	13.6	20.0	30.4	27.7	0.14	0.04	0.03	0.70	1.08	0.77
ENSDARG00000012140	ccnl1b	-0.09	0.81	14.1	15.4	21.1	31.2	28.3	23.2	0.05	0.06	0.23	0.74	0.61	0.76
ENSDARG00000035095	tdgf1	0.30	-0.01	15.2	19.6	27.0	44.2	22.2	20.0	0.05	0.02	0.13	0.24	0.24	0.70
ENSDARG00000016463	trappc6b	-0.20	-0.56	18.9	20.3	25.9	28.6	22.2	24.2	0.00	0.07	0.04	0.03	0.10	0.50
ENSDARG00000038980	txndc12	-0.17	0.01	13.8	13.0	16.9	27.9	26.8	24.0	0.00	0.02	0.13	0.19	0.90	0.61
ENSDARG00000038027	nol12	-0.28	0.05	7.7	9.5	11.2	12.2	14.5	30.3	0.59	0.69	0.78	1.62	1.97	1.55
ENSDARG00000040730	wdr75	-0.59	-0.08	19.0	23.5	29.8	33.4	27.4	27.8	0.18	0.24	0.46	0.57	0.76	1.13
ENSDARG00000029500	rpl34	-0.18	0.42	19.3	19.8	19.1	22.6	29.7	30.2	0.00	0.19	0.08	0.46	0.74	0.34
ENSDARG00000090697	eif3ea	-0.27	0.04	10.4	10.0	12.2	14.4	23.3	34.3	0.29	0.39	0.26	0.63	1.64	0.23
ENSDARG00000022430	ppp1r8b	-0.04	0.17	11.1	17.8	30.8	35.9	25.2	27.7	0.07	0.28	0.53	0.55	0.35	0.91
ENSDARG00000010965	psma8	-0.12	0.39	12.6	11.6	12.6	17.8	27.2	29.1	0.10	0.12	0.42	1.53	0.83	0.58
ENSDARG00000104508	slc10a7	-0.39	-0.46	7.5	9.9	13.4	20.6	20.2	16.3	0.43	0.04	0.19	1.08	1.05	0.92
ENSDARG00000054355	dcaf7	-0.07	0.07	12.8	25.0	29.7	40.5	29.1	29.5	0.04	0.07	0.20	0.18	0.31	0.35
ENSDARG00000100072	mgrn1a	-0.68	0.33	14.0	16.5	18.7	22.0	23.3	26.2	0.00	0.03	0.04	0.01	0.24	0.00
ENSDARG00000021059	alas1	-0.33	-0.23	9.5	10.4	11.3	16.2	14.9	15.7	0.00	0.05	0.17	0.39	0.78	1.29
ENSDARG00000077546	ZDHHC1	-0.64	0.41	19.8	20.7	23.3	26.6	21.6	21.9	0.19	0.44	0.07	0.23	0.60	1.60
ENSDARG00000070688	ncalda	-0.29	0.03	21.0	16.9	22.6	38.4	35.5	35.7	0.00	0.04	0.07	0.30	0.43	0.50
ENSDARG00000037739	zgc:112980	-0.27	0.40	12.3	14.8	20.0	32.6	17.0	14.4	0.03	0.21	0.44	0.33	0.86	0.83
ENSDARG00000070618	tatdn2	-0.27	-0.45	13.8	16.3	21.2	23.6	19.3	20.0	0.20	0.18	0.14	0.58	0.98	1.00
ENSDARG00000097103	zgc:165555	0.76	1.20	7.3	7.6	7.1	8.9	7.9	8.9	0.30	0.39	0.38	0.44	0.36	0.49
ENSDARG00000012572	polr3f	-1.36	0.64	12.1	13.1	13.4	24.1	18.0	19.6	0.09	0.14	0.18	0.00	0.33	0.58
ENSDARG00000001241	puf60b	-0.17	0.16	12.8	17.1	23.9	36.7	22.9	23.5	0.16	0.17	0.41	0.69	0.57	0.78
ENSDARG00000039350	ssbp1	-0.55	0.45	14.4	20.3	21.9	27.0	29.5	25.1	0.11	0.03	0.10	0.19	0.00	0.25
ENSDARG00000093058	si:dkey-13i19.8	-0.32	-0.14	17.5	18.2	23.5	28.9	37.5	21.4	0.00	0.06	0.06	0.28	0.00	1.12
ENSDARG00000043684	bpnt1	-0.51	-0.04	25.9	20.5	22.1	28.3	29.9	27.8	0.00	0.09	0.10	0.06	0.00	0.00
ENSDARG00000009484	arf1	0.15	0.19	19.3	17.0	20.7	31.1	20.3	26.1	0.10	0.25	0.18	0.25	0.33	0.46
ENSDARG00000058041	ndufa8	-1.30	0.54	12.2	10.0	13.0	18.9	18.7	19.5	0.75	0.40	0.31	0.34	0.38	0.86
ENSDARG00000102511	cript	-0.03	-0.17	15.6	18.5	21.3	38.6	41.2	23.6	0.00	0.04	0.09	0.40	0.25	0.64
ENSDARG00000053685	gtf2a2	-0.90	1.00	25.3	15.5	19.9	30.3	27.4	23.9	0.07	0.08	0.02	0.45	0.36	0.86
ENSDARG00000023920	llgl2	-0.13	0.01	27.4	38.7	37.3	48.8	44.5	31.4	0.14	0.03	0.09	0.61	0.22	1.00
ENSDARG00000034956	myclb	-0.70	0.83	10.5	13.2	16.0	22.5	19.2	14.4	0.15	0.09	0.17	0.34	0.00	0.18
ENSDARG00000006019	tktb	-0.19	0.09	13.5	14.6	18.6	36.7	34.8	24.5	0.02	0.06	0.15	0.76	0.84	0.62
ENSDARG00000099631	cmtm6	0.03	0.21	16.2	20.3	23.0	26.0	36.6	28.9	0.48	0.89	1.66	1.81	0.87	1.68
ENSDARG00000002401	gale	-0.38	-0.04	8.2	12.1	15.8	32.6	26.9	32.8	0.08	0.09	0.14	0.46	0.20	0.55

ENSDARG00000014083	wdr82	-0.17	0.18	15.0	18.5	27.9	45.8	34.4	26.1	0.00	0.04	0.14	1.00	0.10	0.48
ENSDARG00000019951	sec62	0.01	0.17	16.6	21.3	26.0	33.8	33.2	26.8	0.07	0.15	0.02	0.75	0.11	0.35
ENSDARG00000038801	klhl20	0.12	-0.09	24.6	29.7	29.2	33.0	28.0	27.8	0.05	0.00	0.07	0.44	0.26	0.30
ENSDARG00000007141	psmc3	0.05	0.08	17.9	21.1	27.3	27.6	34.1	25.9	0.19	0.78	1.13	2.15	0.30	0.43
ENSDARG00000015292	ube2g1a	0.16	-0.10	33.0	35.3	32.9	32.6	33.2	26.7	0.22	0.41	0.17	0.44	0.25	0.57
ENSDARG00000041533	ccdc130	-0.74	0.18	7.3	9.3	9.3	19.0	15.6	21.6	1.00	0.63	0.52	0.65	1.13	0.83
ENSDARG00000019398	psma6a	0.02	0.06	13.9	15.7	19.9	32.6	27.2	30.7	0.08	0.29	0.24	0.27	0.67	0.79
ENSDARG00000039213	prpf38a	0.03	0.16	12.9	17.8	27.8	44.4	31.6	27.7	0.06	0.01	0.10	0.36	0.16	0.92
ENSDARG00000030241	vbp1	-0.62	0.14	9.7	10.5	14.2	22.9	30.0	38.0	0.17	0.21	0.05	0.10	1.06	0.56
ENSDARG00000044565	ola1	-0.36	0.12	12.5	13.8	17.8	38.4	35.3	36.2	0.06	0.04	0.14	0.75	0.46	0.51
ENSDARG00000000018	nrf1	-0.22	-0.05	9.9	15.9	20.6	29.8	26.5	24.4	0.00	0.13	0.21	0.19	0.89	1.61
ENSDARG00000059906	sdc4	-0.14	-0.02	13.7	18.7	26.9	45.4	37.8	31.7	0.23	0.06	0.03	0.44	0.17	0.24
ENSDARG00000099667	snrpg	-1.49	0.94	21.1	19.4	19.0	23.8	31.1	40.1	0.00	0.04	0.03	0.06	0.10	0.21
ENSDARG00000012040	rnf19a	0.04	0.43	9.2	11.9	16.6	21.9	17.2	14.4	0.17	0.03	0.16	0.47	0.34	0.88
ENSDARG00000063295	myh9a	-0.19	-0.26	9.0	13.5	17.8	25.3	22.4	19.5	0.21	0.16	0.42	0.77	0.58	1.73
ENSDARG00000005926	ak2	-0.42	0.01	10.4	11.2	13.8	22.8	26.2	29.3	0.00	0.06	0.09	0.39	0.24	1.07
ENSDARG00000034409	pik3r3b	0.10	0.06	11.6	12.0	14.5	21.7	15.4	16.6	0.21	0.31	0.42	0.50	0.75	0.20
ENSDARG00000003127	zgc:123105	-0.53	0.05	22.0	22.3	30.6	32.4	25.5	26.1	0.14	0.02	0.03	0.10	0.16	0.65
ENSDARG00000056621	ctcf	0.19	-0.03	11.4	12.1	16.2	24.1	22.8	18.4	0.15	0.22	0.23	0.65	0.64	0.53
ENSDARG00000041155	morf4l1	-0.19	0.05	12.7	14.4	22.4	37.3	22.7	27.6	0.07	0.12	0.24	0.14	0.91	1.65
ENSDARG00000045676	calua	-0.08	-0.09	15.2	19.7	30.5	46.7	32.5	21.3	0.00	0.01	0.05	0.30	0.21	0.71
ENSDARG00000104959	dnajc17	0.03	0.15	27.7	25.3	29.1	38.1	27.1	16.6	0.22	0.03	0.00	0.00	0.00	0.27
ENSDARG00000045601	cax1	-0.94	-0.54	8.1	9.6	11.1	15.6	18.0	22.0	0.38	0.47	0.17	0.38	0.09	0.50
ENSDARG00000104647	surf4	-0.92	-0.26	10.9	12.2	12.9	17.6	13.6	15.5	0.14	0.02	0.03	0.11	0.00	0.08
ENSDARG00000016117	exd2	-0.25	-0.34	11.6	14.2	21.6	32.7	23.0	28.9	0.03	0.15	0.31	1.82	1.39	2.17
ENSDARG00000056414	usp1	0.07	-0.38	15.5	28.9	28.8	54.3	19.9	17.6	0.03	0.27	0.26	0.15	0.43	1.03
ENSDARG00000005454	tacc3	-1.19	0.25	16.5	9.6	9.6	10.9	9.2	13.6	0.55	0.48	0.41	0.74	1.50	0.89
ENSDARG00000041853	rbm39b	0.00	0.19	12.7	24.5	34.2	50.4	44.0	25.5	0.09	0.05	0.27	0.00	0.05	0.38
ENSDARG00000000068	slc9a3r1	-0.36	-0.06	13.9	16.6	24.0	37.5	31.5	21.7	0.19	0.09	0.14	0.16	0.21	1.58
ENSDARG00000040443	polr2i	-0.09	0.03	18.4	22.5	31.9	25.0	25.4	24.6	0.23	0.09	0.07	0.26	0.32	1.20
ENSDARG00000069619	atf7ip	0.14	-0.02	23.8	32.1	36.2	48.1	26.3	29.7	0.36	0.00	0.14	0.55	0.34	0.56
ENSDARG00000009862	dcps	-0.06	-0.04	22.1	21.2	25.3	32.0	29.6	26.4	0.13	0.28	0.12	0.20	0.44	0.29
ENSDARG00000005619	nek2	-0.40	0.27	22.1	16.6	18.4	22.8	19.8	14.4	0.00	0.10	0.10	0.13	1.07	0.89
ENSDARG00000016496	cdk8	-0.07	0.17	9.2	11.1	15.4	42.7	17.5	16.2	0.00	0.07	0.22	0.47	0.54	0.50
ENSDARG00000070083	atp5b	-0.24	-0.12	10.1	9.6	11.3	17.0	16.9	24.1	0.00	0.29	0.27	1.26	0.91	1.08
ENSDARG00000044402	nop16	-0.81	-0.02	10.5	11.6	13.1	36.6	43.9	31.5	0.15	0.22	0.15	0.06	1.88	0.73
ENSDARG00000043360	dph3	-0.94	0.69	12.9	15.0	17.5	33.6	18.8	20.1	0.02	0.12	0.15	0.05	0.59	0.82
ENSDARG00000014159	mtdha	-0.19	0.25	13.0	12.7	16.9	17.5	23.9	21.2	0.04	0.11	0.17	1.09	0.19	0.60
ENSDARG00000034291	rpl37	0.09	-0.16	24.3	21.8	22.9	26.5	30.3	35.4	0.09	0.06	0.27	0.39	0.69	0.53
ENSDARG00000004680	dnajb6a	-0.19	-0.18	29.3	35.8	35.2	41.5	47.8	34.9	0.00	0.00	0.00	0.00	0.00	0.54
ENSDARG00000041248	si:dkey-241l7.6	-0.79	-0.05	9.2	10.1	9.8	10.4	9.7	12.4	0.39	0.47	0.49	1.74	2.40	1.17
ENSDARG00000040666	nifk	-0.91	0.06	9.9	9.7	14.2	28.9	32.7	25.2	0.30	0.25	0.09	0.10	0.32	0.65
ENSDARG00000031511	psmb2	-0.39	-0.01	12.3	11.5	13.3	17.7	26.5	34.6	0.07	0.04	0.08	0.20	0.44	0.00
ENSDARG00000068404	tbcb	-0.05	-0.22	16.9	30.8	36.0	47.4	36.0	30.0	0.09	0.05	0.41	0.11	0.48	1.00

Table 2. RNA-seq and TAIL-seq data from zebrafish embryos. The list shows the fold change of genes between 2 and 4 hpf in Control and TUT4/7 morphants detected by RNA-seq, and the mean of poly(A) tail length and average U length of genes at six different time points in wild-type zebrafish embryos measured by TAIL-seq. Genes with≥100 reads in TAIL-seq data were included in the analysis.

국문초록

척추 동물 모계-접합체 전이 과정에서의 전령 RNA 꼬리 조절에 관한 연구

모계-접합체 전이 (Maternal-to-zygotic transition, MZT) 과정은 초기배아의 난자로 부터 유래한 모계 전사체가 새로 합성되는 접합체의 전사체에 의해 대체되는 과정이다. 접합체의 전사는 수정 후 바로 시작되지 않기 때문에, 초기 배아의 발달 과정은 모계 전사체에 의해 결정되고, 모계 전사체의 발현은 세포질에서 일어나는 폴리아데닐화 및 RNA 안정성과 같은 전사 후 기작에 의해 조절된다. 모계 전사체는 접합체 유전자 활성화 (ZGA) 가 시작되기 전에는 안정해야 하고, ZGA 후에는 제거되어야 하므로, 모계 전령 RNA 의 분해되는 시기가 정확하게 조절되는 것이 MZT 과정에서 중요하다. 그러나 척추 동물의 초기 발달 과정에서 전령 RNA의 안정성이 시기적으로 어떻게 조절되는지에 대한 분자적 기작이 아직 알려져 있지 않다.

MZT 과정에서 전령 RNA 의 꼬리조절이 전사체 조절에 어떤 영향을 미치는지 연구하기 위해, 나는 최근 개발된 high-throughput 서열분석 방법 중 하나인 꼬리서열 분석법 (TAIL-seq) 을 zebrafish 초기 배아에 적용하였다. TAIL-seq 은 전사체 수준에서 폴리아데닐산 꼬리 길이를 잴 수 있을 뿐 아니라 3′ 말단 서열에 대한 정확한 정보를 제공한다. ZGA 이 일어나기 이전에는 모계 전령 RNA의 폴리아데닐산 꼬리길이가 늘어나며, 이에 따라 모계 단백질 발현이 증가함을 발견했다. 또한 일부 전령 RNA 경우에는 꼬리길이가 감소하며 이로 인해 발현이 억제됨을 확인했다. 그리고, ZGA 일어남과 동시에 모계 전사체가 광범위하게 탈 아데닐화되면서 분해되는 것을 관찰했다.

흥미롭게도, 모계 전사체가 광범위하게 분해되는 시기와 동일하게 전령 RNA 의

유리딘화가 크게 증가한다는 것을 발견하였다. MZT 과정에서 유리딘화가 증가되는 현상은 무척추동물인 초파리 배아에서는 관찰되지 않지만, *Xenopus* 와 쥐의 배아에서는 동일하게 관찰되는 것을 알아냈다. 이는 유리딘화가 척추동물 배아의 RNA 분해과정에서 진화적으로 보존된 기능을 갖는다는 것을 암시한다.

다음으로 나는 morpholino (MO) 를 매개로한 표적 단백질의 발현 억제 실험과 RNA 대량 서열분석방법을 이용해서 전령 RNA 의 유리딘화가 MZT 진행에 결정적인 역할을 한다는 것을 알아냈다. 이전 연구에서 포유류의 전령 RNA 유리딘화를 담당하는 효소로 확인된 TUT4 와 TUT7 (TUT4/7, 또는 ZCCHC11/6) 의 발현을 zebrafish 초기 배아에서 억제하면, 모계 전령 RNA 분해가 지연되어 접합체 전사의 손상 및 배아 발달의 결함으로 이어진다. 짧은 아데닐산 꼬리를 갖는 모계 전령 RNA 는 TUT4 및 TUT7 에 의해 선택적으로 변형되는 반면, 긴 폴리 아데닐산 꼬리를 갖는 모계 전사체는 유리딘화 활성에 덜 영향을 받는다는 것을 확인했다. 또한, *Xenopus* 배아에서 TUT4/7 의 발현을 억제하였을 때, zebrafish 에서 관찰된 발달상의 표현형과 일치하는 결함이 나타난다는 것을 확인함으로써 초기 배아 발달에서 유리딘화의 필수적인 역할을 검증했다. 다른 서열을 갖는 TUT7 MO 의 사용과 WT TUT7 또는 비활성 돌연변이 TUT7 을 이용한 구조실험을 수행함으로써 TUT7 MO 에 의해 야기된 발달상의 표현형이 유리딘화 억제에 기인한다는 것을 검증했다.

나는 이번 연구를 통해, 척추 동물의 초기 배아 발달 동안 모계 전령 RNA 를 제거하는 과정에서 전령 RNA 의 유리딘화가 진화적으로 보존된 역할을 하는 것을 밝혔다. 또한 MZT 동안 증가하는 전령 RNA 의 유리딘화가 폴리 아데닐산 꼬리가 짧은 모계 전사체를 정확한 시기에 분해함으로써 초기 발달 진행에 중요한 기능을 한다는 것을 제시한다.

Bibliography

Aanes, H., Winata, C. L., Lin, C. H., Chen, J. P., Srinivasan, K. G., Lee, S. G., Lim, A. Y., Hajan, H. S., Collas, P., Bourque, G., Gong, Z., Korzh, V., Alestrom, P., & Mathavan, S. (2011). Zebrafish mrna sequencing deciphers novelties in transcriptome dynamics during maternal to zygotic transition. *Genome Res*, 21(8), 1328–38.

Alizadeh, Z., Kageyama, S., & Aoki, F. (2005). Degradation of maternal mrna in mouse embryos: selective degradation of specific mrnas after fertilization. *Mol Reprod Dev*, 72(3), 281–90.

Aravind, L. & Koonin, E. V. (1999). Dna polymerase beta-like nucleotidyltransferase superfamily: identification of three new families, classification and evolutionary history. *Nucleic Acids Res*, 27(7), 1609–18.

Audic, Y., Omilli, F., & Osborne, H. B. (1997). Postfertilization deadenylation of mrnas in xenopus laevis embryos is sufficient to cause their degradation at the blastula stage. *Mol Cell Biol*, 17(1), 209–18.

Barckmann, B. & Simonelig, M. (2013). Control of maternal mrna stability in germ cells and early embryos. *Biochim Biophys Acta*, 1829(6-7), 714–24.

Bazzini, A. A., Del Viso, F., Moreno-Mateos, M. A., Johnstone, T. G., Vejnar, C. E., Qin, Y., Yao, J., Khokha, M. K., & Giraldez, A. J. (2016). Codon identity regulates mrna stability and translation efficiency during the maternal-to-zygotic transition. *EMBO J*, 35(19), 2087–2103.

Bazzini, A. A., Lee, M. T., & Giraldez, A. J. (2012). Ribosome profiling shows that mir-430 reduces translation before causing mrna decay in zebrafish. *Science*, 336(6078), 233–7.

Bisbee, C. A., Baker, M. A., Wilson, A. C., Haji-Azimi, I., & Fischberg, M. (1977). Albumin phylogeny for clawed frogs (xenopus). *Science (New York, N.Y.)*, 195, 785–787.

Bushati, N., Stark, A., Brennecke, J., & Cohen, S. M. (2008). Temporal reciprocity of mirnas and their targets during the maternal-to-zygotic transition in drosophila. *Curr Biol*, 18(7), 501–6.

Castresana, J. (2000). Selection of conserved blocks from multiple alignments for their use in phylogenetic analysis. *Molecular biology and evolution*, 17, 540–552.

Chang, H., Lim, J., Ha, M., & Kim, V. N. (2014). Tail-seq: genome-wide determination of poly(a) tail length and 3' end modifications. *Mol Cell*, 53(6), 1044–52.

Chu, J., Loughlin, E. A., Gaur, N. A., SenBanerjee, S., Jacob, V., Monson, C., Kent, B., Oranu, A., Ding, Y., Ukomadu, C., & Sadler, K. C. (2012). Uhrf1 phosphorylation by cyclin a2/cyclin-dependent kinase 2 is required for zebrafish embryogenesis. *Mol Biol Cell*, 23(1), 59–70.

Collart, C., Owens, N. D., Bhaw-Rosun, L., Cooper, B., De Domenico, E., Patrushev, I., Sesay, A. K., Smith, J. N., Smith, J. C., & Gilchrist, M. J. (2014). High-resolution analysis of gene activity during the xenopus mid-blastula transition. *Development*, 141(9), 1927–39.

Dobin, A., Davis, C. A., Schlesinger, F., Drenkow, J., Zaleski, C., Jha, S., Batut, P., Chaisson, M., & Gingeras, T. R. (2013). Star: ultrafast universal rna-seq aligner. *Bioinformatics*, 29(1), 15–21.

Duval, C., Bouvet, P., Omilli, F., Roghi, C., Dorel, C., LeGuellec, R., Paris, J., & Osborne, H. B. (1990). Stability of maternal mrna in xenopus embryos: role of transcription and translation. *Mol Cell Biol*, 10(8), 4123–9.

Eisen, J. S. & Smith, J. C. (2008). Controlling morpholino experiments: don't stop making antisense. *Development*, 135(10), 1735–43.

Garneau, N. L., Wilusz, J., & Wilusz, C. J. (2007). The highways and byways of mrna decay. *Nat Rev Mol Cell Biol*, 8(2), 113–26.

Giraldez, A. J., Mishima, Y., Rihel, J., Grocock, R. J., Van Dongen, S., Inoue, K., Enright, A. J., & Schier, A. F. (2006). Zebrafish mir-430 promotes deadenylation and clearance of maternal mrnas. *Science*, 312(5770), 75–9.

Graindorge, A., Le Tonqueze, O., Thuret, R., Pollet, N., Osborne, H. B., & Audic, Y. (2008). Identification of cug-bp1/eden-bp target mrnas in xenopus tropicalis. *Nucleic Acids Res*, 36(6), 1861–70.

Guindon, S., Dufayard, J.-F., Lefort, V., Anisimova, M., Hordijk, W., & Gascuel, O. (2010). New algorithms and methods to estimate maximum-likelihood phylogenies: assessing the performance of phyml 3.0. *Systematic biology*, 59, 307–321.

Hamatani, T., Carter, M. G., Sharov, A. A., & Ko, M. S. (2004). Dynamics of global gene expression changes during mouse preimplantation development. *Dev Cell*, 6(1), 117–31.

Harvey, S. A., Sealy, I., Kettleborough, R., Fenyes, F., White, R., Stemple, D., & Smith, J. C. (2013). Identification of the zebrafish maternal and paternal transcriptomes. *Development*, 140(13), 2703–10.

Heasman, J., Kofron, M., & Wylie, C. (2000). Beta-catenin signaling activity dissected in the early xenopus embryo: a novel antisense approach. *Dev Biol*, 222(1), 124–34.

Heo, I., Ha, M., Lim, J., Yoon, M. J., Park, J. E., Kwon, S. C., Chang, H., & Kim, V. N. (2012). Mono-uridylation of pre-microrna as a key step in the biogenesis of group ii let-7 micrornas. *Cell*, 151(3), 521–32.

Heyn, P., Kircher, M., Dahl, A., Kelso, J., Tomancak, P., Kalinka, A. T., & Neugebauer, K. M. (2014). The earliest transcribed zygotic genes are short, newly evolved, and different across species. *Cell Rep*, 6(2), 285–92.

Hoefig, K. P., Rath, N., Heinz, G. A., Wolf, C., Dameris, J., Schepers, A., Kremmer, E., Ansel, K. M., & Heissmeyer, V. (2013). Eri1 degrades the stem-loop of oligouridylated histone mrnas to induce replication-dependent decay. *Nat Struct Mol Biol*, 20(1), 73–81.

Kahvejian, A., Svitkin, Y. V., Sukarieh, R., M'Boutchou, M.-N., & Sonenberg, N. (2005). Mammalian poly (a)-binding protein is a eukaryotic translation initiation factor, which acts via multiple mechanisms. *Genes & development*, 19(1), 104–113.

Kamachi, Y., Okuda, Y., & Kondoh, H. (2008). Quantitative assessment of the knockdown efficiency of morpholino antisense oligonucleotides in zebrafish embryos using a luciferase assay. *Genesis*, 46(1), 1–7.

Kane, D. A. & Kimmel, C. B. (1993). The zebrafish midblastula transition. *Development*, 119(2), 447–56.

Kent, B., Magnani, E., Walsh, M. J., & Sadler, K. C. (2016). Uhrf1 regulation of dnmt1 is required for pre-gastrula zebrafish development. *Dev Biol*, 412(1), 99–113.

Kimmel, C. B., Ballard, W. W., Kimmel, S. R., Ullmann, B., & Schilling, T. F. (1995). Stages of embryonic development of the zebrafish. *Dev Dyn*, 203(3), 253–310.

Klein, S. L. & Moody, S. A. (2015). Early neural ectodermal genes are activated by siamois and twin during blastula stages. *Genesis*, 53(5), 308–20.

Kwak, J. E. & Wickens, M. (2007). A family of poly(u) polymerases. *RNA*, 13(6), 860–7.

Lackey, P. E., Welch, J. D., & Marzluff, W. F. (2016). Tut7 catalyzes the uridylation of the 3' end for rapid degradation of histone mrna. *RNA*.

Lapointe, C. P. & Wickens, M. (2013). The nucleic acid-binding domain and translational repression activity of a xenopus terminal uridylyl transferase. *J Biol Chem*, 288(28), 20723–33.

Lee, M., Kim, B., & Kim, V. N. (2014). Emerging roles of rna modification: m(6)a and u-tail. *Cell*, 158(5), 980–7.

Lee, M. T., Bonneau, A. R., Takacs, C. M., Bazzini, A. A., DiVito, K. R., Fleming, E. S., & Giraldez, A. J. (2013). Nanog, pou5f1 and soxb1 activate zygotic gene expression during the maternal-to-zygotic transition. *Nature*, 503(7476), 360–4.

Legagneux, V., Bouvet, P., Omilli, F., Chevalier, S., & Osborne, H. B. (1992). Identification of rna-binding proteins specific to xenopus eg maternal mrnas: association with the portion of eg2 mrna that promotes deadenylation in embryos. *Development*, 116(4), 1193–202.

Li, B. & Dewey, C. N. (2011). Rsem: accurate transcript quantification from rna-seq data with or without a reference genome. *BMC bioinformatics*, 12(1), 1.

Lim, J., Ha, M., Chang, H., Kwon, S. C., Simanshu, D. K., Patel, D. J., & Kim, V. N. (2014). Uridylation by tut4 and tut7 marks mrna for degradation. *Cell*, 159(6), 1365–76.

Lim, J., Lee, M., Son, A., Chang, H., & Kim, V. N. (2016). mtail-seq reveals dynamic poly(a) tail regulation in oocyte-to-embryo development. *Genes Dev*, 30(14), 1671–82.

Lund, E., Liu, M., Hartley, R. S., Sheets, M. D., & Dahlberg, J. E. (2009). Deadenylation of maternal mrnas mediated by mir-427 in xenopus laevis embryos. *RNA*, 15(12), 2351–63.

Malecki, M., Viegas, S. C., Carneiro, T., Golik, P., Dressaire, C., Ferreira, M. G., & Arraiano, C. M. (2013). The exoribonuclease dis3l2 defines a novel eukaryotic rna degradation pathway. *The EMBO journal*, 32(13), 1842–1854.

Martin, G. & Keller, W. (2007). Rna-specific ribonucleotidyl transferases. *RNA*, 13(11), 1834–49.

Mendez, R. & Richter, J. D. (2001). Translational control by cpeb: a means to the end. *Nat Rev Mol Cell Biol*, 2(7), 521–9.

Minasaki, R. & Eckmann, C. R. (2012). Subcellular specialization of multifaceted 3'end modifying nucleotidyltransferases. *Current opinion in cell biology*, 24, 314–322.

Mishima, Y. & Tomari, Y. (2016). Codon usage and 3' utr length determine maternal mrna stability in zebrafish. *Mol Cell*, 61(6), 874–85.

Mullen, T. E. & Marzluff, W. F. (2008). Degradation of histone mrna requires oligouridylation followed by decapping and simultaneous degradation of the mrna both 5' to 3' and 3' to 5'. *Genes Dev*, 22(1), 50–65.

Munoz-Tello, P., Rajappa, L., Coquille, S., & Thore, S. (2015). Polyuridylation in eukaryotes: A 3'-end modification regulating rna life. *Biomed Res Int*, 2015, 968127.

Nasevicius, A. & Ekker, S. C. (2000). Effective targeted gene 'knockdown' in zebrafish. *Nat Genet*, 26(2), 216–20.

Newport, J. & Kirschner, M. (1982). A major developmental transition in early xenopus embryos: I. characterization and timing of cellular changes at the midblastula stage. *Cell*, 30(3), 675–86.

Nguyen, T. A., Jo, M. H., Choi, Y.-G., Park, J., Kwon, S. C., Hohng, S., Kim, V. N., & Woo, J.-S. (2015). Functional anatomy of the human microprocessor. *Cell*, 161(6), 1374–1387.

Nieuwkoop, P. & Faber, J. (1994). *Normal Table of Xenopus laevis (Daudin)*. Garland Publishing Inc.

Norbury, C. J. (2013). Cytoplasmic rna: a case of the tail wagging the dog. *Nat Rev Mol Cell Biol*, 14(10), 643–53.

Owens, N. D., Blitz, I. L., Lane, M. A., Patrushev, I., Overton, J. D., Gilchrist, M. J., Cho, K. W., & Khokha, M. K. (2016). Measuring absolute rna copy numbers at high temporal resolution reveals transcriptome kinetics in development. *Cell Rep*, 14(3), 632–47.

Paillard, L. & Osborne, H. B. (2003). East of eden was a poly(a) tail. *Biology of the Cell*, 95(3-4), 211–219.

Paris, J. & Philippe, M. (1990). Poly(a) metabolism and polysomal recruitment of maternal mrnas during early xenopus development. *Dev Biol*, 140(1), 221–4.

Pei, J. & Grishin, N. V. (2007). Promals: towards accurate multiple sequence alignments of distantly related proteins. *Bioinformatics (Oxford, England)*, 23, 802–808.

Peshkin, L., Wuhr, M., Pearl, E., Haas, W., Freeman, R. M., J., Gerhart, J. C., Klein, A. M., Horb, M., Gygi, S. P., & Kirschner, M. W. (2015). On the relationship of protein and mrna dynamics in vertebrate embryonic development. *Dev Cell*, 35(3), 383–94.

Pique, M., Lopez, J. M., Foissac, S., Guigo, R., & Mendez, R. (2008). A combinatorial code for cpe-mediated translational control. *Cell*, 132(3), 434–48.

Quinlan, A. R. & Hall, I. M. (2010). Bedtools: a flexible suite of utilities for comparing genomic features. *Bioinformatics*, 26(6), 841–842.

Rissland, O. S., Mikulasova, A., & Norbury, C. J. (2007). Efficient rna polyuridylation by noncanonical poly(a) polymerases. *Mol Cell Biol*, 27(10), 3612–24.

Rissland, O. S. & Norbury, C. J. (2009). Decapping is preceded by 3' uridylation in a novel pathway of bulk mrna turnover. *Nat Struct Mol Biol*, 16(6), 616–23.

Ro, H., Won, M., Lee, S. U., Kim, K. E., Huh, T. L., Kim, C. H., & Rhee, M. (2005). Sinup, a novel siaz-interacting nuclear protein, modulates neural plate formation in the zebrafish embryos. *Biochem Biophys Res Commun*, 332(4), 993–1003.

Robinson, M. D. & Oshlack, A. (2010). A scaling normalization method for differential expression analysis of rna-seq data. *Genome biology*, 11(3), 1.

Scheer, H., Zuber, H., De Almeida, C., & Gagliardi, D. (2016). Uridylation earmarks mrnas for degradation... and more. *Trends Genet*, 32(10), 607–19.

Schmidt, M.-J., West, S., & Norbury, C. J. (2011). The human cytoplasmic rna terminal u-transferase zcchc11 targets histone mrnas for degradation. *Rna*, 17(1), 39–44.

Session, A. M., Uno, Y., Kwon, T., Chapman, J. A., Toyoda, A., Takahashi, S., Fukui, A., Hikosaka, A., Suzuki, A., Kondo, M., van Heeringen, S. J., Quigley, I., Heinz, S., Ogino, H., Ochi, H., Hellsten, U., Lyons, J. B., Simakov, O., Putnam, N., Stites, J., Kuroki, Y., Tanaka, T., Michiue, T., Watanabe, M., Bogdanovic, O., Lister, R., Georgiou, G., Paranjpe, S. S., van Kruijsbergen, I., Shu, S., Carlson, J., Kinoshita, T., Ohta, Y., Mawaribuchi, S., Jenkins, J., Grimwood, J., Schmutz, J., Mitros, T., Mozaffari, S. V., Suzuki, Y., Haramoto, Y., Yamamoto, T. S., Takagi, C., Heald, R., Miller, K., Haudenschild, C., Kitzman, J., Nakayama, T., Izutsu, Y., Robert, J., Fortriede, J., Burns, K., Lotay, V., Karimi, K., Yasuoka, Y., Dichmann, D. S., Flajnik, M. F., Houston, D. W., Shendure, J., DuPasquier, L., Vize, P. D., Zorn, A. M., Ito, M., Marcotte, E. M., Wallingford, J. B., Ito, Y., Asashima, M., Ueno, N., Matsuda, Y., Veenstra, G. J. C., Fujiyama, A., Harland, R. M., Taira, M., & Rokhsar, D. S. (2016). Genome evolution in the allotetraploid frog xenopus laevis. *Nature*, 538, 336–343.

Sheets, M. D., Fox, C. A., Hunt, T., Vande Woude, G., & Wickens, M. (1994). The 3'-untranslated regions of c-mos and cyclin mrnas stimulate translation by regulating cytoplasmic polyadenylation. *Genes Dev*, 8(8), 926–38.

Shen, B. & Goodman, H. M. (2004). Uridine addition after microrna-directed cleavage. *Science*, 306(5698), 997.

Sive, H. L., Grainger, R. M., & Harland, R. M. (2007). Xenopus laevis in vitro fertilization and natural mating methods. *CSH Protoc*, 2007, pdb prot4737.

Slevin, M. K., Meaux, S., Welch, J. D., Bigler, R., Miliani de Marval, P. L., Su, W., Rhoads, R. E., Prins, J. F., & Marzluff, W. F. (2014). Deep sequencing shows multiple oligouridy-

lations are required for 3' to 5' degradation of histone mrnas on polyribosomes. *Mol Cell*, 53(6), 1020–30.

Su, W., Slepenkov, S. V., Slevin, M. K., Lyons, S. M., Ziemniak, M., Kowalska, J., Darzynkiewicz, E., Jemielity, J., Marzluff, W. F., & Rhoads, R. E. (2013). mrnas containing the histone 3' stem-loop are degraded primarily by decapping mediated by oligouridylation of the 3' end. *RNA*, 19(1), 1–16.

Subtelny, A. O., Eichhorn, S. W., Chen, G. R., Sive, H., & Bartel, D. P. (2014). Poly(a)-tail profiling reveals an embryonic switch in translational control. *Nature*, 508(7494), 66–71.

Suzuki, H., Tsukahara, T., & Inoue, K. (2009). Localization of c-mos mrna around the animal pole in the zebrafish oocyte with zor-1/zorba. *Biosci Trends*, 3(3), 96–104.

Tadros, W. & Lipshitz, H. D. (2009). The maternal-to-zygotic transition: a play in two acts. *Development*, 136(18), 3033–42.

Tharun, S., He, W., Mayes, A. E., Lennertz, P., Beggs, J. D., & Parker, R. (2000). Yeast sm-like proteins function in mrna decapping and decay. *Nature*, 404(6777), 515–8.

Thornton, J. E., Du, P., Jing, L., Sjekloca, L., Lin, S., Grossi, E., Sliz, P., Zon, L. I., & Gregory, R. I. (2014). Selective microrna uridylation by zcchc6 (tut7) and zcchc11 (tut4). *Nucleic Acids Res*, 42(18), 11777–91.

Voeltz, G. K. & Steitz, J. A. (1998). Auuua sequences direct mrna deadenylation uncoupled from decay during xenopus early development. *Mol Cell Biol*, 18(12), 7537–45.

Weill, L., Belloc, E., Bava, F. A., & Mendez, R. (2012). Translational control by changes in poly(a) tail length: recycling mrnas. *Nat Struct Mol Biol*, 19(6), 577–85.

Wells, S. E., Hillner, P. E., Vale, R. D., & Sachs, A. B. (1998). Circularization of mrna by eukaryotic translation initiation factors. *Mol Cell*, 2(1), 135–40.

Yartseva, V. & Giraldez, A. J. (2015). The maternal-to-zygotic transition during vertebrate development: A model for reprogramming. *Curr Top Dev Biol*, 113, 191–232.